Diurnal rodents as pertinent animal models of human retinal physiology and pathology

Daniela M. Verra, Benjamin S. Sajdak, Dana K. Merriman, David Hicks

Diurnal rodents as pertinent animal models of human retinal physiology and pathology

Daniela M. Verra[1], Benjamin S. Sajdak[2], Dana K. Merriman[3] and David Hicks[1*]

Running title: Vision in diurnal rodents

Author affiliations:

1. Department of Neurobiology of Rhythms, Institut des Neurosciences Cellulaires et Intégratives (INCI), CNRS UPR 3212, Strasbourg, France;

2. Morgridge Institute for Research, Madison, WI, USA

3. Department of Biology, University of Wisconsin Oshkosh, Oshkosh, WI, USA

* Author for all correspondence:

David Hicks, INCI CNRS UPR 3212, 5 rue Blaise Pascal, 67000 Strasbourg, France

Tel: 33 388456723

E-mail: photoreceptor67@hotmail.com

Funding Sources: The authors would like to sincerely thank the following for funding parts of the research reported here: Agence Nationale de Recherche (ANR), France; Fondation de Recherche Médicale; International Retinal Research Foundation, USA; Roche Pharmaceuticals Ltd.; UNADEV-ITMO; USIAS (Univ. Strasbourg Inst. Advanced Studies)

Table of contents:

Abstract

This presentation will survey the retinal architecture, advantages, and limitations of several lesser-known rodent species that provide a useful diurnal complement to rats and mice. These diurnal rodents also possess unusually cone-rich photoreceptor mosaics that facilitate the study of cone cells and pathways. Species to be presented include principally the Sudanian Unstriped Grass Rat and Nile Rat (*Arvicanthis spp*.), the Fat Sand Rat (*Psammomys obesus*), the degu (*Octodon degus*) and the 13-lined ground squirrel (*Ictidomys tridecemlineatus*). The retina and optic nerve in several of these species demonstrate unusual resilience in the face of neuronal injury, itself an interesting phenomenon with potential translational value.

1. Introduction

After some general considerations in the introduction, the sections that follow highlight those diurnal species for which we have most experimental data, primarily *Arvicanthis*, *Psammomys*, and *Ictidomys* (formerly *Spermophilus*). We provide an update on the latter species, since Merriman et al., 2016 covers this species in more detail. We also review scattered data concerning visual studies in other diurnal rodents that are less familiar. Finally, we provide our thoughts on future directions on increasingly important diurnal rodents for the study of retinal physiology and pathology. Unless stated otherwise, the common name mouse always refers to *Mus musculus*, rat always refers to *Rattus norvegicus*, and when the species is not stipulated, *Arvicanthis* refers to *Arvicanthis ansorgei*.

1.1. Justification for cone-rich small mammal models

The *Rodentia* form the largest order of the class *Mammalia*, constituting around 40% of the total with 2,276 currently identified species. Of these, the family *Muridae* with around 710 species is further divided into five sub-families, of which the *Murinae* (519 species) contains some of the most familiar examples including the House Mouse *Mus musculus* and the Brown Rat *Rattus norvegicus*. Although the use of animals to explore the structure and function of the human body can be recorded back to ancient Greece, over the course of the last century these two species have come to dominate

laboratory research, because of the many similarities between physiological and pathological parameters compared to humans, and the practical advantages of small size, easy maintenance in captivity and rapid breeding. The decision at the start of the 20th century to extensively in-breed mice, leading to the generation of genetically uniform colonies in order to reduce inter-individual variation, was seminal in accelerating use of mice in research (Ericsson et al., 2013). Indeed mice now together represent around 95% of all animal models used for biomedical research (Foundation for Biomedical Research). However, like the majority of rodents, mice and rats have visual systems evolved for a nocturnal lifestyle, whereas the human visual system evolved for a bright-light diurnal habitat. In light of this, and despite the overwhelming presence and utility of genetically inbred and transgenic strains of mice in research, certain shortcomings with respect to their pertinence for human disease modelling are being increasingly recognized. For example, basic differences in the immune system of mice compared to humans has complicated their use in studying infectious diseases such as tuberculosis or inflammatory processes (Lynch, 2009). Many preclinical trials of promising pharmacological agents using mouse models have given disappointing results when extended to human populations (eg. the combined NMDA receptor blocker and morphine mix MorphiDex™, which despite strong analgesic effects in rodents had no statistically significant effect in epidemiological studies in humans, and was discontinued: Galer et al., 2005). Frequently used to study genes involved in pain mediation, it was shown through comparison of gene profiling data from numerous reports that putative genes in rat models were largely different and separate from those seen in mouse models (LaCroix-Fralish et al., 2011). Similarly, use of mice by the pharmaceutical industry as preclinical models of drug screening in depression or analgesia are complicated by changes in the behavioral tests used (forced swim test or tail suspension test) as a function of time of day, and are quite different from analogous tests performed on diurnal rodents (Bilu and Kronfeld-Schor, 2013; Bilu et al., 2016, 2019). In general terms, it has also been recognised that reliance on a single species (indeed a single strain, the C57BL/6) to model human pathology is necessarily restricted. With respect to the central tenet of the current review, the potential interest of diurnal rodents for vision research,

mice and rats (as examples of nocturnal mammals) have distinct differences in retinal structure and function that make them less suitable for extrapolation to humans (as an example of a diurnal mammal). To paraphrase Daniel Engber (The Slate, Nov. 16 2011 The Mouse Trap : "If you want to know about the visual system, for example, why use an animal that sniffs and whisks its way through the world? How about one that depends on its eyes, like a squirrel?"). This statement is backed up by the fact that both arboreal and ground squirrels have relatively larger dorsolateral cortical areas devoted to visual information processing relative to rats, which on the contrary have greater somatosensory and auditory representation (Campi and Krubitzer, 2010). Similarly, the diurnal Nile Rat *Arvicanthis niloticus* has a disproportionately large superior colliculus attesting to the dominance of visual input (Gaillard et al., 2013). Before considering how diurnally active rodents could represent interesting animal models for vision research, we will start by addressing three related issues: firstly, how does one define diurnality versus nocturnality, secondly what could be the importance of the circadian clock in any observed differences, and thirdly how do "typical nocturnal rodent eyes" compare to "typical diurnal rodent eyes".

1.2. Diurnality versus nocturnality

Our current model of visual system evolution suggests that cones evolved first in vertebrates (Lamb 2013), but there are converging lines of evidence, from the fossil record and comparative genomics that ancestral mammals were nocturnal (the “nocturnal bottleneck”, though see Davies et al. 2012 discussion of the “twilight bottleneck”). The currently accepted hypothesis of a bottleneck in mammalian evolution posits that predatory pressure from the reigning dinosauria pushed early mammals towards a nocturnal phenotype. Their presumptive ability to thermoregulate enabled them to occupy this nocturnal niche, remaining hidden in burrows during the day (Heesy and Hall, 2010). Over the long course of dinosaur planetary dominance, from the early Triassic to late Cretaceous lasting some 220 million years, several features of diurnal vision including absolute cone numbers, different spectral sub-types and additional melanopsin genes, were lost by genetic drift. Disappearance of the dinosaurs released mammals from this predatory pressure, and some lines

adopted a daytime mode of foraging and gradually evolved some diurnal attributes such as increased complement of cones. In extant species, the *Rodentia* family comprises many examples of both temporal niches, as well as animals displaying crepuscular activity. The evolution of primate vision is less clear, with evidence of considerable flexibility between temporal niches (Ankel-Simons & Rasmussen 2008). Both nocturnal and diurnal primates exist today, the former lacking foveal structures (Wikler & Rakic 1990).

As will be seen when discussing individual species, depending on the parameters used these can be defined as "fully nocturnal", "fully diurnal" or "intermediate/crepuscular. Although on the face of it these temporal niches should be easy to define – animals which are active entirely or principally during the day or night hours respectively – the truth is more nuanced. Even in species such as *Arvicanthis* showing diurnal traits under natural conditions, experimental manipulation of the photoperiod leads to shifts in locomotor activity, and some individuals have nocturnal activity profiles (Challet et al., 2002). Some discrete anatomical and physiological differences between diurnal or nocturnal species have been identified, such as robust retinohypothalamic projections to the ventral subparaventricular zone (vSPVZ) in rats but only weak innervation of the same region in *Arvicanthis niloticus* (Todd et al., 2012); or distinctly different temporal profiles of c-Fos expression in the lower subparaventricular zone (LSPZ) between the same two species (Schwarz et al., 2004); or phase-inversed peak levels of, and sensitivity to, serotonin in the suprachiasmatic nucleus (SCN), again between the two same species (Cuesta et al., 2008). Similarly, acute effects of light are almost diametrically opposed between mice and *A. niloticus*, with opposite directions of masking responses and c-fos expression in arousal-related brain regions in *A. niloticus* but not mice (Shuboni et al., 2015). Temporal niche is also behaviorally plastic depending on local conditions of resource competition, at least in rodents. Some species are able to shift between the two niches depending on environmental influences, and these shifts can occur in either direction, ie. diurnal to nocturnal or nocturnal to diurnal. Examples of the first concern several species which are fully diurnal in the wild but when captured and maintained in captivity assume a nocturnal phenotype (Refinetti, 2006; Vivanco et al.,

2010a; Hut et al., 2012). Examples of nocturnal to diurnal shifts are calorie restriction-induced changes from nocturnal to diurnal locomotor activity in rats and mice (Mendoza et al., 2008; Challet, 2010; Sen et al., 2017) (although limiting access to food during the nocturnal period induces nocturnality in diurnal species for as long as the timed feeding paradigm continues: Vivanco et al., 2010b), and exposure to very dim lighting during the day leading to diurnal activity in mice (Doyle et al., 2008). In addition to these structural specializations, diurnality and nocturnality may impose different metabolic backgrounds on which the respective photoreceptor mosaics function. If so, relying exclusively on nocturnal models of human vision in health and disease could be misleading. Phillips et al. (2013) developed a mathematical model that uses physiological-based parameters (simulating connectivity patterns between the SCN and recipient targets), to accurately predict diurnal, nocturnal or bimodal activity patterns, as well as temporal niche switching.

Notwithstanding, in terms of ocular, especially retinal, structure there are clear differences between mammals typically active during the daylight and those typically active during the night time. Eye size is one important parameter, especially in primates which have adopted a nocturnal mode of activity, increasing the size of the pupil to maximise light entry. Additionally, corneal size and curvature, lens size and focal length, are modified between species living in either temporal niche. The presence of a reflecting tapetum behind the neural retina is another common feature of night-dwelling species, increasing light capture by reflecting light back across the retina. The retina itself shows several important adaptations to mode of life. Nocturnal mammals like mice and rats typically have very large numbers of rods within the outer nuclear layer (ONL), again to maximize photon catch. Diurnal mammals have far fewer cell layers in the ONL. Nocturnal species have low proportions of cone photoreceptors, which would be less functionally important in low light levels. Both mice (2.9% cones: Jeon et al., 1998) and rats (0.9% cones: Szel and Röhlich, 1992) have very rod-dominated retinas, whereas ground squirrels and tree shrews are at the opposite extreme, around 85% and 95% cones, respectively (Kryger et al., 1998; Müller and Peichl, 1989). Of course humans have a relatively low cone percentage, too (around 5%), but these are concentrated within the central macula

affording high acuity vision under photopic conditions. A final and fascinating difference concerns nuclear structure: it was demonstrated that nocturnal mammals have a unique inverted chromatin architecture in their rods, whereby the normal configuration of a central core of euchromatin (EC) surrounded by a shell of heterochromatin (HC) has been replaced by a central dense core of HC surrounded by more peripherally distributed EC (Solovei et al., 2009). The authors showed that this structure allowed more efficient light transmission, with the condensed centres acting as microlenses to reduce light scattering during passage through the ONL. Originally described in the mouse, the authors showed that this inverted architecture segregated with nocturnal mode of activity. Simply put, rods in diurnal mammals such as humans are not the strict equivalent of rods in nocturnal mammals such as mice. The underlying assumption is that in limiting light levels encountered at night, adaptations that would improve light transmission would be favourable; such constraints are not present for daytime active species, where the ambient levels are adequate to allow losses. The same authors went on to identify the molecular mechanisms involved in chromatin organisation, showing that continued expression of either lamin B receptor (LBR) and/or lamin A/C was necessary to tether HC to the nuclear envelope (Solovei et al., 2013). Differentiated rods in mice were the only cell type in which expression of both proteins was highly down-regulated, leading to re-distribution of HC to the nuclear centre. Generation of transgenic mice harbouring the lamin B receptor re-established a centralized EC phenotype, so that mutant mice possess “humanized” rod nuclei in which chromatin organisation resembles that of primates (Solovei et al., 2013).

1.3. Circadian clock adaptations

Circadian rhythms, and chronobiology in general, are increasingly recognized as critical determinants of survival in all living organisms. The importance of this subject was recently underscored by the attribution of the 2017 Nobel Prize in Medicine and Physiology to the three scientists pioneering work in this field, Michael Young, Michael Rosbach and Jeffrey Hall. The fundamental influence of this complex temporal organisation upon the physiology, behaviour, health and fitness of biological organisms has come to be appreciated. Practically all species manifest some kind of biological clock, in

accordance with periodic variations of environmental factors and especially the 24-hour day/night cycle. In mammals, circadian rhythms (circadian = about 24 hours) are controlled by conserved, cell autonomous, and self-sustaining mechanisms mainly based on autoregulatory, negative feedback loops capable of tracking time in order to anticipate predictable environmental changes and to control physiology and behavior accordingly. A huge number of cellular clocks exist throughout the body, coordinated by a master clock located in the suprachiasmatic nuclei (SCN) within the hypothalamus, themselves synchronized with the solar day by daily light signals transmitted through the retina. Recently, an exhaustive analysis of rhythmic transcriptional expression profiles in >60 tissues/organs from a diurnal non-human primate was performed (Mure et al., 2018). This genome-wide transcriptome study uncovered a wide array (about 82%) of protein-encoding, ubiquitous, and tissue-specific genes undergoing rhythmic daily changes. This and previous studies emphasize just how pervasive the circadian clock system is, with extensive regulation of major, basic biologic processes such as metabolism, DNA repair and gene expression, but also tissue-specific functions, all intimately coordinated within the 24-hour period.

The day/night cycle is the major environmental factor (also called a zeitgeber or time giver) able to entrain clocks. In mammals, eyes constitute the only light input pathway to the SCN and entrainment of the central clock involves the three main light-sensitive systems of the retina i.e., rods, cones, and the intrinsically sensitive retinal ganglion cells (ipRGCs)]. The latter were discovered about 20 years ago and express the photopigment melanopsin (OPN4) (see section 2.5. for further details). Hence the retina plays a unique double role within the circadian network, both constituting the gateway into the central control module (SCN) but also displaying its own endogenous temporal organization. As the circadian system is so important, an argument can be made that the use of diurnal mammalian species may offer advantages compared to the far more commonly used nocturnal species mice, rats and golden hamsters (*Mesocricetus auratus*) for investigating human-related pathophysiological processes. Although contemporary lifestyles have greatly affected our own endogenous time-keeping systems, we are essentially diurnal animals. As recently outlined by Yan et

al (2018), the effects of light on the circadian timekeeping system are very similar in nocturnal and diurnal animals, whereas the downstream effects/outputs of that system on the myriad rhythms under its control are very different.

1.4. Animal model considerations for studying retinal disease

The human fovea is distinguished by a pronounced increase in cone density with a near absence of rods. It is the dense packing of cones in the fovea that underlies our high-acuity vision. However, while the fovea occupies only about 0.02% of the total retinal area, about 40% of primary visual cortex is devoted to processing cone signals from the fovea (Hendrickson, 2005). As such, diseases that affect cone structure and function are especially devastating – placing severe social and economic burdens on the individual and on society. While several innovative therapeutic strategies for restoring cone function are being pursued, their continued development and translation relies on the availability of animal models that mimic human retinal anatomy, as well as recapitulate the pathophysiology of the disease of interest. Inbred strains of mice and rats have been the most frequently used among vision researchers, but are not ideal models for testing translatable therapies. These rodents are nocturnal, have low visual acuity, small eyes, large lenses, and sparse cone mosaics that frequently do not phenocopy human retinal diseases (Slijkerman et al., 2015), likely due to cellular and molecular differences of photoreceptors (Frohns et al., 2014; Mustafi et al., 2016; Solovei et al., 2009). When choosing an animal model, it's important to consider how comparable the structure and function of the visual system is to humans. Such considerations include: ocular anatomy (e.g. eye size, vasculature, photoreceptor anatomy); presence of a fovea, area centralis or visual streak; and post-receptoral/high-order organization in the visual cortex. With these considerations, non-human primates that possess a fovea would appear to be an ideal model. However, progress in creating non-human primate genetic models of blindness has been slow due to high cost, ethical concerns, and limited (and decreasing) availability. Large mammal models with a cone-rich area centralis [e.g. dogs (Beltran et al., 2014) and pigs (Hendrickson and Hicks, 2002)] are appealing because of lower costs and the existence of natural and genetic models of retinal disease (Kostic and Arsenijevic, 2016).

Despite the many advancements towards large animal modeling, a critical research gap remains between nocturnal rodents and large animal work. Unfortunately, there is no single "perfect" animal model, so balancing practicality and relevance is critical.

2. Sudanian Unstriped Grass Rat (*Arvicanthis ansorgei*)

2.1. *Arvicanthis*: systematics, comparison of *A. ansorgei* and *A. niloticus*.

Although most rodent species are nocturnal, a few diurnal species of African rodents can be found among the *Sciuridae*, *Bathyergidae*, and *Muridae* families. Apart from some species of *Acomys* and *Hybomys*, diurnal *Muridae* species belong to the genera *Arvicanthis*, *Mylomys*, *Pelomys*, *Desmomys*, *Rhabdomys*, or *Lemniscomys*, which constitute the exclusively African branch of the Arvicanthine division. All species in that division share common characteristics (Carleton and Musser, 1984), some of which are probably related to their diurnality (i.e., presence of bands on dorsal coat or pigmentation by melanin of the periosteum at the top of the skull, as well as retinal cellular anatomy to be discussed later). Cytogenetic and molecular analysis demonstrates the monophyly of these genera with estimated times of divergence from other *Muridae* divisions ranging from 4 to 13 million years (Ducroz et al., 2001). The genus *Arvicanthis* is widely distributed in savanna grasslands of sub-saharan Africa. The taxonomy of the genus is problematic, and it remains possible that different investigators have actually been working with different species within the genus *Arvicanthis*. Taxonomists have argued for the existence of one (Misonne, 1969; Honacki et al., 1982) to five (Nowak, 1991) distinct species in this genus. Recent chromosomal work has shown that there are indeed more than one species of *Arvicanthis*, but the exact taxonomic relationships and ranges of these species have yet to be defined (Volobouev et al., 1987; Capanna et al., 1988; Orlov et al., 1992). The various forms of *Arvicanthis* were first grouped into a single species, *A. niloticus*, by Honacki et al. (1982). The forms were then listed as 6 species (i.e., *A. abyssinicus*, *A. blicki*, *A. somalicus*, *A. dembeensis*, *A. nairobae*, and *A. niloticus*) in the following revisions (e.g., Wilson and Reeder, 1993). Several sibling but true species were probably merged into a single but polytypic species, and conversely certain recognized separate species probably belong to a single true species.

Studies cited in the present review stem from work on the two species *A. ansorgei* and *A. niloticus*. A breeding colony of *A. ansorgei* was initiated by the laboratory of Dr. Paul Pevet at the University of Strasbourg, France in 1998 from animals trapped in the southern part of Mali, whereas the laboratory of Dr. Laura Smale (Departments of Zoology and Psychology, Michigan State University, East Lansing, MI, USA) established a colony of *A. niloticus* from individuals trapped in southern Kenya in 1993. Both species are sympatric only in the central region of Mali, but no hybrid forms were caught in the overlapping areas (Sicard et al., 1999). Based on their geographical distributions, *A. ansorgei* probably experiences less variable photoperiods than *A. niloticus*. Because they are morphologically similar, the two species have been confounded until recently. As regards to their retinal organisation, the two species are ostensibly the same although there may be some differences arising from housing conditions and diet used by the different facilities (see further on discussion of diabetic retinopathy). A recent review provides a comprehensive account of circadian and light-driven activities in *Arvicanthis* (principally *A. niloticus*) (Yan et al., 2018).

2.2. Photoreceptor organisation and phagocytosis in *Arvicanthis*

Owing to their scientific interest as a mammalian species occupying a diurnal niche conferring upon them some similarities to humans, many studies have been performed regarding their physiology and behaviour, especially in relation to circadian rhythmicity (Challet et al., 2002; Caldelas et al., 2003; Cuesta et al., 2008; Mendoza et al., 2012; Novak et al., 2007; Yan et al., 2018). Furthermore several studies have demonstrated the interest of diurnal rodents for modelling different disease states in humans, including neurological and metabolic conditions (Ashkenazy et al., 2009; Fonken et al., 2012b; Grosbellet et al., 2015; Bilu et al., 2016). To the best of our knowledge, our laboratory was the first to publish data concerning the cone-rich aspect of the retina in *Arvicanthis ansorgei*. Dissemination of these findings led to similar studies being performed in *Arvicanthis niloticus* (Gaillard et al., 2008). We reasoned that the diurnal status of this species would lead to adaptations to bright photic environments, and our predictions were borne out by initial immunolabeling studies using anti-cone arrestin antibody (Figure 1; Bobu et al., 2006). As was to be expected in a diurnal species, the

outer nuclear layer (ONL) was thinner than that of typical nocturnal species, composed of only about 6 rows of cells, compared to the 11-15 rows seen in mice and rats. The 2-3 scleral-most layers were entirely composed of cone cell bodies, whereas the vitreal-most 4 layers were exclusively rods (Figure 1). This quasi-crystalline organisation has facilitated tissue collection by laser capture microscopy in order to perform transcriptomic analysis of specific populations. The two populations showed highly specific immunostaining using probes made against mouse and rat sequences, rods being exclusively stained by antibodies to rhodopsin, phosducin, rod transducin and RET-P3, cones being labelled with cone arrestin, cone transducin, short- and mid-wavelength cone opsins, and both being stained equally with antisera to arrestin and recoverin (Figure 2). As would be expected, use of the same antibodies on protein extracts analyzed by western blotting showed more intense bands for mid-wavelength opsin and cone arrestin compared to rat retina (Bobu et al., 2006). This high degree of antibody cross-reactivity between mouse, rat and *Arvicanthis* highlights another advantage due to the high degree of homology. Indeed we recently sequenced the entire genome of *Arvicanthis ansorgei* (transfer to public database underway), the overall level of homology being >98% to both mouse and rat. Additionally we have recently published the retinal transcriptome for this species (Liu et al., 2017) (see Figure 3 for comparative phylogenetic tree of selected retinal genes). Our hope is that it may serve the broader research community and provide a foundation for the use of *Arvicanthis sp*. as a model organism for future cellular and molecular investigations related to cone biology and retinal degeneration and for comparison to other common model organisms, including mice and rats.

We studied the regional distribution of short-wavelength cones by immunohistochemistry of flat-mounted whole retinas. This was not possible for mid-wavelength cones which are too numerous. There were no statistical differences between short wavelength cone density for any of the quadrants, but overall cone density diminished from the centre and mid-periphery (average of ~40 cones/2250µ2 field) towards the far periphery (average ~14 cones/2250µ2 field) (Bobu et al., 2006). Roughly similar findings were subsequently reported for *A. niloticus*, although they observed peak densities in the dorso-temporal central retina whereas *A. ansorgei* had highest densities in the ventro-temporal area

(Gaillard et al., 2009). Like these authors, partial sequencing of *A. ansorgei* short wavelength opsin showed it to be ultraviolet sensitive (unpublished data). Functional visual recordings were performed in *A. niloticus*, where in keeping with the high cone numbers it was seen that pure cone ERG a wave amplitudes were ~5 times higher than rats or mice, and flicker fusion occurred >60 Hz (Gilmour et al., 2008). We saw comparable characteristics in *A. ansorgei* (Boudard et al., 2010, 2011), and noted the lower sensitivity compared to mice recorded under dim light cotopic conditions, predicted from the lower rod numbers (Figure 4). These and other functional visual features are more similar to human visual physiology than are those of mice and rats, underlining the potential usefulness of *Arvicanthis* to modelling human retinal pathophysiology.

This rod-cone configuration prompted us to examine the issue of photoreceptor phagocytosis by the retinal pigmented epithelium (RPE). Due to their elevated metabolic activity and vulnerability to oxidative stress, photoreceptors undergo large scale membrane turnover whereby the distal-most portions of the outer segments (OS) are engulfed and ingested by the adjacent RPE, which recycles many of the membrane components for re-use by the photoreceptors. Extensive data have been gathered concerning the chain of events linking OS shedding and their subsequent internalization by the RPE. Initially, OS bind to the RPE apical surface, triggering activation of an intracellular second-messenger cascade, which in turn activates the ingestion of bound OS. Binding of OS requires the activation of αVβ5-integrin receptors, which interact with MerTK via the focal adhesion kinase (FAK) signaling pathway (Feng et al., 2002; Finnemann, 2003). In brief, OS binding to αVβ5-integrin receptors activates FAK, which in turn phosphorylates MerTK, leading to phosphorylation and activation of the second messenger cascade (Finnemann and Nandrot, 2006; Mao and Finnemann, 2012; Nandrot et al., 2012; Ruggiero et al., 2012). But it should be stressed that these data pertain only to rod phagocytosis, and it is currently unknown whether the same molecular machinery is involved in cone internalisation. Especially given that in many mammalian species cone OS do not contact directly the RPE apical surface, but their shed membranes appear to be shuttled towards the RPE within microdomains or require specific expansions of the RPE (Steinberg et al., 1977; Anderson

et al., 1978). Be that as it may, the critical importance of regulated photoreceptor turnover is shown by the fact that perturbation in the phagocytosis pathway leads to retinal degeneration, as observed in the RCS rat (Mullen and LaVail, 1976; D'Cruz et al., 2000) and a subset of patients with retinitis pigmentosa (Gal et al., 2000).

Photoreceptor phagocytosis is under circadian control, with phagocytic activity showing robust rhythmic profiles during the 24 hour period (LaVail, 1980). In all nocturnal and diurnal vertebrates examined, both cold- and warm-blooded, rod OS uptake occurs maximally shortly after light onset. In rats, this daily rhythm is established by 2 weeks of age and is irrespective of the lighting conditions during development (Tamai and Chader, 1979). It persists for up to 14 days in constant darkness (LaVail, 1980) and is independent from the brain's biological clock since it is maintained after optic nerve section or destruction of the suprachiasmatic nucleus (Terman et al., 1993). Pioneering work by R.W. Young in western fence lizards (Young, 1977) and chickens (Young, 1978), both species with strongly cone dominated retinas (~90%), showed a peak in cone phagocytosis shortly after light offset, and he proposed that rods and cones had phase-inverted profiles in accordance with their functional roles. However, the timing of cone shedding was subsequently seen to be more variable, since in many species (goldfish: O'Day and Young, 1979; western fence lizards: Young, 1977; chickens: Young, 1978; and eastern grey squirrels: Tabor et al., 1980) it occurs during early-middle night time, whereas in rhesus monkeys (Anderson et al., 1980), tree shrews (Immel and Fisher, 1985) and cats (Fisher et al., 1983) rod and cone OS shedding both occur concomitantly just after light onset.

This latter scenario was also true for *Arvicanthis*, which showed a large discrete peak in immunopositive phagosome numbers 1 hour after light onset for both rods and cones (Figure 5). The peak activity for rods was 30-40 fold higher than in retinas examined at the end of the day, whereas cone phagosome numbers were some 20-30 higher than those seen in early night. Also of note, rod activity was ten times higher than that of cones, which indicates that even adjusting for the rod: cone ratio of ~2:1, rod OS turnover exceeds that for cones.

2.3. Effects of excessive light exposure and pharmacological treatment on retinas in *Arvicanthis*

These original data were obtained from animals maintained in a standard 12 hour light/12 hour dark (LD) cycle. To examine light-induced and circadian effects on phagocytosis profiles, we performed similar studies on animals maintained under different lighting conditions. In conditions of constant darkness (DD), the overall profile was very similar and a robust peak continued to be observed in retinas isolated at circadian time 1 (corresponding to 1 hour after expected light onset in the subjective daytime). Indeed the absolute numbers of phagosomes were even higher than in standard LD cyclic light (Figure 5). In addition, the presence of a smaller but statistically significant secondary peak was seen during the subjective night (Bobu and Hicks, 2009). Although there was also a tendency (not statistically significant) for this secondary peak in LD-raised animals it was much greater in animals in DD, perhaps an equivalent response to behavioural negative masking. By contrast, animals subjected to a single 24 hour period of constant moderate light (LL) (~300 lux measured at the level of the cages) showed a completely scrambled phagocytic activity, with no discernible peak at any time (Figure 5). Even more pronounced, absolute numbers of cone, but not rod, phagosomes increased by 250% compared to LD (Bobu and Hicks, 2009). Since these latter features suggested that phagocytosis (especially that of cones) was highly perturbed by LL, and with the knowledge that correct phagocytic regulation is critical for retinal health, we examined the effects of more extended (7 days of continuous moderate intensity white light) lighting on *A. ansorgei* retinas. As opposed to the acute effects, one week of LL led to strong down-regulation of both rod (80%) and cone (50%) phagosome counts respectively (Mehdi and Hicks, 2010), possibly in parallel with down regulation of *de novo* disc formation to maintain OS integrity. Analysis of retinal structure (cell numbers, OS length) and phenotype showed no deleterious changes. Thus it seems that there are protective responses triggered by excessive light exposure, but they require more than one night to be activated.

This protective response was further studied by exposing animals to lighting conditions reported in the literature to lead to photoreceptor damage. There is a long history of using mice and rats in light damage (phototoxicity) experiments as a model system for studying retinal degeneration

in humans (reviewed in Wenzel et al., 2005; Organisciak and Vaughan, 2010; De Vera Mudry et al., 2013; van Norren and Vos, 2016). Light damage is typically confined to rod photoreceptors and retinal cell loss is largely restricted to the ONL. Retinal light damage is a graded response, with areas containing little or no damage adjacent to more severely affected regions. Many studies have reported light-induced cell loss to be less in the inferior compared to the superior hemisphere, which may be related to a number of factors including the angle of light exposure. Light damage to the retina has been documented extensively during the past five decades, ever since Noell et al. 1966 showed that relatively low intensity illumination led to photoreceptor degeneration in albino rats. Early studies by Noell et al. (1966), Kaitz and Auerbach (1979), and Williams and Howell (1983) all pointed to rhodopsin bleaching as the trigger for retinal light damage. Both rhodopsin and RPE65 knockout mice are protected against light damage. Studies have shown the critical importance of rhodopsin regeneration rates within the visual cycle: protection against light damage is seen in mice strains expressing polymorphic variants of RPE65 in which rhodopsin regenerates less rapidly, and slowing rhodopsin regeneration with 13-cis retinoic acid prevents light damage in the rat. Noell et al., 1966 also measured the first action spectrum of light damage in rat, which turned out to be identical to the absorption spectrum of rhodopsin. However, Ham et al. (1976, 1982) found a quite different spectrum in monkeys, peaking at short wavelengths. The latter spectrum, but not the former, was confirmed in numerous subsequent publications with animal models including rat, and gave rise to the idea of a blue light hazard in humans. These numerous studies showed that nocturnal mammals like mice and rats, especially albino strains such as Balb/C and Wistar respectively, were extremely vulnerable to light exposure. Indeed a consistent finding in both rodents and primates is differential vulnerability between diurnal and nocturnal retinas. Our analyses of *Arvicanthis* retinas falls clearly within this scenario, since animals were extremely resistant to white light exposure: despite testing multiple conditions of intensity, duration, timing and light history, there was little or no damage on either tissue structure, phenotypic expression or functional light sensitivity (Figure 6). The most extreme condition we tried involved blue light at a corneal irradiance of 30mW/cm^2, fed directly onto

the eye by optic fibre lamp: whereas there was no structural difference after 5 or 15 minutes of exposure, 45 minutes of intense blue light led to a focused spot of complete tissue collapse, more in keeping with thermochemical damage than photochemical because the entire retina was affected. Although structural damage after 45 minutes was confined to a narrow spot, a more generalized response was evident since glial fibrillar acidic protein (GFAP) immunostaining, often used as a marker of cellular stress in the retina, was up-regulated across the entire retina (Figure 7).

The relative resistance of diurnal retinas is likely due to multiple factors that may either operate less robustly in nocturnal retinas, or may be absent from them altogether. One reason may be due to the inverted chromatin architecture in nocturnal species increasing photon capture per rod cell compared to that of the rods of diurnal species (Solovei et al., 2009). Thus, outer segments (OS) of nocturnal animals may simply collect more light energy from incident radiation, particularly at low light intensities. By having a lower quantum catch, diurnal rods would be less vulnerable to damage and less able to exert a bystander effect on cones, whereas the capture of photons in nocturnal rods would enhance the likelihood of rod and cone damage. Indeed, mouse rods exhibit specific defects (compared to other cell populations in the mouse retina, including cones) in double strand DNA repair mechanisms when irradiated (Frohns et al., 2014), and similar defects may occur in single strand DNA breaks occurring in light-induced cytotoxic insults. On the other hand, resistance could be mediated by endogenous neuroprotective mechanisms activated in diurnal retinas which are regularly exposed to potentially harmful radiation under natural conditions. To see whether this high degree of resistance was specific to intense light or a more general feature, we also explored photoreceptor degeneration using another commonly used experimental paradigm, injection of N-methylnitrosourea (MNU), an alkylating agent which induces DNA strand breaks and has been reported to lead to rapid and complete loss of photoreceptors in a variety of nocturnal mammals (mice, rats and hamsters) (Yuge et al., 1996; Taomoto et al., 1998; Yoshizawa et al., 1999). Injection of MNU at doses shown to eliminate rod photoreceptors in mice (75 mg/kg body weight), had no visible effect on *Arvicanthis*, even after 2 months post-injection. Parallel studies performed in our laboratory using pigmented Long

Evans rats confirmed that this dose was rapidly (by 9 days post-injection) and completely effective in destroying rod photoreceptors (Boudard et al., 2009). We thus injected *A. ansorgei* with more concentrated doses (100 and 150 mg/kg body weight). Even under these more extreme conditions photoreceptor degeneration was slow (no statistical difference between control saline-injected and MNU-injected animals before 20 days) and only partial (even 3 months after injection, degeneration was marked within the superior hemisphere while the inferior hemisphere was intact) (Boudard et al., 2010) (Figure 8). This regional difference is often observed in light damage studies in other species, although the reasons are not clear. It may indicate that the MNU-injected *Arvicanthis* underwent additive light damage once the retina was weakened by MNU-induced cytotoxic stress. Intriguingly then, photoreceptor resistance in *Arvicanthis* is not restricted to light damage, neither it is restricted to cones since rods also demonstrated heightened resistance within the inferior retina. Extreme resistance against light damage has been seen in other diurnal species [eastern grey squirrel: Collier et al. (1989), but in this case resistance to drug-induced aggression is unknown].

2.4. Retinal circadian clock and effects of evening light exposure in *Arvicanthis*

As mentioned in the introduction, in mammals the retina represents the only entrance for solar light information to reach the central circadian clock in the SCN (in contrast to other vertebrate and invertebrate groups in which additional light sensitive organs such as the pineal gland or ocelli exist). Eye physiology is also itself subject to circadian regulation, which adapts vision to the alternating day-night cycle (i.e., high and low light intensities), and also modulates the capacity of the retina to signal to the circadian system (Felder-Schmittbuhl et al., 2018). In mammals, the retina was actually the first tissue described outside of the SCN to display circadian clock properties, based on its capacity to synthesize and release melatonin *in vitro* with a ~24 hour rhythm (Tosini and Menaker, 1996). This observation triggered extensive analysis of retinal physiology over the 24 hour cycle, and many molecular and cellular processes are now known to be controlled of a molecular clock or clocks (McMahon et al., 2014; Felder-Schmittbuhl et al., 2018). These activities include the daily expression of photopigments (Von Schantz et al., 1999; Bobu et al., 2013); visual sensitivity, as reflected in ERG by

the amplitude of the photopic b-wave (Barnard et al., 2006; Storch et al., 2007; Ait-Hmyed et al., 2016); rhythms in shedding of rod and cone OS and phagocytosis by the underlying RPE (LaVail, 1980; Bobu and Hicks, 2009); and the vulnerability to phototoxicity (Organisciak et al., 2000) (discussed above). The molecular organisation of the endogenous retinal circadian clock(s) has been quite well studied, and has already been the subject of previous reviews (McMahon et al., 2014; Besharse and McMahon, 2016; Ko, 2018). The basic layout resembles that of the SCN, but there is some controversy concerning certain features (see below). This molecular time-keeping system is generated by interlocking transcriptional-translational feedback loops (Figure 9) (Takahashi, 2017). The clock core loop involves the activator proteins complex CLOCK-BMAL1 (or NPAS2-BMAL1) which binds to E-box sequences in the promoters of the repressor genes Period (Per) 1–3 and Cryptochrome (Cry) 1–2 to induce their transcription. PER proteins form complexes with CRY proteins, undergo phosphorylation by casein kinase CK1ε/δ within the cytoplasm and are then translocated back to the nucleus to repress the transcriptional activity of the CLOCK-BMAL1 complex, thereby repressing their own transcription. In addition, the CLOCK-BMAL1 complex activates the Ror and RevErb nuclear receptor genes also via the E-box enhancers. The ROR and REVERB proteins compete at the retinoic acid-related orphan receptor binding elements (RORE) sites to either activate or repress Bmal1 transcription respectively. These interlocking feedback loops build a network of rhythmic clock genes and clock-controlled genes in which expression patterns are finely shaped by post-translational processes such as proteasomal degradation, ubiquitination, sumoylation, phosphorylation and acetylation in order to set the phase coherence of cellular and tissue functions over a 24 hour cycle. The multiple cellular populations in the retina may blur whole tissue studies of circadian rhythms, since different types may present different phase relationships which would be lost during averaging. This may explain why a recent study on non-human primate retina did not observe clock gene rhythmicity, whereas overall weak rhythmicity has been previously reported in several studies in rodents (Peirson et al., 2006; Storch et al., 2007; Ruan et al., 2008; Sandu et al., 2011; Mure et al., 2018). *Ex vivo* studies of clock gene expression have demonstrated rhythms in photoreceptor layers in

some studies (Sandu et al., 2011; Dhkissi-Benyahya et al., 2013), and in the inner nuclear layer (INL) in others (Ruan et al., 2006). Nevertheless, specific ablation of the Bmal1 core clock gene in the retina leads to abnormal retinal transcriptional responses to light (Storch et al., 2007), while in retinal explants Per1 (but not Per2 and Per3), Cry1 (but not Cry2), and Clock are necessary for sustained circadian rhythms (Ruan et al., 2012; Wong et al., 2018).

Single cell PCR and immunohistochemistry studies show broad expression of core clock proteins in retinal cells: CLOCK, BMAL1, NPAS2, PER1, PER2, and CRY2 are all expressed in retinal ganglion cells (RGC), amacrine cells, bipolar cells, horizontal cells and cones, but not in rods (Ruan et al., 2006). Clear diurnal and circadian rhythms were observed only in mouse cones (Liu et al., 2012) suggesting that cones and not rods are cell autonomous circadian clocks (Ruan et al., 2006; Liu et al., 2012). If rods are not strong oscillators, the weak overall amplitude in whole retinal clock rhythms in mice and rats may stem from their rod-dominated structure. We observed stronger rhythms of identified clock genes seen in *Arvicanthis* retina: whereas in whole rat retina the difference in arbitrary units of expression of the core clock genes Bmal1, Per1, Per2 and Cry1 between the peak and the trough is ~0.2, 0.25, 0.9 and 0.5 fold respectively (Sandu et al., 2011), values for the same genes in whole *A. ansorgei* retina are ~4, 7, 4 and 6 fold respectively (Bobu et al., 2013), around 20 times higher. Since the major difference between the two retinas is the proportion of cones (0.9% in rats: Szel and Rohlich, 1992; 33% in *Arvicanthis*: Bobu et al., 2006), perhaps this increased amplitude is an indirect reflection of this. Since data on clock gene expression profiles in diurnal mammals are very limited, we dissected retinas from *Arvicanthis* at different time points during a standard LD cycle (12 hour light/12 hour dark), and also under conditions of DD and LL as for the phagocytosis experiments. These retinas were used to analyze expression levels of circadian clock genes across the 24 hour period by real-time PCR. The results showed that under standard LD cycles there was a robust rhythm for almost all genes, exhibiting a peak at or close to the night/day transition boundary (Figure 10). Under conditions of DD, although there was some dampening of the amplitudes, basic profiles were unchanged. However, as with photoreceptor phagocytosis, a single night of moderate intensity LL led

to widespread changes in clock gene expression, with the peaks being shifted between 4 to 10 hours relative to those seen under LD cycles (Bobu et al., 2013) (Figure 10). We performed similar analyses of key clock output genes in the retina, especially those involved in phototransduction and retinal physiology. As for the clock genes, rhodopsin and both short- and mid-wavelength cone opsins, showed high amplitude robust cyclic behaviour under conditions of both LD and DD. These were greatly perturbed by LL, now peaking in the middle of the subjective night period. In summary, use of a diurnal rodent has enabled us to show that exposure to artificial light at night provokes numerous dramatic changes in retinal clock gene expression, output of key phototransduction genes, and phagocytic regulation. It remains to be seen whether these changes may lead to long-term decline in retinal health or function (apparently not the case for cones at least after a week of exposure), or whether such processes may be operating in humans.

2.5. Intrinsically photosensitive retinal ganglion cells in *Arvicanthis*

In addition to the important role(s) of the endogenous retinal circadian clock, the mammalian retina also constitutes the unique pathway for light information to reach the brain and synchronize the central clock in the SCN with solar time. This information is carried by the intrinsically photosensitive retinal ganglion cells (ipRGCs), discovered around 20 years ago (Provencio et al., 2002; Panda et al., 2002; Hattar et al., 2002). This special sub-class of RGC expresses a novel visual pigment, melanopsin, which conveys upon them the ability to directly detect and transduce light, although they also receive synaptic input from upstream rod- and cone-driven pathways similar to conventional RGCs (Hattar et al., 2003). Practically all experimental data come from nocturnal mice and rats, and hence it was valuable to characterize this population in a diurnal mammal. Using multi-electrode array set-ups to record from explanted newborn *A. ansorgei* retinas stimulated by LED light flashes of 505±30 nm, we described three physiological sub-classes of ipRGCs (type I, II and III) as was described for mice (Tu et al., 2005), distinguished by their light sensitivity, response strength, latency and duration (Figure 11) (Karnas et al., 2013a). Type I cells (20%) were the most sensitive, with very short latencies to activity onset, high spike rates and prolonged response durations, characteristics which correspond most

closely to mouse type III cells (Tu et al., 2005). *Arvicanthis* type II ipRGCs were the most frequent sub-type (59%), characterized by intermediate latencies and durations with spike rates and response durations lower than in *Arvicanthis* type I cells. This population most closely resembles mouse type I cells. Finally, type III (21%) showed low photosensitivity, very long latencies and short response durations, features resembling mouse type II ipRGCs (Tu et al., 2005). A surprising result was that type I cells in *Arvicanthis* displayed a remarkably high sensitivity to brief light flashes, with robust responses to pulses as short as 10 msec, not seen in parallel recordings from mouse retinas (Karnas et al., 2013a) (Figure 11). In fact for all flash durations, *Arvicanthis* type I ipRGCs showed more prolonged and robust responses compared to identical recording conditions in mouse retinas, as did the type II and III subtypes for longer light pulses. It has been shown widely that mouse ipRGCs respond only sluggishly to light stimulation and are relatively insensitive to brief light pulses (Nelson and Takahashi, 1991; Van den Pol et al., 1998; Berson et al., 2002; Berson, 2003), leading to the proposal that this matches well with their function of measuring ambient light levels, as it would filter out potentially conflicting information such as lightning flashes. The *Arvicanthis* data, at least at the single cell level, stand in apparent contradiction to such a hypothesis, especially as one might imagine the system should be even less light sensitive in a diurnal species. However the observation is in agreement with the described ability of ipRGCs to detect single-photon absorption (Do et al., 2009), or that downstream integration of repetitive millisecond light exposures is effective at phase-shifting the circadian clock (van den Pol et al., 1998 ; Zeitzer et al., 2011). Only type I ipRGC responded to very short flashes (10 and 50 ms), adding a new feature to their description as the most sensitive ipRGC type. Moreover, it indicates an extremely large range of ipRGC light sensitivity, showing responses to millisecond flashes up to many hours of illumination (Wong, 2012). A further difference compared to the mouse retina was the relative proportions of M1 and M2 sub-types of ipRGCs: whereas these are roughly similar in the mouse (estimated by our immunohistochemical studies as 44% M1 and 50% M2 – Karnas et al., 2013b), in *Arvicanthis* M1 constituted 74% and M2 25%. Another study using *A. niloticus* revealed that M1 (of which 25% were displaced to the INL) and M3 together accounted for 94% of total ipRGC, with

the M2 sub-type representing only 6%) (Langel et al., 2015). Another diurnal rodent, the Mongolian gerbil (*Meriones unguiculatus*) also had an extreme M1/M2 ratio, with >95% M1 and no detectable M2 ipRGC (Jeong and Jeon, 2015). These data tentatively point to a dominant role for M1 ipRGCs in diurnal rodents, with a correspondingly very strong input to the SCN.

In the mouse, M1 ipRGCs project to brain regions involved in circadian behaviour, principally the SCN, the intergeniculate leaflet (IGL) and the ventral lateral geniculate nucleus (vLGN), but also to the shell of the olivary pretectal nucleus (OPTN) for mediation of the pupillary light reflex (Hattar et al., 2006). These different innervation patterns possibly originate from molecularly distinct sub-populations of M1 ipRGCs, where Brn3b-negative M1 ipRGCs innervate the SCN and part of the intergeniculate leaflet and Brn3b-positive ipRGCs innervate other targets in the brain including the OPTN (Chen et al., 2011). In mice the innervation pattern of non-M1 (mainly M2 on a numerical basis) types shares some central targets with the M1 type, including the SCN and OPTN (Baver et al., 2008; Hattar et al., 2006), but there is also innervation of the dorsal LGN and superior colliculus which represent retinotopically organized nuclei mediating object localization and discrimination (Brown et al., 2010; Ecker et al., 2010). Anterograde tracing studies in *A. niloticus* using cholera B toxin showed reduced ipRGC innervation of the ventral subparaventricular zone (vSPV) compared to nocturnal rats (Todd et al., 2012), although the projection sites of ipRGC subtypes remain unknown. They reported that a robust retina-to-vSPVZ projection develops in rats around the end of the second postnatal week, coincident with the emergence of nocturnal wakefulness and a pattern of neuronal activity in-phase with the SCN. In *A. niloticus*, however, such a projection does not develop and the emergence of an anti-phase pattern between the vSPV and the SCN during the second postnatal week is accompanied by increased diurnal wakefulness. Furthermore, Novak et al. (2000) and Schwartz et al. (2011) used neuronal tracing techniques to reveal that distribution patterns of SCN and vSPV efferents were highly conserved in diurnal *A. niloticus* and nocturnal rats. Labeled fibres originating in each region were heavily concentrated in the medial preoptic area (mPO), PV thalamic nucleus, the SPV zone, and the hypothalamic PV and dorsomedial nuclei. Labeled fibres from the SCN and vSPVZ

formed appositions with orexin neurons and gonadotropin-releasing hormone neurons, two cell populations whose rhythms in c-fos expression illustrate temporally reversed patterns of locomotor and reproductive behaviour in diurnal and nocturnal rodents. Thus vSPV zone projections may modulate the responsiveness of target cells to signals from the SCN. An older study using *A. niloticus* showed only weak innervation of the ventrolateral preoptic (vlPO) zone, a region known to be involved in sleep (Novak et al., 1999). Using c-fos immunohistochemistry as a marker of neuronal activation they concluded that the vlPO may function similarly in *A. niloticus* and rats – modulating the onset and maintenance of slow wave sleep. In a more recent study, central projections of *A. niloticus* ipRGCs were seen in the SCN, LGN, pretectum, and superior colliculus, although the vLGN and dLGN and caudal OPTN received less innervation from ipRGCs compared to nocturnal rodents. Finally, direct retinal projections to the IGL have also been reported in *A. niloticus* (Smale and Boverhof, 1999; Gaillard et al., 2013), and bilateral IGL lesioning led to remarkable changes in masking behaviour depending on the phase: light pulses during the night increased activity in control animals but decreased it in animals with IGL lesions; whereas dark pulses had no effect on controls, but significantly increased activity in lesioned animals in the day (Gall et al., 2013). Lesions also significantly increased activity, primarily during the dark phase of a standard LD cycle, and during the subjective night when animals were kept in constant conditions. These results suggest that the IGL plays a vital role in the maintenance of species-specific masking responses to light, as well as the circadian contribution to diurnality in grass rats.

In summary, studies on *Arvicanthis* ipRGCs and their central projection sites show an overall resemblance to those reported in mice and rat retinas, but with notable differences in both phenotype (M1/M2 ratios), physiology (light sensitivity) and innervation (vSPV, VLPO and LGN). Along with the strong cone component of light information delivered to the brain, the heterogeneity of ipRGC central projections might suggest different functions in non-visual photoreception which could influence temporal niche switching. *Arvicanthis* represents an interesting animal model to compare

how light, circadian, and homeostatic influences combine to affect sleep differently in diurnal and nocturnal species.

2.6. Retinal endocrinology and *Arvicanthis*

Of the potential messengers/outputs of the circadian network, melatonin is by far the best characterized (Pevet and Challet, 2011). This indolamine was discovered over 50 years ago, and as a prominent output of the central circadian clock it modulates a wide array of physiological functions such as the sleep/wake cycle (Burke et al., 2013), reproduction (Barrett and Bolborea, 2012) and immune modulation (Sande et al., 2008). Principally secreted by the pineal gland during the night time, this neurohormone is rapidly taken up by the bloodstream where it reaches many peripheral organs. It also diffuses throughout the central nervous system where it acts through two high affinity adenylate cyclase-coupled membrane receptors, MT1 and MT2 (Klosen et al., 2019). Its secretion by the pineal gland is under circadian control, since rhythmic synthesis continues in constant darkness, but exposure to light at night suppresses melatonin through a direct pathway. This inhibition is thought to be one of the ways that artificial light at night can affect metabolism and health, as well as short-term sleep difficulties. For the purposes of the present review, the second main source of melatonin synthesis is the retina, where it was shown to also be under rhythmic control by an endogenous clock since explanted retinas continued to secrete melatonin during the (subjective) night periods and also could be re-entrained by new light/dark cycles (Tosini and Menaker, 1996). Melatonin can exert local effects on photoreceptor phagocytosis (Besharse and Dunis, 1983; White and Fisher, 1989; Laurent et al., 2017), neuronal electrical activity (Baba et al., 2009; Sengupta et al., 2011), dark adaptation (Wiechmann et al., 2003) and light sensitivity (Baba et al., 2013), by way of MT1 and MT2 receptors expressed in the eye (Alarma-Estrany and Pintor, 2007; Wiechmann and Summers, 2008). In nocturnal rodents MT1 receptors have been localized in photoreceptors, inner nuclear layer (INL), and retinal ganglion cells (RGCs) (Sengupta et al., 2011; Gianesini et al., 2015), although recent investigations using genetically engineered mice containing LacZ reporter gene under control of the MT1 promoter showed a much more restricted distribution, very faint in the OS and

only scattered cells in the INL and ganglion cell layer (GCL) (Klosen et al., 2019). Furthermore, melatonin-proficient mice that lack MT1 display reduced viability of rods and RGC (Baba et al., 2009) as well as cones (Gianesini et al., 2016) during aging, and show altered phagocytic profiles leading to increased accumulation of lipofuscin in the RPE (Laurent et al., 2017). The available evidence shows that melatonin synthesis in nocturnal rodent retinas shares many classical features with that of the pineal gland, such as the biochemical substrates (tryptophan and serotonin) and enzymatic machinery (notably the terminal enzymes in the synthetic pathway, arylalkylamine Nacetyltransferase [AA-NAT] and hydroxyindole-O-methyl-transferase [HIOMT]). Scattered reports indicate it is synthesized within a sub-population of photoreceptors, seemingly cones (Niki et al., 1998), although others have shown a more widespread distribution across all layers (Liu et al., 2004). But the published data are fragmentary and there had been no comprehensive studies of the cellular sites of retinal melatonin synthesis, rhythmic expression profile and receptor distribution in a single species, especially in mammals. Because of earlier reports indicating that the enzymes involved in melatonin synthesis were detected in cones (Niki et al., 1998), we reasoned that *Arvicanthis* with its high cone complement would be a good experimental model.

Since melatonin itself is very labile and diffuses rapidly from its site of synthesis, we first examined the expression of AA-NAT and HIOMT mRNA by non-radioactive in situ hybridization and AANAT protein by immunohistochemistry and western blotting. Because previous publications for nocturnal rodents reported a nocturnal peak in AA-NAT mRNA levels, we first examined retinal sections prepared at ZT19 (corresponding to midnight). Staining was observed specifically within the 2 scleral-most rows of cells in the ONL, corresponding to cones (Figure 12), with no detectable signal elsewhere in the retina, neither rods nor inner layers. By contrast, in the middle of the day (ZT6), hybridisation signal was no longer apparent in the cones but was now detected strongly in the GCL (Figure 12). When we performed an entire series of *in situ* hybridization studies across the 24 hour period under standard LD cycles, it was seen that expression within the cones was faint or undetectable throughout the day but intense during the night; and expression in the GCL was

moderate to strong during the day but below detection levels at night. Thus these two sites of expression are in phase opposition, cone AA-NAT peaking in the night as seen in the pineal gland, and GCL AA-NAT peaking in the day. Melatonin expression in RGC during the day has been previously reported in fish (Falcon et al., 2010) and birds (Garbarino-Pico et al., 2004; Contin et al., 2006), though it was not known previously in mammals. Given the relative proportions of cones and RGC, contributions from the former type predominate. Unexpectedly, AA-NAT protein, as seen by western blotting using two different specific antisera, was present also largely throughout the day except for the early morning. Furthermore, AA-NAT activity was present during both day and night periods, although somewhat higher at night (Gianesini et al., 2015). This indicates that in *Arvicanthis* the AA-NAT protein is not rapidly degraded in light as has been shown in chickens (Iuvone et al., 2002; Pozdeyev et al., 2006), and opens the question as to the regulation of the melatonin synthetic pathway in diurnal rodents. HIOMT, the terminal enzyme actually responsible for converting N-acetyl serotonin into melatonin, was expressed at very low levels across the 24 hour period, which was consistent with the low levels of melatonin detected by RIA compared with other vertebrate species. This is another puzzling result, since if cones are a major source of retinal melatonin then one would expect its concentration to be higher in *Arvicanthis* compared to cone-poor nocturnal species: in fact we observed the contrary, with rats containing far greater levels (do Carmo Buonfiglio et al., 2011). These data reveal the complexity of the melatonin signalling system in retina, where it may influence processes in the outer retina (phagocytosis, cell survival, light sensitivity) and inner retina (cell survival), potentially deriving from the two opposing cellular sources. The picture is further complicated by the possibility that the melatonin precursor N-acetyl serotonin acts as a neuromodulator in its own right (Tosini et al., 2012), capable of acting as a ligand for trkB receptors (Jang et al., 2010).

3. Fat Sand Rat (*Psammomys obesus*)

3.1. General features

Although widely known as the Fat Sand Rat, *Psammomys* is in fact a gerbil, first described by P. Cretzschmar in 1828. It is a rodent from the sub-family *Gerbillinae* and lives across North African and Middle East regions, in semi-arid, desertic areas from Morocco to the east of Arabia (Osborn and Helmy, 1980). When maintained under laboratory conditions with *ad libitum* access to food (rat chow), a large proportion of the animals become overweight and insulin resistant (Schmidt-Nielsen, 1964). Diabetic features spanned from mild hyperglycaemia with hyperinsulinemia, to individuals advancing to a terminal stage with combined hypoinsulinemia and ketoacidosis (Haines et al., 1965). These characteristics led to it becoming of great interest to researchers as a novel animal model of type 2 diabetes-like (T2D) induced by nutritional manipulation.

3.2. Induction of diabetes in *P. obesus*

Animals in the wild are herbivorous, eating a low digestible energy (LE) (1.92 kcal/g), electrolyte-rich saltbush (*Atriplex halimus*). When fed with a high digestible energy diet (HE) in captivity, a proportion of the animals develop a metabolic syndrome that resembles human T2D. HE diet results in excess nutrient availability that enhances insulin secretion, reduction of the glucose-stimulated insulin secretion threshold (Pertusa et al., 2002) and rapid depletion of pancreatic insulin stores, correlating with the appearance of postprandial hyperglycemia (Nesher et al., 1999; Donath et al., 1999). Islets of newborn or adult *P. obesus* have no functional gene product of the homeodomain transcription factor *Ipf1/Pdx1* (Leibowitz et al., 2001), required by β-cells for efficient expression of insulin, glucose transporter 2, and prohormone convertases 1/3 and 2. A recent study sequenced the *P. obesus* genome and identified an unusual, extensive, and mutationally biased GC-rich genomic domain encompassing several functionally essential genes, including *Pdx1*. The sequence of *P. obesus* Pdx1 is grossly affected by GC-biased mutation, leading to the highest divergence observed for this gene across the entire Bilateria (Hargreaves et al., 2017).

Kalman et al. (1993) described two distinct lines of *P. obesus* with genotypic and phenotypic differences, the “Diabetic Prone” (DP) and “Diabetic Resistant” (DR). Animals from the DP line exert

hyperinsulinemia (non-fasted plasma insulin over 150 u/ml) after 7-28 days of being fed HE diet, followed by hyperglycemia (non-fasted glucose levels over 200 mg/dl) (Shafrir and Ziv, 1998; Shafrir et al., 2006). In DP strains, sensitivity to diabetes induction by HE diet increases from weaning, being maximal around 5 months of age (Ziv et al, 1999). The DR sub-strain is completely refractory to induction of diabetes. The difference is possibly due to the gene *beacon*, which is overexpressed in the hypothalamus of DP *P. obesus* compared to DR (Collier et al., 2000). The *beacon* gene product is involved in the regulation of energy balance (Walder et al., 2002).

Nevertheless, change in environment is also of importance. *P. obesus* shows diurnal activity patterns in the wild but when transferred to controlled laboratory conditions becomes nocturnal or arrhythmic (Barak and Kronfeld-Schor, 2013; Touati et al., 2018). Recent observations from the Kronfeld-Schor group, comparing diabetes development in *P. obesus* raised on HE diets and held in captivity either in cages outdoors (and hence following a natural LD cycle) or inside the laboratory, found that the latter developed diabetes while the former did not. This suggests that in addition to dietary factors, the change of environment with a concomitant loss of thermal and ecological cues and the dysregulation of daily rhythm contributes to the development of diabetes (Bilu et al., 2019).

3.3. Interest of *P. obesus* in retinal research

As stated previously, *P. obesus* is a diurnal species, at least in its natural habitat, and its retina resembles that of humans in several respects. They have larger eyes (~8 mm in diameter) compared to those of rats (4-5 mm) possibly increasing their visual capacities and facilitating experimental manipulations. Saidi et al. (2011a) showed that the retina has a typical stratified structure, with cones accounting for ~40% of total photoreceptor cells. Short and mid-wavelength cones are present in typical relative proportions (about 10% for the former and 90% for the latter). In addition, there is an interesting expression pattern at the level of horizontal cells: in addition to expressing classic horizontal cells markers such as calbindin and parvalbumin, they also exhibited highly unusual ones including occludin. This is expressed throughout the cell and does not appear to be localised in tight

junctions, where it is known as an integral component of tight junctions. In *P. obesus* retina it is possibly serving as a relay or sensor for signalling cascades, modulating barrier functions as suggested by Chiba et al. (2008). The importance of the cone system was later confirmed by functional electrophysiological measurements in *P. obesus* captured from the wild and maintained on LE saltbush diet. While scotopic electroretinogram (ERG) measurements are comparable between Wistar rats, humans and *P. obesus*, in photopic conditions the ERG measurements in *P. obesus* share several characteristics with human ERG responses, quite different to the rat (Dellaa et al., 2017a) (Figure 13). A strong, cone-driven retinal response is indicated by the photopic a-wave amplitude, very similar to that seen in humans and much higher than in rats. While the b-wave is significantly larger for *P. obesus* compared to both human and rat responses, the photopic b-/a- ratio is lower than in rats, and closer to the value for humans, showing another discrepancy with nocturnal rodents. Matsui et al. (1994) demonstrated that the value of the photopic b-/a- wave ratio can be used to follow changes in retinal ischemia due to central vein obstruction. Another striking feature shared by *P. obesus* and humans concerns the post b-wave photopic ERG responses: the i wave and the photopic negative response (PhNR) (Figure 13). Similar post b-wave events were also seen in another gerbil, *Meriones unguiculatus* (Yang et al., 2015), but not in nocturnal rodents (Rosolen et al., 2004), suggesting gerbils may represent a valuable group as animal models of human DR. Since these electrical variations are thought to derive at least in part from RGC activity (Rousseau et al., 1996; Viswanathan et al., 2001), and RGC degeneration has also been implicated in DR (Meyer-Rusenberg et al., 2007; Gastinger et al., 2008; Saidi et al., 2011b), this is yet one more salient feature in these species. The PhNR has been stated as useful in the evaluation of human disorders that involve retinal ischemia (Machida et al., 2004), such as DR. Other results from Dellaa et al (2017a) dealt with fast-flicker ERG and d-wave analysis (photopic OFF-response), showing additional physiological resemblances with human retina. Finally, fundus observations and fluorescent angiography show a pronounced *area centralis* or visual streak extending across the superior hemisphere close to the optic nerve head, from which major blood vessels are largely absent (Figure 14). Such vascular arrangements resemble the human macula.

Altogether, these results characterise the retina of *P. obesus* as that of a diurnal mammal, structurally and functionally closer to the central retina in humans than the retinas of mice or rats.

3.4. *P. obesus*, a model for studying multiple features of diabetic retinopathy

Diabetic retinopathy constitutes the main cause of vision loss for working-age persons in developed countries (Wong et al., 2006). Long considered as a microvascular complication of diabetes, nowadays it is regarded as a neurovascular disease, where abnormal visual function, such as decreased contrast sensitivity (Dosso et al., 1996), colour vision defects (Gregori et al., 2011; Roy et al., 1986; Yamamoto et al., 1996) and functional abnormalities (Kohzaki et al., 2008) actually precede clinically detectable signs of retinopathy, suggesting that vascular abnormalities are not the first events to occur in DR. Various mice and rat models have allowed to uncover molecular mechanisms operating during the pathogenesis of DR, but no animal model recapitulates all the neural and vascular complications associated with DR, especially the key feature of human PDR, retinal non-perfusion and pre-retinal neovascular stage, secondary to diabetes, possibly because of the short lifespan of the animals once the disease manifests. Some studies reported the presence of cataracts in *P. obesus* that become hyperglycemic and hyperinsulinemic under HE diet after 2-4 months, but not in the groups that are only hyperinsulinemic (Ulmansky et al., 1984; Kohler and Knospe, 1980; Hackel et al. 1965). Unpublished observations from our laboratory indicate the incidence of cataracts in a low proportion (<5%) of obese normoglycemic and normo-insulinemic animals (unpublished observations). Our original studies on the incidence of DR in *P. obesus* (Saidi et al., 2011b) were performed using animals captured in the Tunisian desert and subsequently maintained in captivity. After 7 months of HE diet, individuals displayed one of two phenotypes: they either became both obese (~2x body mass of controls) and hyperglycemic (OH) (~400 mg/dl glucose compared to <100 mg/dl in controls), or obese but remaining normoglycemic (ON), in approximately equal numbers. This recalls the DP and DR substrains previously mentioned. Control animals maintained on a halophilic plant diet remained lean and normoglycemic (LN). At the vascular level, blood vessels in OH animals displayed abnormal features like irregular width with constrictions and dilations, vascular sprouts with blind ends and

balloon-like swellings resembling microaneurysms (Figure 15). Furthermore, unlike the regular network of uniform capillaries in LN retinas, retinal digests from OH animals contained thin acellular non-functional capillaries, as seen in human DR (Mizutani et al., 1996). Very notably, blood vessels in LN samples were completely covered by pericytes while blood vessels from OH retinas were practically devoid of pericytes (Figure 15). Pericyte dropout represents the earliest detectable vascular change in animal models of DR and is a hallmark feature of human DR (Hammes et al., 2002). One of the most telltale signs of developing DR is a rise within the vitreous of pro-angiogenic, and a corresponding decrease in anti-angiogenic factors (Aiello et al., 1994; Ambati et al., 1997; Ogata et al., 2002). Vitreous levels of vascular endothelial cell growth factor (VEGF), a pro-angiogenic factor, and pigment epithelium derived growth factor (PEDF), an anti-angiogenic factor, showed huge imbalances in OH versus LN animals: VEGF concentrations were ~8x higher, and PEDF concentrations ~100x lower, leading to a VEGF/PEDF ratio some 300-fold different in OH compared to LN animals (Figure 16). Such conditions are reported to precede development of neovascularization. In addition, hyperproteinemia in the vitreous of OH animals indicate leakage of newly forming blood vessels. Many other characteristics of human DR were observed - most notably in line with the hypothesis that cone degeneration is a central feature in DR, large significant reductions in short- and mid-wavelength cone opsins are seen, whereas rhodopsin levels remain unaltered (Figure 17).

Hence these findings position *Psammomys obesus* as a potentially valuable animal model for investigating the cellular and molecular events involved in triggering and executing retinal damage. Together with recent functional data confirming the prominent role of cone malfunction in *P. obesus* and Shaw's gerbil *Meriones shawi* (Hammoum et al., 2017a, b; Dellaa et al., 2017, 2018, dealt with in more detail in sections 5.1 and 6.2), we believe these animals could be of tremendous value to the research community by not only mapping the temporal sequence and order of events preceding and including PDR, but also providing a non-genetically modified organism in which to screen potential therapies. Of added value, though not much is known about them, the ON group presents a potentially unique means to tease out genetic and metabolic differences related to obesity rather

than glucose imbalance. For example, retinal thinning is seen in OH and ON animals, and thus may be more linked to obesity than glucose mismanagement *per se*. This could be of critical importance given the fact that retinal thinning was retained as a consistent clinical feature in diabetic macula edema (Browning et al., 2008). The manner by which diabetes occurs in such animals, namely the natural adaptation to living on meagre resources becoming rapidly overwhelmed in the face of abundant nutrition known as the thrifty metabolism theory (Neel, 1962; Coleman, 1978), has obvious close parallels to the rise of T2D in humans.

4. 13-Lined Ground Squirrel (*Ictidomys tridecemlineatus*)

For in-depth overviews on the ground squirrel visual system, its response to retinal detachment, and retinal remodeling during hibernation, the readers are steered toward past reviews (Merriman et al., 2016; Van Hooser and Nelson, 2006). Ground squirrels have cone dominant retinas with around 90% of central photoreceptors being cones (Kryger et al., 1998), which make them an attractive model for studying cone photoreceptors and modeling associated diseases. The 13-Lined ground squirrel (13-LGS; Ictidomys tridecemlineatus, native to North America) is a promising diurnal rodent model for vision research because it can be reliably bred in captivity (Merriman et al., 2012). This species has emerged as the most prominent ground squirrel in the literature, so the following sections will provide an update on 13-LGS vision research.

4.1. Reversible cone deconstruction during hibernation

Nature presents many unique adaptations and evolved solutions to things that ail us humans. Hibernation is one such “model of nature” that we can use to learn more about cell survival during drastic metabolic inhibition. The 13-LGS is an annual obligate hibernator, and such physiological fluctuations are inevitably juxtaposed on visual system, which may be undesirable depending on the study. This ought to be utilized as a strength of the 13-LGS as a model in vision research. This seasonal adaptation can be triggered experimentally by housing these animals in a cold hibernaculum in autumn and winter months (Merriman et al., 2012), and accompanies drastic metabolic fluctuations

(Staples, 2016), transcriptomic remodeling (Luan et al. 2018), ischemia tolerance (Dave et al. 2012), and of particular interest and potential to cone disease, reversible deconstruction of cone structure. The later phenomenon was originally reported in the 70's with a pair of electron microscopy studies that revealed shortened (in some cases absent) cone outer segments and depleted inner segment mitochondria (Kuwabara, 1975; Reme and Young, 1977). Many of these initial observations of reversible cone deconstruction were recently replicated with comparative electron microscopy and noninvasive retinal imaging (Sajdak et al. 2018; Sajdak et al. 2019b). While hibernation is not disease, cone remodeling during hibernation offers natural, predictable, and readily reversible deconstruction of the subcellular components of cones. The resilience to damage after ischemia has not been directly studied in the context of the visual system, and offers additional avenues of fascinating and potentially valuable research in neuroprotection.

4.2. Ground squirrel potential in disease modeling

The 13-LGS was one of the few rodents selected for genome sequencing (Clark et al. 2016). This species' mitochondrial genome has been sequenced as well (Zhang et al. 2016). Thus, the 13-LGS is primed for transgenic modeling of retinal disease, especially in light of photoreceptor specific transcriptomics of this species potentially more relevant to primates than nocturnal mice and rats (Mustafi et al., 2016). A limitation overshading progress in developing a transgenic ground squirrel lines is that they naturally breed once a year; in the spring following hibernation (Merriman et al., 2012). Ou and colleagues recently took developed induced pluripotent stem cells (iPSC) from 13-LGS, which circumvents the need for in vivo genetic manipulation (Ou et al., 2018). In this work, they took advantage of the hibernation physiology of the 13-LGS to discover microtubule-associated proteins involved in cold tolerance. By pharmacologically targeting cellular pathways associated with microtubule cold-intolerance in rat and human neuronal iPSC lines, they demonstrated increased microtubule integrity at near-freezing temperatures (4°C). This work represents a novel and exciting start to uncovering neuroprotective mechanisms in the 13-LGS retina that can be translated to other species, and could have profound impact on stem cell applications in disease modeling across many

organ systems. Another core methodology for retinal research that remains in development is gene delivery to retinal cells. Treatments to retinal diseases may be slowed by a reliance on large animal models. Supplementary studies of the safety and efficacy of retinal cell targeting using rAAV vectors can be performed in 13-LGS as a potential avenue for pre-clinical therapies. For example, clinical trials aimed at treating inherited cone disorder have had mixed success, often requiring invasive sub-retinal placement of gene therapy material. Intravitreal injections are a less-invasive approach, and the challenges of targeting photoreceptors from the vitreous are being overcome (Reid et al., 2017; Boyd et al., 2016). Therefore, intraocular injections of recombinant adeno-associated viral vectors (rAAV) for the manipulation of cells may be one of the most promising avenues for creating 13-LGS models of retinal disease in the short term. Previous studies assessing rAAV-mediated overexpression of GFP in the 13-LGS retina following intravitreal administration have demonstrated cone bipolar cell transduction with rAAV encoding green fluorescent protein using capsid mutant vectors (Light et al., 2012). Optimizing gene delivery to retinal cells via intravitreal administration of rAAV is particularly important in the ground squirrel because they have a uniquely rapid photoreceptor degenerative response following retinal detachment (Fisher et al., 2005; Sakai et al., 2003). However, ground squirrels also have a uniquely attenuated glial cell response to these retinal detachments (Lewis et al., 2005; Linberg et al., 2002; Merriman et al., 2016). While a lack of gliosis and inflammatory response theoretically makes these animals more amenable to photoreceptor transduction with rAAV via subretinal injection, where glial scarring can impede transduction of gene delivery in other species (Hippert et al., 2016), the rapid and prolific photoreceptor death observed following retinal detachment contraindicates the use of subretinal injection for gene delivery in the ground squirrel (Fisher et al., 2005). While subretinal injections indeed have visual consequences, limited gliosis in response to retinal detachment may be a benefit of the ground squirrel model when developing ocular therapies delivered subretinally (Graca et al., 2018).

The 13-LGS continues to serve as an animal model to uncover cone mechanisms, including S-cone synapse recovery after insult (Beier et al., 2018). And now with the capability of longitudinal

non-invasive assessment of the retinal structures with in vivo retinal imaging (Sajdak et al., 2016; Sajdak et al., 2018), the 13-LGS has great potential to answer questions about human retinal disease. Differences in chromatic packing, lipid content, and transcriptomics of rods and cones accompanying an animals visual ecology is mounting evidence in support of diurnal animal models like the 13-LGS for translational relevance when studying retinal disease (Agbaga et al., 2018; Mustafi et al., 2016; Solovei et al., 2009, 2013).

5. Honorable mentions in diurnal animal models

Several prior reviews have examined various vertebrate models for vision research outside the rat and mouse mainstream, to which the reader is referred (Huber et al. 2010; Slijkerman et al, 2015; Kostic and Arsenijevic, 2016; Wisely et al., 2017). It is not our intention to repeat that work here. The three species described in detail above are not the only diurnal small mammals available to vision research. Many other rodents are available that may also prove useful as counterpoints to traditional nocturnal rodent models. Comparative anatomy of 18 species within the family *Rodentia* can provide a useful starting-point when pursuing such "non-traditional" rodent models (Fernandez and Dubielzig, 2013). In this final section, we briefly highlight a few additional rodents that have been active in retinal research.

5.1. Gerbils

In addition to *Psammomys*, a few other gerbil species have been investigated with regard to the visual system. Huber et al. (2010) have provided a thoughtful characterization of two species of gerbil, the pale gerbil (*Gerbillus perpallidus*, native to Egypt) and the Mongolian gerbil (*Meriones unguiculatus*, native to Inner Mongolia). Gerbils are appealing animal models due to possessing both increased regions of cone density (approximately 15% cones; M:S ratio of 4:1) and a vascular pattern that circumvents the *area centralis*, mimicking the situation seen in the human macula (as in *P. obesus*, see Figure 15). This retinal anatomy may prove critical for modeling retinal diseases like age-related macular degeneration and diabetic retinopathies as recently studied in *Meriones shawi*

(Hammoum et al., 2017a, 2017b, 2018). These latter papers also used a protocol similar to our original one for inducing diabetes by 3 or 7 month high calorie diets, and observed retinal thinning, reduced cone numbers and increased gliosis, consistent with human DR (Hammoum et al., 2017a, b). The same group also more recently published functional (ERG) and non-invasive imaging data (OCT) to show that diabetic individuals exhibit a number of pathological modifications, including significantly delayed scotopic and photopic ERG responses and decreases in scotopic and photopic a- and b-wave amplitudes at both time points. Immunohistochemical analyses detected decreased expression of glutamine synthetase, vesicular glutamate transporter 1 and synaptophysin. Overall the data show that in addition to *P. obesus*, *Meriones shawi* could represent another interesting model of DR. Gerbils also breed year-round, which makes the development of transgenic animal models feasible but largely unexplored. Due to the wide use of the Mongolian gerbil in auditory research (Keplinger et al., 2018), this species has the potential to more accurately model Usher's Syndrome, where mouse models often fail to demonstrate the retinal phenotype associated with this disorder (Williams, 2008). Extant vision literature also includes retinal anatomy, ERG, UV sensitivity, visual pathways and circadian rhythms. They are domesticated and available from established laboratory animal vendors (although the susceptibility to diabetes may be lost with selective in-breeding - see sections 3 and 6.2). Husbandry of these rodents is also documented (including a useful but inactive egerbil.com). While the Mongolian gerbil seems to be the most well characterized in this category, caution is advised when choosing a species strain, as some exhibit nocturnal behaviors (24% of the 29 studied in Refinetti 2006).

5.2. Degu (*Octodon degus*)

The common degu (*Octodon degus*) is another cone-rich rodent (approximately 30% cones; mid-wavelength: short wavelength ratio of 13:1) that can be bred in captivity. However, this species is exclusive to central Chile, and to our knowledge the only colony exists at the Universidad de Valparaiso. This institution has provided a wealth of knowledge pertaining to this species as an animal model for biomedical research and laboratory care (Ardiles et al., 2013; Palacios and Lee, 2013). Social

housing seems to be required for optimal health, but antagonistic behaviors are frequent, so they must be monitored to avoid serious injury. Visual spectral sensitivity, RGC function and retinal histology during ageing have been reported and nicely characterize this model for retinal research (Jacobs et al., 2003; Chavez et al. 2003; Szabadfi et al., 2015; Escobar et al., 2018). Owing to its long lifespan for a rodent (up to 7 years), the degu has also been a valuable model for sporadic Alzheimer's disease, and could therefore contribute to a growing area examining retinal biomarkers for this and other age-related cognitive impairments (Du et al., 2015). In addition, this animal model has a rich history of research in circadian biology (Vivanco et al., 2010a, b; Otalora et al., 2013). There is uncertainty in the true diurnality of this species as well, with more than half exhibiting nocturnal behavior (52% of the 25 studied in Refinetti 2006).

5.3. Miscellaneous murids

A single study has reported the retinal anatomy and phenotype in the Striped Desert Mouse *Lemniscomys barbarus*, which shares much of the same geographical distribution as *Arvicanthis ansorgei*. Similar to the latter, retinas in this diurnal rodent had a high proportion of cones (>30%) which were immunopositive for a number of cone-specific markers (Bobu et al., 2008). Discrete differences in binding of a panel of monoclonal anti-rhodopsin antibodies for which the exact epitopes are known indicate slight differences in the amino acid sequence of this visual pigment between *A. ansorgei* and *L. barbarus*.

6. Future Directions and Conclusions

Non-human mammalian research has been paramount in making many significant advances in understanding and combating debilitating and life-threatening diseases. Although there is a heavy reliance on standardized laboratory animal models, the mouse *Mus musculus* having a pre-eminent position because of the accumulated genetic knowledge, there is a place for species which can complement existing fields of investigation. There is a recognition in organizations funding eye research that cone-rich animal models are of priority interest – the Foundation Fighting Blindness/

National Eye Institute have for several years listed among their priority axes of Individual Investigator Research Awards: "Cell and Molecular Mechanisms of Retinal Disease (CMM): Applications that target the following areas are of particular interest: Develop and characterize cone-rich and/or non-rodent animal models for retinal degenerative disease (RDD) that are relevant to human RDD." This overview has laid out the areas that have been explored using particular cone-rich rodents, but it is clear much more could be done, especially in terms of retinal disease modelling. The diurnal nature of these animals should not be underestimated, as experimental data shows that their circadian organization is not a simple reversal of that seen in mice and rats but leads to differential responses to anxiety or stress for example (Ashkenazy et al., 2009; Flaisher-Grinberg et al., 2011; Yan et al., 2018). We will highlight some domains where use of diurnal rodents may further our understanding of underlying mechanisms and provide a means to test potential beneficial strategies.

6.1. Non-invasive imaging to study research models of retinal disease

The retina is a uniquely accessible neural tissue, but historically observing the retina was limited to gross ophthalmoscopy and histological assessment. Traditional methods of studying the retina when developing animal models, like immunohistochemistry and electron microscopy, require the animal to be euthanized—offering just a single time point for analysis. Recent technological advances allow direct *in vivo* visualization of retinal structures to examine layers and individual cell types. The ability to examine the same living retinal structures over time with advances in optical coherence tomography (OCT) and adaptive optics ophthalmoscopy has revolutionized how the retina is studied and is shaping the future of how retinal disease is detected, monitored and treated (Fujimoto and Swanson, 2016; Burns et al., 2019). When adaptive optics scanning light ophthalmoscopy (AOSLO) is applied to the cone-dominant 13-lined ground squirrel, for example, comparable structure of the human retina is observed (Figure 18). Small diurnal mammals like the 13-LGS and northern tree shrew are highly amenable to non-invasive retinal imaging (Sajdak et al., 2016; Sajdak et al., 2018; Abbott et al., 2009; Sajdak et al. 2019a). The northern tree shrew, while not a rodent, is a small mammal with a nearly cone-exclusive retina (>95% of photoreceptors are cones) and highly advanced visual

processing. These animals do not seem to develop anesthesia-induced cataracts, as seen in mice (Bermudez et al., 2011), allowing consistent visualization of the living retinal layers with OCT, and of their cone-rich photoreceptor mosaics and other retinal structures with AOSLO. Rather than actively fixating, small anesthetized animals can be rotated about the optical axis, and retinal landmarks can be utilized (i.e. pores of the optic nerve head and retinal vasculature) to return to the same retinal location for longitudinal assessment. Many questions exist about the sub-cellular origins of the structures we see during *in vivo* retinal imaging, or which visible biomarkers indicate proper function or disease progression. This is a particularly popular area of investigation for photoreceptors and related diseases (Litts et al. 2017). Mysteries of specific origin of hyper-reflective signals and dynamics over time are difficult to answer using only human subjects, in part due to the challenges of obtaining samples for histological correlation, but also limits in resolution (up to 1 micron resolution for most of these *in vivo* techniques, while many cellular functions are visualized on nanoscopic scale). Imaging retinal structure and function non-invasively represents a promising future direction in the way we model and subsequently treat retinal disease. Studying small diurnal mammals with these same techniques used to directly examine human retinal health and disorder has potentially immediate translational value.

6.2. Use as research models of diabetic retinopathy

One avenue of potentially valuable research is diabetic retinopathy (DR). It is acknowledged that DR is a neurovascular disease in which neurodegenerative changes occur earlier than clinically detectable vascular alterations (Simo et al., 2012). Multiple clinical and experimental studies have observed that colour vision defects precede vascular alterations (Roy et al., 1986; Tzekov and Arden, 1999; Yamamoto et al., 1996; Klemp et al., 2005; Gualtieri et al., 2013), and that cones are preferentially impacted in DR animal models (Alvarez et al., 2010) and humans with DR (Cho et al., 2000). Numerous rodent models of DR exist, with varying degrees of similarity to the human disease, although no single animal model recapitulates all the neural and vascular complications associated with DR, especially the late-stage proliferative form, PDR (Rees and Alcolado, 2005). Animal models can be classified as

drug-induced, as with the destruction of pancreatic β cells by streptozotocin (Armstrong and Al-Awadi, 1991); genetic, as with the widely used Ins2akita mouse strain (Barber et al., 2005); and spontaneously occurring diabetes brought on by aging and/or dietary modification (Shafrir and Ziv, 2009). This last category includes the Fat Sand Rat *P. obesus*. Considering the strong evidence implicating early cone malfunction in DR, a particularly valuable characteristic of this animal is the high cone number, facilitating detailed structural and functional scrutiny of this population. As detailed in section 3, many of the features of human DR were observed in animals maintained on HE diets, including a reduction in both short wavelength and mid-wavelength cone opsins, whereas rhodopsin levels were not changed (Saidi et al., 2011b), underlining the enhanced vulnerability of cones to pre-diabetic states.

Recently, using the same protocol as in our original study it was shown that two gerbil species, *P. obesus* and *M. shawi*, displayed severely reduced amplitudes and increased implicit times for both scotopic and photopic ERGs, as well as blunted oscillatory potentials (Dellaa et al., 2018; Hammoum et al., 2018). Altered oscillatory potentials is another prominent characteristic of human DR (Kizawa et al., 2006). There were interesting differences between the two models, notably the lack of susceptibility of the short wavelength-sensitive cones in *M. shawi*, whereas this population is reported as being especially vulnerable in human DR (Cho et al., 2000). This difference was confirmed in a subsequent study by the same group, with an actual increase in this cone population compared to controls (Hammoum et al., 2017b). The same group also showed that short-term treatment of diabetic *P. obesus* with the xanthophyll astaxanthin reversed some phenotypic features of induced DR (Baccouche et al., 2018). These results are very encouraging but currently limited by two factors: firstly, the studies were performed on animals captured in their natural habitat, which is not compatible with routine repeatable experimentation under controlled sanitary conditions in multiple laboratories; and secondly, functional changes were only reported after 7 months of dietary overload, whereas perhaps the main interest of this model is to non-invasively track retinal alterations as a progression of DR over time in order to identify primary lesions (particularly cone functional deficits)

which may be of predictive value as “biomarkers”. We are currently performing such analyses using *P. obesus* raised in clean animal house conditions and monitored daily for their health status.

Diabetes has also been observed to occur in *Arvicanthis niloticus*: Noda et al. (2010) showed that metabolic syndrome and T2D were widespread in older animals (~1 year), predominantly in males. Studies of over 1100 animals in fed normal rat chow in captivity, revealed that most of these animals spontaneously develop dyslipidemia and hyperglycemia by 1 year. Diabetic individuals developed liver steatosis, abdominal fat accumulation, nephropathy, atrophy of pancreatic islets of Langerhans, fatty streaks in the aorta, and hypertension. The same group (Noda et al., 2014) later used this model to explore retinopathy – although they only examined vasculopathic features, they observed that advanced diabetes in *A. niloticus* was associated with reduced expression of intercellular adhesion molecule 1 compared to normal animals. As opposed to the streptozotocin-induced model of DR, in diabetic *A. niloticus* most leukocytes accumulated in the retinal arteries. Diabetic animals also showed substantial retinal endothelial injury, primarily in the microvessels, including vascular tortuosity, obliterated acellular capillaries, and pericyte ghosts.

Aware of these findings, we examined aged (1-2.5 years) individuals in our *A. ansorgei* colony. Although occasional individuals were detected with elevated blood glucose concentrations, metabolic syndrome did not develop in a systematic manner. Of note, a recent study showed that pre-diabetic states accompanied with premature cellular aging could be induced in young *A. ansorgei* subjected to circadian desynchronisation (Grosbellet et al., 2015), underscoring the importance of the circadian clock in regulating metabolic status. This difference in diabetic prevalence between the two *Arvicanthis* species in captivity may represent altered genetic susceptibility, or alterations in animal nutrition or maintenance (though both locations use standard rat chow formulas).

6.3. Use as research models of macular degeneration

A second research domain where cone-rich rodents may help advance knowledge concerns modelling of inherited retinal diseases, especially maculopathies. Mice and rat retinas at best approximate

peripheral retina in humans, with cone numbers between 1 and 3%. Although not as numerous as in the ground squirrel, the 33% cone numbers in *Arvicanthis* are roughly similar to the human macula (except for its very centre at the foveola). Efforts are thus justified to generate genetically modified animals with either deleted genes of interest or carrying human disease-related mutations. Although thus far we have been unable to prepare such strains (see section 6.5.), we have embarked on performing subretinal injections of plasmids containing CRISPR-Cas9 constructs directed against *abca4*, the gene in which mutations are responsible for the early onset inherited maculopathy Stargardts Disease (Allikmets, 1997). Although the disease has a complicated genotype-phenotype relationship, many patients exhibit a preferential loss of cone-mediated vision, often with rod function fully preserved (Fujinami et al., 2013). This characteristic has not been reported in the mouse model (*abca4*$^{-/-}$) of Stargardts Disease (Weng et al., 1999), and we believe *Arvicanthis* represents a rare setting to compare directly the effects of experimental *abca4* inhibition on rod and cone structure, function and survival.

6.4. Use as research models of environmental (lighting) effects on health and disease

An area of major current interest concerns the potential deleterious effects of exposure to artificial light at night on human health. Both experimental and epidemiological data point to short and long-term effects on sleep but also cancer, metabolic stress and depression (Cho et al., 2015; Lunn et al., 2017; Touitou et al., 2017; Russart and Nelson, 2018). There is debate on whether the generalized introduction of LED technology will exacerbate these problems, because of the high percentage of emitted blue light amplifying perturbation of the circadian clock (Kyba et al., 2017). Diurnal rodents such as *Arvicanthis* represent a useful means of investigating the relationship between night-time light exposure and downstream effects on pathophysiology, once again because their circadian system is constructed in a similar manner to humans, and they have been shown to develop neurological (Fonken et al., 2012b), metabolic (Grosbellet et al., 2015) and immune system (Fonken et al., 2012a) malfunction upon exposure to dim light at night. Our studies, reported in section 2.3., showed that a single night of continued moderate illumination leads to widespread modifications in temporal

profiles of retinal clock genes and their downstream targets (Bobu and Hicks, 2009; Mehdi and Hicks, 2010; Bobu et al., 2013). Conversely, both *Arvicanthis* and *Psammomys* develop signs of neurological stress and impairment when raised in a lighting environment whereby daytime levels are relatively dim (Ashkenazy et al., 2009; Leach et al., 2013). This is also similar to contemporaneous human lifestyles, where people frequently spend the entire day indoors under lighting regimes in which intensity is very inferior to outdoors, and appear inadequate to correctly synchronize the circadian clock. Furthermore *Arvicanthis* exhibits a pronounced nocturnal peak of circulating melatonin similar to humans, and absent from many inbred mouse strains. Since melatonin is a key intermediate in many of the downstream effects of circadian disruption seen in humans this is an important parameter.

6.5. Current drawbacks

Finally, there are certain caveats that need to be mentioned, despite the claim by Yan et al. (2018) that "… the Nile grass rat is an ideal diurnal model (sic: for the visual system)". Except for the Mongolian gerbil, diurnal rodents lack the long domestication history of commercially available laboratory rats and mice. That can make them difficult to obtain in large numbers necessary to undertake systematic studies with sufficient sample size. Animal facilities are not accustomed to non-domesticated rodents, so their husbandry presents a learning curve. These obstacles are surmountable, and the higher yield of cones and cone pathway circuitry may well be worth the effort for projects centered on cone-based vision. As is true for the great majority of mammals other than old world primates and humans (which are trichromats possessing distinct blue, green and red cone subtypes), diurnal rodents are dichromats lacking the red cone subtype.

A further caveat is that the diurnal murids (at least the two species *Arvicanthis* and *Psammomys*) do not have "fully diurnal retinas". In the introduction we outlined how a distinction could be made between nocturnal and diurnal mammals based on the distribution of euchromatin and heterochromatin within the rod nucleus, such that nocturnal species (such as mice and rats) have

a uniquely inverted structure with a dense central heterochromatin core and surrounding euchromatin shell which is thought to be an evolutionary adaptation to maximize light gathering (Solovei et al., 2009, 2013). On the contrary, diurnal species (such as pigs and macaques) have re-acquired a "conventional" chromatin architecture, with a large central euchromatin core and narrow heterochromatin shell. Ground squirrels also have this conventional rod nuclear layout (Figure 19). We were thus surprised to discover that rods in *Arvicanthis* and *Psammomys* in fact display a nocturnal-type inverted chromatin distribution (Figure 19), putting them in a “grey zone” of having evolved some diurnal features (thinner ONL, large numbers of cones) but retaining some nocturnal ones (rod nuclear organisation). Although there are no data to show this is a disadvantage in terms of faithfully modelling human retinal pathophysiology - indeed one study showed that the distribution of nuclear speckles was similar between nocturnal and diurnal rodent rods, suggesting that transcription and splicing are not radically different (Derlig et al., 2015) - it should nevertheless be borne in mind.

Another current limitation, at least in our hands, is the inability to generate a germline transgenic strain. This an important goal to strive for, as successful creation of a line with gene deletion of abca4 for example, would provide the scientific community with a means to compare rod and cone degeneration in the severe maculopathy Stargardts Disease. We (DV, DH) have repeatedly tried unsuccessfully to produce such a strain, especially hindered by the lack of knowledge of experimental procedures suitable for creating tansgenic diurnal rodents. The reproductive cycle in *A. ansorgei* is not very marked, there is no cornification of the squamous epithelium during oestrous and the presence of a vaginal plug does not systematically indicate successful fertilization (pers. obs.). Our attempts to date to induce superovulation in *A. ansorgei* using the standard protocol of gonadotropin injection in terms of dose and timing developed for mice has not yielded positive results. Data from *A. niloticus* show that sexual hormone surge is phase-inverted respective to diurnal rats (McElhinny et al., 1999; Mahoney et al., 2004), indicating that timing of gonadotropin injections should probably also be inverted with respect to the protocol defined for mice. Culture media optimized for survival of mice ova do not sustain *Arvicanthis* oocytes >24 hours (pers. obs.). Hence all these parameters need

to be redefined in order to maximize the chances of generating a germline deletion of gene of interest.

7. Figure Legends

Figure 1: Toluidine blue-stained histological section (left) and cone arrestin-immunostained cryostat section (right) of adult *Arvicanthis ansorgei* retina. The clear separation of cone (CCB) and rod (RCB) cell bodies within the outer nuclear layer (ONL) can be seen; CCB in the histological section have less intensely stained nuclei, and on the right are specifically and intensely stained with anti-cone arrestin. The antibody outlines the entire cell, including cone outer (COS) and inner (CIS) segments, with traces of cone axons visible running through the RCB layer and terminating in intensely stained cone synaptic pedicles in the outer plexiform layer (OPL). The rod OS (ROS) are unstained and extend beyond the COS to contact the overlying retinal pigmented epithelium (RPE). Additional abbreviations: Ch, choroid. Scale bar in bottom right = 25µm.

Figure 2: Immunostaining of *Arvicanthis* retina using antibodies directed against rod-, cone- or rod/conespecific proteins. A) DAPI staining of outer nuclear layer (ONL), divided clearly into the upper row of cone cell bodies (CCB) and lower rod cell bodies (RCB). Note the paler stained cone nuclei. Rod-specific antibodies: B) Same area stained with RET-P3, a monoclonal antibody specific for plasma membrane of rod cell bodies (Barnstable, 1980). The staining extending up through the CCB is actually on rod cell extensions joining to their inner/outer segments. C) Monoclonal antibody specific for cGMP-gated cation channel staines heavily the OS of rods. D) Phosducin antibody stains throughout the rod cell cytoplasm – notice the dark band corresponding to the absence of staining in CCB. Cone-specific antibodies: polyclonal antibodies to mid-wavelength cone opsin (E) and short wavelength cone opsin (F) respectively, label the OS in cones. The former are ~10 fold more numerous than the latter. Rod/cone antbodies: polyclonal antibodies to panarrestin (S-antigen) (G) and recoverin (H) stainheavily CCB and RCB, as well as IS and OS. Additional immunolabelled images can be seen in Bobu et al., 2006, 2008.

Figure 3: Phylogenetic analysis for selected retinal genes in *Arvicanthis ansorgei*. Multiple sequence alignment for the CDS of A) rhodopsin, B) short-wave-sensitive (blue) opsin, C) melanopsin and D) cone-rod homeobox for *A. ansorgei* and other model organisms performed using MUSCLE. The Maximum Composition Likelihood model was used to construct Neighbor-Joining phylogenetic trees. Taken from Liu et al., 2017.

Figure 4: Comparative electroretinographic recordings from adult C57/Bl mice (black traces) and *Arvicanthis ansorgei* (grey traces). Animals (n=3 for each group) were anesthetised and stimulated with increasing intensities of white light. Representative single flash (A, B) and flicker (C) ERG recordings. The lightning symbol above the second vertical line indicates the time of the light flash. Comparison of representative records under dark-adapted (A) and light-adapted conditions (B, C). Open arrows indicate the a-wave, solid arrows indicate the trailing edge of the b-wave. The flash intensity for flicker recordings was 0.5 log cd×s/m2. ERG, electroretinogram. The overlay in (A) demonstrates lower amplitude rod responses in *A. ansorgei* compared to *M. musculus*, to be expected given the lower rod numbers; and the overlay in (B) shows clearly the higher corresponding cone responses in *A. ansorgei* for each flash intensity. The overlays further indicate the differential light sensitivities in the two species, since under scotopic conditions mice already give weak responses at 10^{-4} cd/s/m^2, not seen in *Arvicanthis*; and conversely pure cone responses are intiated in *Arvicanthis* at $5x10^{-2}$ cd/s/m^2, not seen in mice. Taken from Boudard et al., 2010.

Figure 5: Double-label immunohistochemistry of rod and cone phagocytosis, and quantitative analysis of rhythmic daily rod and cone phagocytosis in *A. ansorgei* retina. A-D: Sections obtained at 09.00 hours (1 hour after lights on) were stained with rho-4D2 anti-rhodopsin (staining rods and rod phagosomes, green) and red/green cone opsin antibody (staining cones and cone phagosomes, red). (A) Bright-field image showing the outer retina and RPE; (B) rho-4D2 labeling of the same field, including several immunopositive phagosomes (circles); (C) red/green cone opsin labeling of the same field, including several immunopositive phagosomes (white arrows); (D) merged image of (B) and (C), showing presence of both rod and red/green cone phagosomes in the RPE. Double-headed arrow:

width of the RPE. ONL, outer nuclear layer; COS, cone outer segments; ROS, rod outer segments. Scale bar, 15 µm. E, F: Phagosome counts were made every 3 hours throughout both the light and dark periods. (E) Rod phagocytosis: as seen in other species, a large burst in the number of rod phagosomes was seen 1 hour after light onset, significantly different from all other values ($P < 0.0001$). Phagosome numbers were lowest in late daytime, but showed a smaller but noticeable peak late at night. (F) Cone phagocytosis: similar to the kinetic profile for rods, cone phagocytosis peaked shortly after light onset, but the order of magnitude was always 10 times lower than that of rods (note difference in y-axis scales). When animals were raised under DD conditions, rod (G) and cone (H) phagosome counts actually increased, although there was a similar profile to LD. On the contrary, exposure to LL led to completely random profiles for both rods (I) and cones (J), and in addition cone phagosome numbers were significantly increased compared to LD. Modified from Bobu et al., 2006 and Bobu and Hicks, 2009.

Figure 6: Intense light exposure (ILE) does not elicit apoptosis in *A. ansorgei* photoreceptors but does injure mice photoreceptors. (A–D) Hematoxylin and eosin staining. (A) Control (-ILE) *A. ansorgei* retina; (B) *A. ansorgei* sacrificed one week after receiving 2 hour ILE at 12 klux. There was no observable alteration of retinal structure following exposure; (C) Control (-ILE) pigmented mouse (129S6) retina; (D) Pigmented mouse (129S6) sacrificed one week after receiving 2 hour ILE at 13 klux. There was complete loss of the ONL after light exposure. (E) Control (-ILE) *A. ansorgei*, and (F) +ILE *A. ansorgei* retinas taken 36 hours after exposure to 15 klux white light for 8 hours. No TUNEL reaction is seen in either case. (G) Retinal sections of albino Balb/c mice exposed to 5 klux for 1 hour (ie. 24 times less total light) already show widespread apoptotic nuclei within the ONL. Scale bar, 50 µm. Taken from Boudard et al., 2011).

Figure 7: Exposure to intense blue light does not lead to photoreceptor-specific light damage but thermal damage in *A. ansorgei* neural retina. Haematoxylin-stained retinal sections were prepared from animals exposed to (A) 15 minutes or (B) 45 minutes of narrow band intense blue light (30 mW/cm2, 403±10 nm) delivered via a fibre optics lamp apposed to the cornea, and killed 10 days

later. Retinal histology was normal 10 days after 15 minute exposure to blue light, whereas a ~1-mm-diameter circular lesion, corresponding to the area illuminated by the fibre optics beam, was observed after 45 minute exposure (flanked by arrows in the image B). (C) DAPI-stained section of same eye from animal 10 days after 45 min intense blue light exposure. Higher magnification of lesion site shown in C'. D-F, sections taken immediately adjacent to lesion site in 45 min-exposed animals, and D'-F' corresponding sections taken inside the lesion site. DAPI, rhodopsin and cone arrestin staining show typical staining in D, E and F respectively, with an intact ganglion cell layer (GCL, inner nuclear layer (INL) and outer nuclear layer (ONL). Rhodopsin immunorectivity was especially strong in the outer segments (OS), whereas cone arrestin immunoreactivity was visible throughout the cone cells. Within the lesion site, DAPI staining showed a disorganized mass of scar tissue (ST) (D'). No staining with rhodopsin or cone arrestin antibodies was detected within the lesion site, as seen in E' and F' respectively. (G, H) GFAP staining provides an indicator of general retinal stress. After 15 minutes of intense blue light exposure, outside the lesion site GFAP staining was confined to retinal astrocytes in the nerve fibre layer (NFL) (G), whereas in retinas exposed to 45 minutes of intense blue light there was generalized radial glial staining across the width of the retina, from the NFL to the external limiting membrane (ELM), outside of the lesion site (H). Notice the absence of GFAP immunoreactivity in the central retina denoted by * in G, and widespread staining in Müller glia in the same zone (*) in H. Scale bar in F': 300 µm (A-C); 100 µm (C'); 60 µm (D–H). Taken from Boudard et al., 2011 and thesis dissertation).

Figure 8: Immunohistochemistry labelling showing partial regional loss of rod- and cone-specific proteins in *Arvicanthis* receiving elevated doses of MNU. Fluorescence microscopy of an entire retinal section of 90 dpi (days post-injection)-MNU (100 mg/ml) *Arvicanthis* stained with DAPI (scale: 250 µm), showing the gradient of the degeneration along the vertical meridian from superior to inferior hemisphere. The entire section was reconstructed with adjacent images taken at ×20 magnification. Eight different regions (A–H) of this section are shown in higher detail (scale: 50 µm). (A–E) are located in the inferior hemisphere and (F–H) in the superior hemisphere. The approximate position of

the optic nerve head is shown with a white arrow (located 50-100 µm away in sister section). Same regions of adjacent sections labelled with rhodopsin, r-trans. (r-transducin), MW-cone opsin (red/green cone opsin), and cone arrestin (c-arr.) are shown in serial panels. Control (Ctrl) retina labelled with the same antibodies is given as reference. CCB, cone cell bodies; CIS, cone inner segments; COS, cone outer segments; GCL, ganglion cell layer; INL, inner nuclear layer; MNU, N-methyl-N-nitrosourea; MW opsin, red/green cone opsin; ONL, outer nuclear layer; RCB, rod cell bodies; RIS, rod inner segments; ROS, rod outer segments. Adapted from Boudard et al., 2010).

Figure 9: The molecular clock pathways and retinal clocks. Schematic representation of the transcriptional/translational feedback loops model for the molecular clock. The BMAL1/CLOCK (or BMAL1/NPAS2) dimer activates transcription of the Per and Cry genes upon binding to the Ebox sequences in their promoters. In turn, PER and CRY proteins form heterodimers able to inhibit transcriptional activity of BMAL1/CLOCK, thus turning down their own transcription. Meanwhile, these factors undergo posttranslational modifications, in particular, phosphorylation of PER proteins by the Casein Kinases 1δ or 1ε, signaling for ubiquitination and proteasomal degradation, and then allowing the cycle to restart. BMAL1/CLOCK likewise activates the expression of Rev-Erb and Ror genes, which products respectively repress and activate transcription of the Bmal1 gene at retinoic acid-related orphan receptor binding elements (RORE) sites. This generates an additional loop interlocked with the previous one, all together contributing to the robustness of the clockwork. The presence of Ebox and/or RORE sequences throughout the genome supports the rhythmic regulation of a set of target genes (CCG) for BMAL1/CLOCK, BMAL1/NPAS2, REV-ERB, and ROR transcription factors. Clock gene expression dynamics over the 24-hour cycle conforming to this model have been described in the ONL and in the inner retina (INL + GCL) in several ex vivo studies, as symbolized next to the eosin/hematoxylin stained transversal section of a rat retina shown in the upper-right corner of the figure. Taken from Felder-Schmittbuhl et al., 2018.

Figure 10: Expression profile of core clock genes Bmal1 over a single 24 h period in *Arvicanthis* maintained under different lighting conditions. Vertical columns, left to right : Bmal1, Per1, Per2, Cry1

and Cry2. Horizontal rows, top to bottom: top, 12 h light: 12 h dark cycle (LD); middle, constant darkness (DD); bottom, constant light (LL). Illumination conditions are depicted as backgrounds of white (light) and dark grey (darkness), right hatched (subjective day) and left hatched (subjective night). Statistically significant rhythmic changes are seen in all genes under LD, with most maxima occurring at the night-day transition point; the pattern is basically similar albeit dampened in DD. However LL leads to large phase shifts in expression profiles, with peak expression now occurring in early night. These data underline the highly disruptive effects of artifical light at night upon the retinal circadian clock. One-way analysis of variance (ANOVA) and cosinor levels of significance (PA and Pc respectively) are given in the upper right corner of each panel. Modified from Bobu et al., 2013.

Figure 11: Light-induced responses of ipRGCs in *Arvicanthis* (left) and mouse retina (right) to short flashes of constant irradiance (14.3 log NQ * cm-2 * s-1). The most sensitive ipRGC type (type I) responds to very short light flashes of 10 ms in *Arvicanthis* but only poorly to even 50 ms in the mouse, respectively. We did not try shorter pulses. Type II and type III ipRGCs were insensitive to flashes shorter than 1 s in both species, although *Arvicanthis* displayed greater activity. Modified from Karnas et al., 2013a.

Figure 12: Melatonin synthesis pathway shows two phase-opposed sites of expression in *Arvicanthis* retina. A, DAPI staining of a 10-µm section of *A. ansorgei* retina indicates the area of interest; from top to bottom. B, Aa-nat antisense probe at ZT19 (night time) stains inner segments (IS) and the scleral-most part of the outer nuclear layer (ONL). C, Aa-nat antisense probe at ZT6 stains ganglion cell layer (GCL). D, Immunostaining of *A. ansorgei* retina with anti-cone arrestin (red) clearly showing retinal organization with cone cell bodies (CCB) located sclerally to rod cell bodies (RCB). E, At ZT19, Aa-nat mRNA staining is restricted to the 2 scleral-most cell body rows (CCB) and IS. F, At ZT19 Aa-nat antisense probe does not stain GCL. G and H, At ZT6, Aa-nat antisense probe stains GCL (H) but not ONL (G). I, Use of Aa-nat sense probe at ZT19 does not stain any structures. Scale bar, 10 µm. Additional abbreviations, INL, inner nuclear layer; OS, outer segments; RPE, retinal pigmented epithelium. Taken from Gianesini et al., 2015.

Figure 13: Scotopic and photopic electroretinograms of *Psammomys obesus*, humans and rats. Two different intensities are shown under scotopic mode, faint intensity (0.01 cd/s/m^2) to evoke a pure rod response, and high intensity (3 cd/s/m^2) to evoke a mixed rod-cone reponse. The single photopic recording, under background light adaptation (3 cd/s/m^2), shows a pure cone response. The greater similarities between recordings from *P. obesus* and humans compared to those made in Wistar rats can be seen, including similar amplitudes and waveforms under scotopic conditions, and the presence of post b wave components (the i wave and photoreceptor negative response, PhNR) not seen in rats. Other abbreviations: a = a wave (hyperpolarisation), b = b wave (depolarisation). Modified from Dellaa et al., 2017.

Figure 14: Fundus Fluorescent angiography showing organisation of major blood vessels in *Psammomys obesus*. Vessels present as two beds, one spreading laterally from the optic nerve head (ONH), the other branching laterally in the superior hemisphere. Between the two lies a poorly vascularized region corresponding to the area centralis (outlined by dotted lines). Photoimage made from images captured using Phoenix Micron III camera and anaethetised adult female *P. obesus* injected i.v. with fluorescein, courtesy of Dr. M. Roux, IGBMC, Illkirch, France.

Figure 15: Vascular modifications during diabetes in *P. obesus*. (A–D) Retinas stained with *B. simplicifolia* isolectin. Although the vessel aspect in control retinas (lean normal, LN) showed a regular smoothly branching aspect (A), diabetic retinas (obese hyperglycemic, OH) showed a range of abnormalities, including irregular diameter and constrictions (B, open bracket), neovascular buds (C, arrow), and balloon-like swellings (D, arrow). Vascular and blood-retinal barrier modifications during diabetes in *P. obesus*. LN retinas labeled with *B. simplicifolia* lectin (Bs, red) to outline blood vessels (E) and anti-smooth muscle actin antibody (SMA, green) to stain pericytes (F) demonstrate the dense pericyte coverage (examples shown by arrows). On the contrary, OH retinas labeled under identical conditions showed that lectin-stained vessels (G) are completely lacking pericytes (H). Modified from Saidi et al., 2011b.

Figure 16: Pro-angiogenic and anti-angiogenic growth factors in the vitreous of control and diabetic eyes from *P. obesus*. (A) top panel: VEGF-immunoreactive bands in vitreous samples from three control (lean normal, LN, left) and three diabetic (obese hyperglycemic, OH, right) animals. Lower panel: the bands were analyzed by densitometry and normalized to tubulin in stripped membranes from the same samples. Black column: LN controls; white column: OH animals. ***P<0.001. (B) top panel : PEDF-immunoreactive bands in vitreous samples from three control (LN, left) and three diabetic (OH, right) animals. Lower panel: the bands were analyzed by densitometry and normalized to tubulin in stripped membranes from the same samples. Black column: LN controls; white column: OH animals. ***P<0.001. Relative levels given in arbitrary units. Modified from Saidi et al., 2011b.

Figure 17: Rod and cone photoreceptor opsins in control and diabetic *P. obesus* retina. A-C: Rhodopsin (Rho) immunolabeling showed strong expression in rod outer segments (OS, green) in lean normal (LN), obese normoglycemic (ON), and obese hyperglycemic (OH) animals respectively. D-F: Staining of red/green, or mid-wavelength, cone opsin (MOp) was localized to numerous cone outer segments (OS, red) in LN (D) and ON (E) animals, whereas there were many less immunolabeled cells in OH tissue (F). This was also the case for blue or short wavelength cone opsin (SOp) immunostaining in OS of LN (G) and OH animals (H). To the right of each immunostaining series are shown western blot analyses and quantification of Rho, MOp, and SOp expression. (I) Rho and tubulin (Tub) immunoreactivity showed no difference in intensity between samples. Triplicate samples are shown above corresponding columns: LN (black), ON (gray), OH (white). (J) MOp immunoreactivity showed a roughly 50% decrease in OH retinas when normalized to Tub (***P < 0.001, ANOVA). (K) Similarly, SOp immunoreactivity was also reduced by 50% in OH retinas (***P< 0.001, ANOVA). Scale bar, 80 µm. Modified from Saidi et al., 2011b.

Figure 18: Use of Adaptive Optics Scanning Light Ophthalmoscopy (AOSLO) to show the similar appearance of cone photoreceptors between human fovea (left) and 13-Lined ground squirrel visual streak (right) *in vivo.* Scale bar = 20 µm.

Figure 19: Chromatin organization in nocturnal and diurnal rodent retinas. (A) *Mus musculus* rod nuclei have a uniquely inverted chromatin structure, with heterochromatin (HC, red) concentrated into a central mass surrounded by euchromatin (EC, green). This is the opposite of the situation seen in every other differentiated cell type, in which EC forms a large central area surrounded by a shell of HC (see nuclei in INL). This conventional organization is also seen in rods of diurnal rodents like the ground squirrel, shown at low (B) and high magnification (C) (HC in red, EC in green). Surprisingly, *Psammomys obesus* (and *Arvicanthis*, not shown) possess inverted rod nuclei similar to nocturnal *Mus musculus*, again shown at low (D) and high magnification (E) (HC in red, EC in green). Panel A modified from Solovei et al., 2009, other panels unpub. data and pers. comm. Dr. I. Solovei, with permission).

8. References

1. Agbaga, M.P., Merriman, D.K., Brush, R.S., Lydic, T.A., Conley, S.M., Naash, M.I., Jackson, S., Woods, A.S., Reid, G.E., Busik, J.V., Anderson, R.E., 2018. Differential composition of DHA and very-long-chain PUFAs in rod and cone photoreceptors. J Lipid Res. 59, 1586-1596.
2. Aiello, L.P., DCCT/EDIC Research Group, 2014. Diabetic Retinopathy and Other Ocular Findings in the Diabetes Control and Complications Trial/Epidemiology of Diabetes Interventions and Complications Study. Diabetes Care 37, 17–23.
3. Ait-Hmyed Hakkari, O., Acar, N., Savier, E., Spinnhirny, P., Bennis, M., Felder-Schmittbuhl, M.P., Mendoza, J., Hicks, D., 2016. Rev-Erbalpha modulates retinal visual processing and behavioral responses to light. Faseb j. 30, 3690-3701.
4. Alarma-Estrany, P., Pintor, J., 2007. Melatonin receptors in the eye: location, second messengers and role in ocular physiology. Pharmacol Ther. 113, 507-522.
5. Allikmets, R., 1997. A photoreceptor cell-specific ATP-binding transporter gene (ABCR) is mutated in recessive Stargardt macular dystrophy. Nat Genet. 17, 122.
6. Alvarez, Y., Chen, K., Reynolds, A.L., Waghorne, N., O'Connor, J.J., Kennedy, B.N., 2010. Predominant cone photoreceptor dysfunction in a hyperglycaemic model of non-proliferative diabetic retinopathy. Dis Model Mech. 3, 236-245.
7. Ambati, J., Chalam, K. V, Chawla, D.K., D'Angio, C.T., Guillet, E.G., Rose, S.J., Vanderlinde, R.E., Ambati, B.K., 1997. Elevated gamma-aminobutyric acid, glutamate, and vascular endothelial growth factor levels in the vitreous of patients with proliferative diabetic retinopathy. Arch. Ophthalmol. (Chicago, Ill. 1960) 115, 1161–6.
8. Anderson, D.H., Fisher, S.K., 1975. Disc shedding in rodlike and cone like photoreceptors of tree squirrels. Science. 187, 953-955.
9. Anderson, D.H., Fisher, S.K., Steinberg, R.H., 1978. Mammalian cones: disc shedding, phagocytosis, and renewal. Invest Ophthalmol Vis Sci. 17, 117-133.
10. Anderson, D.H., Fisher, S.K., Erickson, P.A., Tabor, G.A., 1980. Rod and cone disc shedding in the rhesus monkey retina: a quantitative study. Exp Eye Res. 30, 559-574.
11. Anderson, J.W., 1985. Physiological and metabolic effects of dietary fiber. Fed Proc. 44, 2902-2906.
12. Ankel-Simons, F., Rasmussen, D.T., 2008. Diurnality, nocturnality, and the evolution of primate visual systems. Am J Phys Anthropol Suppl. 47, 100-117.
13. Ardiles, A.O., Ewer, J., Acosta, M.L., Kirkwood, A., Martinez, A.D., Ebensperger, L.A., Bozinovic, F., Lee, T.M., Palacios, A.G., 2013. Octodon degus (Molina 1782): a model in comparative biology and biomedicine. Cold Spring Harb Protoc. 2013, 312-318.

14. Armstrong, D., al-Awadi, F., 1991. Lipid peroxidation and retinopathy in streptozotocin-induced diabetes. Free Radic Biol Med. 11, 433-436.
15. Ashkenazy, T., Einat, H., Kronfeld-Schor, N., 2009. We are in the dark here: induction of depression- and anxiety-like behaviours in the diurnal fat sand rat, by short daylight or melatonin injections. Int J Neuropsychopharmacol. 12, 83-93.
16. Baba, K., Pozdeyev, N., Mazzoni, F., Contreras-Alcantara, S., Liu, C., Kasamatsu, M., Martinez-Merlos, T., Strettoi, E., Iuvone, P.M., Tosini, G., 2009. Melatonin modulates visual function and cell viability in the mouse retina via the MT1 melatonin receptor. Proc Natl Acad Sci USA. 106, 15043-15048.
17. Baba, K., Benleulmi-Chaachoua, A., Journe, A.S., Kamal, M., Guillaume, J.L., Dussaud, S., Gbahou, F., Yettou, K., Liu, C., Contreras-Alcantara, S., Jockers, R., Tosini, G., 2013. Heteromeric MT1/MT2 melatonin receptors modulate photoreceptor function. Sci Signal. 6, ra89.
18. Baccouche, B., Benlarbi, M., Barber, A.J., Ben Chaouacha-Chekir, R., 2018. Short-Term Administration of Astaxanthin Attenuates Retinal Changes in Diet-Induced Diabetic Psammomys obesus. Curr Eye Res. 43, 1177-1189.
19. Barak, O., Kronfeld-Schor, N., 2013. Activity rhythms and masking response in the diurnal fat sand rat under laboratory conditions. Chronobiol Int. 30, 1123-1134.
20. Barber, A.J., Antonetti, D.A., Kern, T.S., Reiter, C.E., Soans, R.S., Krady, J.K., Levison, S.W., Gardner, T.W., Bronson, S.K., 2005. The Ins2Akita mouse as a model of early retinal complications in diabetes. Invest Ophthalmol Vis Sci. 46, 2210-2218.
21. Barnard, A.R., Hattar, S., Hankins, M.W., Lucas, R.J., 2006. Melanopsin regulates visual processing in the mouse retina. Curr Biol. 16, 389-395.
22. Barnstable, C.J., 1980. Monoclonal antibodies which recognize different cell types in the rat retina. Nature 286, 231–235.
23. Barrett, P., Bolborea, M., 2012. Molecular pathways involved in seasonal body weight and reproductive responses governed by melatonin. J Pineal Res. 52, 376-388.
24. Baver, S.B., Pickard, G.E., Sollars, P.J., Pickard, G.E., 2008. Two types of melanopsin retinal ganglion cell differentially innervate the hypothalamic suprachiasmatic nucleus and the olivary pretectal nucleus. Eur J Neurosci. 27, 1763-1770.
25. Beier, C., Palanker, D., Sher, A., 2018. Stereotyped Synaptic Connectivity Is Restored during Circuit Repair in the Adult Mammalian Retina. Curr Biol. 28, 1818-1824.e1812.
26. Beltran, W.A., Cideciyan, A.V., Guziewicz, K.E., Iwabe, S., Swider, M., Scott, E.M., Savina, S.V., Ruthel, G., Stefano, F., Zhang, L., Zorger, R., Sumaroka, A., Jacobson, S.G., Aguirre, G.D., 2014. Canine retina has a primate fovea-like bouquet of cone photoreceptors which is affected by inherited macular degenerations. PLoS One. 9, e90390.
27. Bermudez, M.A., Vicente, A.F., Romero, M.C., Arcos, M.D., Abalo, J.M., Gonzalez, F., 2011. Time course of cold cataract development in anesthetized mice. Curr Eye Res. 36, 278-284.
28. Berson DM, Dunn FA, Takao M, 2002. Phototransduction by retinal ganglion cells that set the circadian clock. Science. 295, 1070-3.
29. Berson, D.M., 2003. Strange vision: ganglion cells as circadian photoreceptors. Trends Neurosci. 26, 314-20.

30. Besharse, J.C., Dunis, D.A., 1983. Methoxyindoles and photoreceptor metabolism: activation of rod shedding. Science. 219, 1341-1343.
31. Besharse, J.C., McMahon, D.G., 2016. The Retina and Other Light-sensitive Ocular Clocks. J Biol Rhythms. 31, 223-243.
32. Bilu, C., Kronfeld-Schor, N., 2013. Effects of circadian phase and melatonin injection on anxiety-like behavior in nocturnal and diurnal rodents. Chronobiol Int. 30, 828-836.
33. Bilu, C., Einat, H., Kronfeld-Schor, N., 2016. Utilization of Diurnal Rodents in the Research of Depression. Drug Dev Res. 77, 336-345.
34. Bilu C, Zimmet P, Vishnevskia-Dai V, Einat H, Agam G, Grossman E, Kronfeld-Schor N, 2019. Diurnality, Type 2 Diabetes, and Depressive-Like Behavior. J Biol Rhythms. 34, 69-83.
35. Bobu, C., Craft, C.M., Masson-Pevet, M., Hicks, D., 2006. Photoreceptor organization and rhythmic phagocytosis in the nile rat Arvicanthis ansorgei: a novel diurnal rodent model for the study of cone pathophysiology. Invest Ophthalmol Vis Sci. 47, 3109-3118.
36. Bobu, C., Hicks, D., 2009. Regulation of retinal photoreceptor phagocytosis in a diurnal mammal by circadian clocks and ambient lighting. Invest Ophthalmol Vis Sci. 50, 3495-3502.
37. Bobu, C., Lahmam, M., Vuillez, P., Ouarour, A., Hicks, D., 2008. Photoreceptor organisation and phenotypic characterization in retinas of two diurnal rodent species: potential use as experimental animal models for human vision research. Vision Res. 48, 424-432.
38. Bobu, C., Sandu, C., Laurent, V., Felder-Schmittbuhl, M.P., Hicks, D., 2013. Prolonged light exposure induces widespread phase shifting in the circadian clock and visual pigment gene expression of the Arvicanthis ansorgei retina. Mol Vis. 19, 1060-1073.
39. Boudard, D.L., Acar, N., Bretillon, L., Hicks, D., 2011. Retinas of the diurnal rodent Arvicanthis ansorgei are highly resistant to experimentally induced stress and degeneration. Invest Ophthalmol Vis Sci. 52, 8686-8700.
40. Boudard, D.L., Mendoza, J., Hicks, D., 2009. Loss of photic entrainment at low illuminances in rats with acute photoreceptor degeneration. Eur J Neurosci. 30, 1527-1536.
41. Boudard, D.L., Tanimoto, N., Huber, G., Beck, S.C., Seeliger, M.W., Hicks, D., 2010. Cone loss is delayed relative to rod loss during induced retinal degeneration in the diurnal cone-rich rodent Arvicanthis ansorgei. Neuroscience. 169, 1815-1830.
42. Boyd, R.F., Sledge, D.G., Boye, S.L., Boye, S.E., Hauswirth, W.W., Komaromy, A.M., Petersen-Jones, S.M., Bartoe, J.T., 2016. Photoreceptor-targeted gene delivery using intravitreally administered AAV vectors in dogs. Gene Ther. 23, 223-230.
43. Brown, T.M., Gias, C., Hatori, M., Keding, S.R., Semo, M., Coffey, P.J., Gigg, J., Piggins, H.D., Panda, S., Lucas, R.J., 2010. Melanopsin contributions to irradiance coding in the thalamo-cortical visual system. PLoS Biol. 8, e1000558.
44. Browning DJ, Glassman AR, Aiello LP, Bressler NM, Bressler SB, Danis RP, Davis MD, Ferris FL, Huang SS, Kaiser PK, Kollman C, Sadda S, Scott IU, Qin H; Diabetic Retinopathy Clinical Research Network, 2008. Optical coherence tomography measurements and analysis methods in optical coherence tomography studies of diabetic macular edema. Ophthalmol. 115, 1366-1371.

45. Burke, T.M., Markwald, R.R., Chinoy, E.D., Snider, J.A., Bessman, S.C., Jung, C.M., Wright, K.P., Jr., 2013. Combination of light and melatonin time cues for phase advancing the human circadian clock. Sleep. 36, 1617-1624.
46. Burns, S.A., Elsner, A.E., Sapoznik, K.A., Warner, R.L., Gast, T.J., 2019. Adaptive optics imaging of the human retina. Prog Retin Eye Res. 68, 1-30.
47. Caldelas, I., Poirel, V.J., Sicard, B., Pevet, P., Challet, E., 2003. Circadian profile and photic regulation of clock genes in the suprachiasmatic nucleus of a diurnal mammal Arvicanthis ansorgei. Neuroscience. 116, 583-591.
48. Campi, K.L., Krubitzer, L., 2010. Comparative studies of diurnal and nocturnal rodents: differences in lifestyle result in alterations in cortical field size and number. J Comp Neurol. 518, 4491-4512.
49. Capanna, E., Civitelli, M.V., 1988. A cytotaxonomic approach of the systematics of Arvicanthis niloticus (Desmarest 1822) (Mammalia Rodentia). Tropical Zoology. 1, 29-37.
50. Carleton M.D., Musser G.G., 1984. Muroid rodents. In Orders and Families of Recent Mammals of the World. Anderson, S., Jones, J.K. (Eds), John Wiley, New York. pp 289-379.
51. Challet, E., Pitrosky, B., Sicard, B., Malan, A., Pevet, P., 2002. Circadian organization in a diurnal rodent, *Arvicanthis ansorgei* Thomas 1910: chronotypes, responses to constant lighting conditions, and photoperiodic changes. J Biol Rhythms. 17, 52-64.
52. Challet, E., 2010. Interactions between light, mealtime and calorie restriction to control daily timing in mammals. J Comp Physiol B. 180, 631-644.
53. Chavez, A.E., Bozinovic, F., Peichl, L., Palacios, A.G., 2003. Retinal spectral sensitivity, fur coloration, and urine reflectance in the genus octodon (rodentia): implications for visual ecology. Invest Ophthalmol Vis Sci. 44, 2290-2296.
54. Chen, S.K., Badea, T.C., Hattar, S., 2011. Photoentrainment and pupillary light reflex are mediated by distinct populations of ipRGCs. Nature. 476, 92-95.
55. Chiba, H., Osanai, M., Murata, M., Kojima, T., Sawada, N., 2008. Transmembrane proteins of tight junctions. Biochim. Biophys. Acta - Biomembr. 1778, 588–600.
56. Cho, N.C., Poulsen, G.L., Ver Hoeve, J.N., Nork, T.M., 2000. Selective loss of S-cones in diabetic retinopathy. Arch Ophthalmol. 118, 1393-1400.
57. Cho, Y., Ryu, S.H., Lee, B.R., Kim, K.H., Lee, E., Choi, J., 2015. Effects of artificial light at night on human health: A literature review of observational and experimental studies applied to exposure assessment. Chronobiol Int. 32, 1294-1310.
58. Clark, K., Karsch-Mizrachi, I., Lipman, D.J., Ostell, J., Sayers, E.W., 2016. GenBank. Nucleic Acids Res. 44, D67-72.
59. Coleman, D.L., 1978. Diabetes and obesity: thrifty mutants? Nutr. Rev. 36, 129–32.
60. Collier, R.J., Waldron, W.R., Zigman, S., 1989. Temporal sequence of changes to the gray squirrel retina after near-UV exposure. Invest Ophthalmol Vis Sci. 30, 631-637.
61. Collier, G.R., McMillan, J.S., Windmill, K., Walder, K., Tenne-Brown, J., de Silva, A., Trevaskis, J., Jones, S., Morton, G.J., Lee, S., Augert, G., Civitarese, A., Zimmet, P.Z., 2000. Beacon: a novel gene involved in the regulation of energy balance. Diabetes 49, 1766–1771.
62. Contin, M.A., Verra, D.M., Guido, M.E., 2006. An invertebrate-like phototransduction cascade mediates light detection in the chicken retinal ganglion cells. FASEB J. 20: 2648–2650.

63. Cuesta, M., Mendoza, J., Clesse, D., Pevet, P., Challet, E., 2008. Serotonergic activation potentiates light resetting of the main circadian clock and alters clock gene expression in a diurnal rodent. Exp Neurol. 210, 501-513.
64. D'Cruz, P.M., Yasumura, D., Weir, J., Matthes, M.T., Abderrahim, H., LaVail, M.M., Vollrath, D., 2000. Mutation of the receptor tyrosine kinase gene Mertk in the retinal dystrophic RCS rat. Hum Mol Genet. 9, 645-651.
65. Dave, K.R., Christian, S.L., Perez-Pinzon, M.A., Drew, K.L., 2012. Neuroprotection: lessons from hibernators. Comp Biochem Physiol B Biochem Mol Biol. 162, 1-9.
66. Davies, W.I., Collin, S.P., Hunt, D.M., 2012. Molecular ecology and adaptation of visual photopigments in craniates. Mol Ecol. 21, 3121-3158.
67. De Vera Mudry, M.C., Kronenberg, S., Komatsu, S., Aguirre, G.D., 2013. Blinded by the light: retinal phototoxicity in the context of safety studies. Toxicol Pathol. 41, 813-825.
68. Dellaa, A., Polosa, A., Mbarek, S., Hammoum, I., Messaoud, R., Amara, S., Azaiz, R., Charfeddine, R., Dogui, M., Khairallah, M., Lachapelle, P., Ben Chaouacha-Chekir, R., 2017. Characterizing the Retinal Function of Psammomys obesus: A Diurnal Rodent Model to Study Human Retinal Function. Curr Eye Res. 42, 79-87.
69. Dellaa, A., Benlarbi, M., Hammoum, I., Gammoudi, N., Dogui, M., Messaoud, R., Azaiz, R., Charfeddine, R., Khairallah, M., Lachapelle, P., Ben Chaouacha-Chekir, R., 2018. Electroretinographic evidence suggesting that the type 2 diabetic retinopathy of the sand rat Psammomys obesus is comparable to that of humans. PLoS One. 13, e0192400.
70. Derlig, K., Giessl, A., Brandstatter, J.H., Enz, R., Dahlhaus, R., 2015. Special characteristics of the transcription and splicing machinery in photoreceptor cells of the mammalian retina. Cell Tissue Res. 362, 281-294.
71. Dkhissi-Benyahya, O., Coutanson, C., Knoblauch, K., Lahouaoui, H., Leviel, V., Rey, C., Bennis, M., Cooper, H.M., 2013. The absence of melanopsin alters retinal clock function and dopamine regulation by light. Cell Mol Life Sci. 70, 3435-3447.
72. do Carmo Buonfiglio, D., Peliciari-Garcia, R.A., do Amaral, F.G., Peres, R., Nogueira, T.C., Afeche, S.C., Cipolla-Neto, J., 2011. Early-stage retinal melatonin synthesis impairment in streptozotocin-induced diabetic wistar rats. Invest Ophthalmol Vis Sci. 52, 7416-7422.
73. Do, M.T., Kang, S.H., Xue, T., Zhong, H., Liao, H.W., Bergles, D.E., Yau, K.W., 2009. Photon capture and signalling by melanopsin retinal ganglion cells. Nature. 457, 281-287.
74. Donath, M.Y., Gross, D.J., Cerasi, E., Kaiser, N., 1999. Hyperglycemia-induced beta-cell apoptosis in pancreatic islets of Psammomys obesus during development of diabetes. Diabetes. 48, 738-744.
75. Dosso, A.A., Bonvin, E.R., Morel, Y., Golay, A., Assal, J.P., Leuenberger, P.M., 1996. Risk factors associated with contrast sensitivity loss in diabetic patients. Graefes Arch. Clin. Exp. Ophthalmol. 234, 300–5.
76. Doyle, S.E., Yoshikawa, T., Hillson, H., Menaker, M., 2008. Retinal pathways influence temporal niche. Proc Natl Acad Sci U S A. 105, 13133-13138.
77. Du, L.Y., Chang, L.Y., Ardiles, A.O., Tapia-Rojas, C., Araya, J., Inestrosa, N.C., Palacios, A.G., Acosta, M.L., 2015. Alzheimer's Disease-Related Protein Expression in the Retina of Octodon degus. PLoS One. 10(8), e0135499.

78. Ducroz, J.F., Volobouev, V., and Granjon, L. 2001. An assessment of the systematics of Arvicanthine rodents using mitochondrial DNA sequences: Evolutionary and biogeographical implications. J Mammal Evol. 8, 173-206.
79. Ecker, J.L., Dumitrescu, O.N., Wong, K.Y., Alam, N.M., Chen, S.K., LeGates, T., Renna, J.M., Prusky, G.T., Berson, D.M., Hattar, S., 2010. Melanopsin-expressing retinal ganglion-cell photoreceptors: cellular diversity and role in pattern vision. Neuron. 67, 49-60.
80. Ericsson, A.C., Crim, M.J., Franklin, C.L., 2013. A brief history of animal modeling. Mo Med. 110, 201-205.
81. Escobar, M.J., Reyes, C., Herzog, R., Araya, J., Otero, M., Ibaceta, C., Palacios, A.G., 2018. Characterization of Retinal Functionality at Different Eccentricities in a Diurnal Rodent. Front Cell Neurosci. 12, 444.
82. Falcón, J., Migaud, H., Munoz-Cueto, J.A., Carrillo, M., 2010. Current knowledge on the melatonin system in teleost fish. Gen Comp Endocrinol. 165, 469-482.
83. Felder-Schmittbuhl, M.P., Buhr, E.D., Dkhissi-Benyahya, O., Hicks, D., Peirson, S.N., Ribelayga, C.P., Sandu, C., Spessert, R., Tosini, G. 2018. Ocular Clocks: Adapting Mechanisms for Eye Functions and Health. Invest Ophthalmol Vis Sci. 59, 4856-4870.
84. Feng, W., Yasumura, D., Matthes, M.T., LaVail, M.M., Vollrath, D. 2002. Mertk triggers uptake of photoreceptor outer segments during phagocytosis by cultured retinal pigment epithelial cells. J Biol Chem. 277, 17016–17022.
85. Finnemann, S.C., 2003. Role of alphavbeta5 integrin in regulating phagocytosis by the retinal pigment epithelium. Adv Exp Med Biol. 533, 337-342.
86. Finnemann, S.C., Nandrot, E.F., 2006. MerTK activation during RPE phagocytosis in vivo requires alphaVbeta5 integrin. Adv Exp Med Biol. 572, 499-503.
87. Fisher, S.K., Pfeffer, B.A., Anderson, D.H., 1983. Both rod and cone disc shedding are related to light onset in the cat. Invest Ophthalmol Vis Sci. 24, 844-856.
88. Fisher, S.K., Lewis, G.P., Linberg, K.A., Verardo, M.R., 2005. Cellular remodeling in mammalian retina: results from studies of experimental retinal detachment. Prog Retin Eye Res. 24, 395-431.
89. Flaisher-Grinberg, S., Gampetro, D.R., Kronfeld-Schor, N., Einat, H., 2011. Inconsistent effects of photoperiod manipulations in tests for affective-like changes in mice: implications for the selection of appropriate model animals. Behav Pharmacol. 22, 23-30.
90. Fonken, L.K., Haim, A., Nelson, R.J., 2012a. Dim light at night increases immune function in Nile grass rats, a diurnal rodent. Chronobiol Int. 29, 26-34.
91. Fonken, L.K., Kitsmiller, E., Smale, L., Nelson, R.J., 2012b. Dim nighttime light impairs cognition and provokes depressive-like responses in a diurnal rodent. J Biol Rhythms. 27, 319-327.
92. Frohns, A., Frohns, F., Naumann, S.C., Layer, P.G., Lobrich, M., 2014. Inefficient double-strand break repair in murine rod photoreceptors with inverted heterochromatin organization. Curr Biol. 24, 1080-1090.
93. Fujimoto, J., Swanson, E., 2016. The Development, Commercialization, and Impact of Optical Coherence Tomography. Invest Ophthalmol Vis Sci. 57, OCT1-OCT13.
94. Fujinami, K., Lois, N., Davidson, A.E., Mackay, D.S., Hogg, C.R., Stone, E.M., Tsunoda, K., Tsubota, K., Bunce, C., Robson, A.G., Moore, A.T., Webster, A.R., Holder, G.E.,

Michaelides, M., 2013. A longitudinal study of stargardt disease: clinical and electrophysiologic assessment, progression, and genotype correlations. Am J Ophthalmol. 155, 1075-1088.e1013.
95. Gaillard, F., Bonfield, S., Gilmour, G.S., Kuny, S., Mema, S.C., Martin, B.T., Smale, L., Crowder, N., Stell, W.K., Sauve, Y., 2008. Retinal anatomy and visual performance in a diurnal cone-rich laboratory rodent, the Nile grass rat (Arvicanthis niloticus). J Comp Neurol. 510, 525-538.
96. Gaillard, F., Kuny, S., Sauve, Y., 2009. Topographic arrangement of S-cone photoreceptors in the retina of the diurnal Nile grass rat (Arvicanthis niloticus). Invest Ophthalmol Vis Sci. 50, 5426-5434.
97. Gaillard, F., Karten, H.J., Sauve, Y., 2013. Retinorecipient areas in the diurnal murine rodent Arvicanthis niloticus: a disproportionally large superior colliculus. J Comp Neurol. 521, 1699-1726.
98. Gal, A., Li, Y., Thompson, D.A., Weir, J., Orth, U., Jacobson, S.G., Apfelstedt- Sylla, E., Vollrath, D., 2000. Mutations in MERTK, the human orthologue of the RCS rat retinal dystrophy gene, cause retinitis pigmentosa. Nat Genet. 26, 270-271.
99. Galer, B.S., Lee, D., Ma, T., Nagle, B., Schlagheck, T.G., 2005. MorphiDex (morphine sulfate/dextromethorphan hydrobromide combination) in the treatment of chronic pain: three multicenter, randomized, double-blind, controlled clinical trials fail to demonstrate enhanced opioid analgesia or reduction in tolerance. Pain. 115, 284-295.
100. Gall, A.J., Smale, L., Yan, L., Nunez, A.A., 2013. Lesions of the Intergeniculate Leaflet Lead to a Reorganization in Circadian Regulation and a Reversal in Masking Responses to Photic Stimuli in the Nile Grass Rat. PLoS One. 8, e67387.

101. Garbarino-Pico, E., Carpentieri, A.R., Contin, M.A., Sarmiento, M.I., Brocco, M.A., Panzetta, P., Rosenstein, R.E., Caputto, B.L., Guido, M.E., 2004. Retinal ganglion cells are autonomous circadian oscillators synthesizing N-acetylserotonin during the day. J Biol Chem. 279, 51172-51181.
102. Gastinger, M.J., Kunselman, A.R., Conboy, E.E., Bronson, S.K., Barber, A.J., 2008. Dendrite remodeling and other abnormalities in the retinal ganglion cells of Ins2 Akita diabetic mice. Invest Ophthalmol Vis Sci. 49, 2635-2642.
103. Gianesini, C., Clesse, D., Tosini, G., Hicks, D., Laurent, V., 2015. Unique Regulation of the Melatonin Synthetic Pathway in the Retina of Diurnal Female Arvicanthis ansorgei (Rodentia). Endocrinology. 156, 3292-3308.
104. Gianesini, C., Hiragaki, S., Laurent, V., Hicks, D., Tosini, G., 2016. Cone Viability Is Affected by Disruption of Melatonin Receptors Signaling. Invest Ophthalmol Vis Sci. 57, 94-104.
105. Gilmour, G.S., Gaillard, F., Watson, J., Kuny, S., Mema, S.C., Bonfield, S., Stell, W.K., Sauve, Y., 2008. The electroretinogram (ERG) of a diurnal cone-rich laboratory rodent, the Nile grass rat (Arvicanthis niloticus). Vision Res. 48, 2723-2731.
106. Graca, A.B., Hippert, C., Pearson, R.A., 2018. Muller Glia Reactivity and Development of Gliosis in Response to Pathological Conditions. Adv Exp Med Biol. 1074, 303-308.

107. Gregori, B., Papazachariadis, O., Farruggia, A., Accornero, N., 2011. A differential color flicker test for detecting acquired color vision impairment in multiple sclerosis and diabetic retinopathy. J. Neurol. Sci. 300, 130–134.
108. Grosbellet, E., Zahn, S., Arrive, M., Dumont, S., Gourmelen, S., Pevet, P., Challet, E., Criscuolo, F., 2015. Circadian desynchronization triggers premature cellular aging in a diurnal rodent. FASEB J. 29, 4794-4803.
109. Gualtieri, M., Feitosa-Santana, C., Lago, M., Nishi, M., Ventura, D.F., 2013. Early visual changes in diabetic patients with no retinopathy measured by color discrimination and electroretinography. Psychol & Neurosci. 6, 227-234.
110. Hackel, D.B., Frohman, L.A., Mikat, E., Lebovitz, H.E., Schmidt-Nielsen, K., Kinney, T.D., 1965. Review of current studies on effect of diet on the glucose tolerance of the sand rat (Psammomys Obesus) Ann. N. Y. Acad. Sci. 131, 459–463.
111. Haines, H., Hackel, D.B., Schmidt-Nielsen, K., 1965. Experimental diabetes mellitus induced by diet in the sand rat. Am. J. Physiol. 208, 297–300.
112. Ham, W.T., Jr., Mueller, H.A., Ruffolo, J.J., Jr., Guerry, D., 3rd, Guerry, R.K., 1982. Action spectrum for retinal injury from near-ultraviolet radiation in the aphakic monkey. Am J Ophthalmol. 93, 299-306.
113. Ham, W.T., Jr., Mueller, H.A., Sliney, D.H., 1976. Retinal sensitivity to damage from short wavelength light. Nature. 260, 153-155.
114. Hammes, H.-P., Lin, J., Renner, O., Shani, M., Lundqvist, A., Betsholtz, C., Brownlee, M., Deutsch, U., 2002. Pericytes and the pathogenesis of diabetic retinopathy. Diabetes 51, 3107–12.
115. Hammoum, I., Benlarbi, M., Dellaa, A., Szabo, K., Dekany, B., Csaba, D., Almasi, Z., Hajdu, R.I., Azaiz, R., Charfeddine, R., Lukats, A., Ben Chaouacha-Chekir, R., 2017a. Study of retinal neurodegeneration and maculopathy in diabetic Meriones shawi: A particular animal model with human-like macula. J Comp Neurol. 525, 2890-2914.
116. Hammoum, I., Mbarek, S., Dellaa, A., Dubus, E., Baccouche, B., Azaiz, R., Charfeddine, R., Picaud, S., Ben Chaouacha-Chekir, R., 2017b. Study of retinal alterations in a high fat diet-induced type ii diabetes rodent: Meriones shawi. Acta Histochem. 119, 1-9.
117. Hammoum, I., Benlarbi, M., Dellaa, A., Kahloun, R., Messaoud, R., Amara, S., Azaiz, R., Charfeddine, R., Dogui, M., Khairallah, M., Lukats, A., Ben Chaouacha-Chekir, R., 2018. Retinal dysfunction parallels morphologic alterations and precede clinically detectable vascular alterations in Meriones shawi, a model of type 2 diabetes. Exp Eye Res. 176, 174-187.
118. Hargreaves AD, Zhou L, Christensen J, Marlétaz F, Liu S, Li F, Jansen PG, Spiga E, Hansen MT, Pedersen SVH, Biswas S, Serikawa K, Fox BA, Taylor WR, Mulley JF, Zhang G, Heller RS, Holland PWH, 2017. Genome sequence of a diabetes-prone rodent reveals a mutation hotspot around the ParaHox gene cluster. Proc Natl Acad Sci U S A. 114,:7677-7682.
119. Hattar, S., Liao, H.W., Takao, M., Berson, D.M., Yau, K.W., 2002. Melanopsin-containing retinal ganglion cells: architecture, projections, and intrinsic photosensitivity. Science. 295, 1065-1070.

120. Hattar, S., Lucas, R.J., Mrosovsky, N., Thompson, S., Douglas, R.H., Hankins, M.W., Lem, J., Biel, M., Hofmann, F., Foster, R.G., Yau, K.W., 2003. Melanopsin and rod-cone photoreceptive systems account for all major accessory visual functions in mice. Nature. 424, 76-81.
121. Hattar, S., Kumar, M., Park, A., Tong, P., Tung, J., Yau, K.W., Berson, D.M., 2006. Central projections of melanopsin-expressing retinal ganglion cells in the mouse. J Comp Neurol. 497, 326-349.
122. Heesy, C.P., Hall, M.I., 2010. The nocturnal bottleneck and the evolution of mammalian vision. Brain Behav Evol. 75, 195-203.
123. Hendrickson, A., Hicks, D., 2002. Distribution and density of medium- and short-wavelength selective cones in the domestic pig retina. Exp Eye Res. 74, 435-444.
124. Hendrickson, A., 2005. Organization of the adult primate fovea, in: Penfold, P.L., Provis, J.M. (Eds.), Macular Degeneration. Springer-Verlag, Heidelberg, pp. 1-20.
125. Hippert, C., Graca, A.B., Pearson, R.A., 2016. Gliosis Can Impede Integration Following Photoreceptor Transplantation into the Diseased Retina. Adv Exp Med Biol. 854, 579-585.
126. Honacki, J.H., Kinman, K.E., Koeppl, J.W. 1982. Mammalian Species of the World: A Taxonomic and Geographic Reference. Lawrence: Allen Press, Inc..
127. Huber, G., Heynen, S., Imsand, C., vom Hagen, F., Muehlfriedel, R., Tanimoto, N., Feng, Y., Hammes, H.P., Grimm, C., Peichl, L., Seeliger, M.W., Beck, S.C., 2010. Novel rodent models for macular research. PLoS One. 5, e13403.
128. Hut, R.A., Kronfeld-Schor, N., van der Vinne, V., De la Iglesia, H., 2012. In search of a temporal niche: environmental factors. Prog Brain Res. 199, 281-304.
129. Immel, J.H., Fisher, S.K., 1985. Cone photoreceptor shedding in the tree shrew (Tupaia belangerii). Cell Tissue Res. 239, 667-675.
130. Iuvone, P.M., Brown, A.D., Haque, R., Weller, J., Zawilska, J.B., Chaurasia, S.S., Ma, M., Klein, D.C., 2002. Retinal melatonin production: role of proteasomal proteolysis in circadian and photic control of arylalkylamine N-acetyltransferase. Invest Ophthalmol Vis Sci. 43, 564-572.
131. Jacobs, G.H., Calderone, J.B., Fenwick, J.A., Krogh, K., Williams, G.A., 2003. Visual adaptations in a diurnal rodent, Octodon degus. J Comp Physiol A Neuroethol Sens Neural Behav Physiol. 189, 347-361.
132. Jang, S.W., Liu, X., Pradoldej, S., Tosini, G., Chang, Q., Iuvone, P.M., Ye, K., 2010. N-acetylserotonin activates TrkB receptor in a circadian rhythm. Proc Natl Acad Sci USA. 107, 3876-3881.
133. Jeon, C.J., Strettoi, E., Masland, R.H., 1998. The major cell populations of the mouse retina. J Neurosci. 18, 8936-8946.
134. Jeong, M.J., Jeon, C.J., 2015. Localization of melanopsin-immunoreactive cells in the Mongolian gerbil retina. Neurosci Res. 100, 6-16.
135. Jörns, A., Tiedge, M., Ziv, E., Shafrir, E., Lenzen, S., 2002. Gradual loss of pancreatic beta-cell insulin, glucokinase and GLUT2 glucose transporter immunoreactivities during the time course of nutritionally induced type-2 diabetes in Psammomys obesus (sand rat). Virchows Arch. 440, 63–9.

136. Kaitz, M., Auerbach, E., 1979. Action spectrum for light-induced retinal degeneration in dystrophic rats. Vision Res. 19, 1041-1044.
137. Kalderon, B., Gutman, A., Levy, E., Shafrir, E., Adler, J.H., 1986. Characterization of Stages in Development of Obesity-Diabetes Syndrome in Sand Rat (Psammomys obesus). Diabetes 35, 717–724.
138. Kalman, R., Adler, J.H., Lazarovici, G., Bar-On, H., Ziv, E., 1993. The efficiency of sand rat metabolism is responsible for development of obesity and diabetes. J Basic Clin Physiol Pharmacol. 4, 57-68.
139. Karnas, D., Hicks, D., Mordel, J., Pevet, P., Meissl, H., 2013a. Intrinsic photosensitive retinal ganglion cells in the diurnal rodent, Arvicanthis ansorgei. PLoS One. 8, e73343.
140. Karnas, D., Mordel, J., Bonnet, D., Pevet, P., Hicks, D., Meissl, H., 2013b. Heterogeneity of intrinsically photosensitive retinal ganglion cells in the mouse revealed by molecular phenotyping. J Comp Neurol. 521, 912-932.
141. Keplinger, S., Beiderbeck, B., Michalakis, S., Biel, M., Grothe, B., Kunz, L., 2018. Optogenetic Control of Neural Circuits in the Mongolian Gerbil. Front Cell Neurosci. 12, 111.
142. Kizawa, J., Machida, S., Kobayashi, T., Gotoh, Y., Kurosaka, D., 2006. Changes of oscillatory potentials and photopic negative response in patients with early diabetic retinopathy. Jpn J Ophthalmol. 50, 367-373.
143. Klemp, K., Sander, B., Brockhoff, P.B., Vaag, A., Lund-Andersen, H., Larsen, M., 2005. The multifocal ERG in diabetic patients without retinopathy during euglycemic clamping. Invest Ophthalmol Vis Sci. 46, 2620-2626.
144. Klosen, P., Lapmanee, S., Schuster, C., Guardiola, B., Hicks, D., Pevet, P., Felder-Schmittbuhl, M.P., 2019. MT1 and MT2 melatonin receptors are expressed in nonoverlapping neuronal populations. J Pineal Res. e12575.
145. Ko, G.Y., 2018. Circadian regulation in the retina: From molecules to network. Eur J Neurosci.
146. Kohler, E., Knospe, S., 1980. Glucose metabolism and responsiveness of muscle to insulin during the development of diabetes in sand rats. Endokrinologie 75, 225–234.
147. Kohzaki, K., Vingrys, A.J., Bui, B. V., 2008. Early Inner Retinal Dysfunction in Streptozotocin-Induced Diabetic Rats. Investig. Ophthalmology Vis. Sci. 49, 3595.
148. Kostic, C., Arsenijevic, Y., 2016. Animal modelling for inherited central vision loss. J Pathol. 238, 300-310.

149. Kryger, Z., Galli-Resta, L., Jacobs, G.H., Reese, B.E., 1998. The topography of rod and cone photoreceptors in the retina of the ground squirrel. Vis Neurosci. 15, 685-691.
150. Kuwabara, T., 1975. Cytologic changes of the retina and pigment epithelium during hibernation. Invest Ophthalmol. 14, 457-467.
151. Kyba, C.C.M., Kuester, T., Sanchez de Miguel, A., Baugh, K., Jechow, A., Holker, F., Bennie, J., Elvidge, C.D., Gaston, K.J., Guanter, L., 2017. Artificially lit surface of Earth at night increasing in radiance and extent. Sci Adv. 3, e1701528.
152. LaCroix-Fralish, M.L., Austin, J.S., Zheng, F.Y., Levitin, D.J., Mogil, J.S., 2011. Patterns of pain: meta-analysis of microarray studies of pain. Pain. 152, 1888-1898.
153. Lamb, T.D., 2013. Evolution of phototransduction, vertebrate photoreceptors and retina. Prog Retin Eye Res. 36, 52-119.
154. Langel, J.L., Smale, L., Esquiva, G., Hannibal, J., 2015. Central melanopsin projections in the diurnal rodent, Arvicanthis niloticus. Front Neuroanat. 9, 93.
155. Laurent, V., Sengupta, A., Sánchez-Bretaño, A., Hicks, D., Tosini, G. 2017 Melatonin signaling affects the timing in the daily rhythm of phagocytic activity by the retinal pigment epithelium. Exp Eye Res. 165, 90-95.
156. LaVail, M.M., 1980. Circadian nature of rod outer segment disc shedding in the rat. Invest Ophthalmol Vis Sci. 19, 407-411.
157. Leach, G., Adidharma, W., Yan, L., 2013. Depression-like responses induced by daytime light deficiency in the diurnal grass rat (Arvicanthis niloticus). PLoS One. 8, e57115.
158. Lewis, G.P., Sethi, C.S., Carter, K.M., Charteris, D.G., Fisher, S.K., 2005. Microglial cell activation following retinal detachment: a comparison between species. Mol Vis. 11, 491-500.
159. Leibowitz, G., Ferber, S., Apelqvist A, Å., Edlund, H., Gross, D.J., Cerasi, E., Melloul, D., Kaiser, N., 2001. IPF1/PDX1 deficiency and beta-cell dysfunction in Psammomys obesus, an animal With type 2 diabetes. Diabetes 50, 1799–806.
160. Light, A.C., Zhu, Y., Shi, J., Saszik, S., Lindstrom, S., Davidson, L., Li, X., Chiodo, V.A., Hauswirth, W.W., Li, W., DeVries, S.H., 2012. Organizational motifs for ground squirrel cone bipolar cells. J Comp Neurol. 520, 2864-2887.
161. Lim, L.S., Liew, G., Cheung, N., Mitchell, P., Wong, T.Y., 2010. Mixed messages on systemic therapies for diabetic retinopathy. Lancet 376, 1461. h
162. Linberg, K.A., Sakai, T., Lewis, G.P., Fisher, S.K., 2002. Experimental retinal detachment in the cone-dominant ground squirrel retina: morphology and basic immunocytochemistry. Vis Neurosci. 19, 603-619.
163. Litts, K.M., Cooper, R.F., Duncan, J.L., Carroll, J., 2017. Photoreceptor-Based Biomarkers in AOSLO Retinal Imaging. Invest Ophthalmol Vis Sci. 58, BIO255-BIO267
164. Liu, C., Fukuhara, C., Wessel, J.H., 3rd, Iuvone, P.M., Tosini, G., 2004. Localization of Aa-nat mRNA in the rat retina by fluorescence in situ hybridization and laser capture microdissection. Cell Tissue Res. 315, 197-201.
165. Liu, X., Zhang, Z., Ribelayga, C.P., 2012. Heterogeneous expression of the core circadian clock proteins among neuronal cell types in mouse retina. PLoS One. 7(11), e50602.

166. Liu, M.M., Farkas, M., Spinnhirny, P., Pevet, P., Pierce, E., Hicks, D., Zack, D.J., 2017. De novo assembly and annotation of the retinal transcriptome for the Nile grass rat (Arvicanthis ansorgei). PLoS One. 12, e0179061.
167. Luan, Y., Ou, J., Kunze, V.P., Qiao, F., Wang, Y., Wei, L., Li, W., Xie, Z., 2018. Integrated transcriptomic and metabolomic analysis reveals adaptive changes of hibernating retinas. J Cell Physiol. 233, 1434-1445.
168. Lunn, R.M., Blask, D.E., Coogan, A.N., Figueiro, M.G., Gorman, M.R., Hall, J.E., et al., 2017.
169. Health consequences of electric lighting practices in the modern world: A report on the National Toxicology Program's workshop on shift work at night, artificial light at night, and circadian disruption. Sci Total Environ. 607-608, 1073-1084.
170. Lynch, L., O'Shea, D., Winter, D.C., Geoghegan, J., Doherty, D.G., O'Farrelly, C., 2009. Invariant NKT cells and CD1d(+) cells amass in human omentum and are depleted in patients with cancer and obesity. Eur J Immunol. 39, 1893-1901.
171. Machida, S., Gotoh, Y., Tanaka, M., Tazawa, Y., 2004. Predominant loss of the photopic negative response in central retinal artery occlusion. Am. J. Ophthalmol. 137, 938–940.
172. Mahoney, M.M., Sisk, C., Ross, H.E., Smale, L., 2004. Circadian regulation of gonadotropin-releasing hormone neurons and the preovulatory surge in luteinizing hormone in the diurnal rodent, Arvicanthis niloticus, and in a nocturnal rodent, Rattus norvegicus. Biol Reprod. 70, 1049-1054.
173. Mao, Y., Finnemann, S.C., 2012. Essential diurnal Rac1 activation during retinal phagocytosis requires alphavbeta5 integrin but not tyrosine kinases focal adhesion kinase or Mer tyrosine kinase. Mol Biol Cell. 23, 1104-1114.
174. Marek, G., Pannu, V., Shanmugham, P., Pancione, B., Mascia, D., Crosson, S., Ishimoto, T., Sautin, Y.Y., 2015. Adiponectin resistance and proinflammatory changes in the visceral adipose tissue induced by fructose consumption via ketohexokinase-dependent pathway. Diabetes 64, 508–18.
175. Matsui, Y., Katsumi, O., Sakaue, H., Hirose, T., 1994. Electroretinogram b/a wave ratio improvement in central retinal vein obstruction. Br. J. Ophthalmol. 78, 191–198.
176. McElhinny, T.L., Smale, L., Holekamp, K.E., 1997. Patterns of body temperature, activity, and reproductive behavior in a tropical murid rodent, Arvicanthis niloticus. Physiol Behav. 62, 91-96.
177. McElhinny, T.L., Sisk, C.L., Holekamp, K.E., Smale, L., 1999. A morning surge in plasma luteinizing hormone coincides with elevated Fos expression in gonadotropin-releasing hormone-immunoreactive neurons in the diurnal rodent, Arvicanthis niloticus. Biol Reprod. 61, 1115-1122.
178. McMahon, D.G., Iuvone, P.M., Tosini, G., 2014. Circadian organization of the mammalian retina: from gene regulation to physiology and diseases. Prog Retin Eye Res. 39, 58-76.
179. Mehdi, M.K., Hicks, D., 2010. Structural and physiological responses to prolonged constant lighting in the cone-rich retina of Arvicanthis ansorgei. Exp Eye Res. 91, 793-799.

180. Mendoza, J., Pevet, P., Challet, E., 2008. High-fat feeding alters the clock synchronization to light. J Physiol. 586, 5901-5910.
181. Mendoza, J., Gourmelen, S., Dumont, S., Sage-Ciocca, D., Pévet, P., Challet, E., 2012. Setting the main circadian clock of a diurnal mammal by hypocaloric feeding. J Physiol. 590, 3155-3168.
182. Merriman, D.K., Lahvis, G., Jooss, M., Gesicki, J.A., Schill, K., 2012. Current practices in a captive breeding colony of 13-lined ground squirrels (Ictidomys tridecemlineatus). Lab Anim (NY). 41, 315-325.
183. Merriman, D.K., Sajdak, B.S., Li, W., Jones, B.W., 2016. Seasonal and post-trauma remodeling in cone-dominant ground squirrel retina. Exp Eye Res. 150, 90-105.
184. Meyer-Rusenberg, B., Pavlidis, M., Stupp, T., Thanos, S., 2007. Pathological changes in human retinal ganglion cells associated with diabetic and hypertensive retinopathy. Graefes Arch Clin Exp Ophthalmol. 245, 1009-1018.
185. Misonne, X. 1969. African and Indo-Australian muridae: Evolutionary trends. Ann. Mus. Roy. Afr. Centr.
186. Mizutani, M., Kern, T.S., Lorenzi, M., 1996. Accelerated death of retinal microvascular cells in human and experimental diabetic retinopathy. J. Clin. Invest. 97, 2883–2890.
187. Moreno, J.A., Hong, E., 2013. A single oral dose of fructose induces some features of metabolic syndrome in rats: Role of oxidative stress. Nutr. Metab. Cardiovasc. Dis. 23, 536–542.
188. Mullen, R.J., LaVail, M.M., 1976. Inherited retinal dystrophy: primary defect in pigment epithelium determined with experimental rat chimeras. Science. 192, 799-801.
189. Muller, B., Peichl, L., 1989. Topography of cones and rods in the tree shrew retina. J Comp Neurol. 282, 581-594.
190. Mure, L.S., Le, H.D., Benegiamo, G., Chang, M.W., Rios, L., Jillani, N., Ngotho, M., Kariuki, T., Dkhissi-Benyahya, O., Cooper, H.M., Panda, S., 2018. Diurnal transcriptome atlas of a primate across major neural and peripheral tissues. Science. 359.
191. Mustafi, D., Kevany, B.M., Bai, X., Golczak, M., Adams, M.D., Wynshaw-Boris, A., Palczewski, K., 2016. Transcriptome analysis reveals rod/cone photoreceptor specific signatures across mammalian retinas. Hum Mol Genet. 25, 4376-4388.
192. Nandrot, E.F., Silva, K.E., Scelfo, C., Finnemann, S.C., 2012. Retinal pigment epithelial cells use a MerTK-dependent mechanism to limit the phagocytic particle binding activity of alphavbeta5 integrin. Biol Cell. 104, 326-341.
193. Neel, J. V, 1962. Diabetes mellitus: a “thrifty” genotype rendered detrimental by “progress”? Am. J. Hum. Genet. 14, 353–62.
194. Nelson, D.E., Takahashi, J.S., 1991. Sensitivity and integration in a visual pathway for circadian entrainment in the hamster (Mesocricetus auratus). J Physiol. 439, 115-145.
195. Nesher, R., Gross, D.J., Donath, M.Y., Cerasi, E., Kaiser, N., 1999. Interaction between genetic and dietary factors determines beta-cell function in Psammomys obesus, an animal model of type 2 diabetes. Diabetes. 48, 731-737.

196. Niki, T., Hamada, T., Ohtomi, M., Sakamoto, K., Suzuki, S., Kako, K., Hosoya, Y., Horikawa, K., Ishida, N., 1998. The localization of the site of arylalkylamine N-acetyltransferase circadian expression in the photoreceptor cells of mammalian retina. Biochem Biophys Res Commun. 248, 115-120.
197. Noda, K., Melhorn, M.I., Zandi, S., Frimmel, S., Tayyari, F., Hisatomi, T., Almulki, L., Pronczuk, A., Hayes, K.C., Hafezi-Moghadam, A., 2010. An animal model of spontaneous metabolic syndrome: Nile grass rat. FASEB J. 24, 2443-2453.
198. Noda, K., Nakao, S., Zandi, S., Sun, D., Hayes, K.C., Hafezi-Moghadam, A., 2014. Retinopathy in a novel model of metabolic syndrome and type 2 diabetes: new insight on the inflammatory paradigm. FASEB J. 28, 2038-2046.
199. Noell, W.K., Walker, V.S., Kang, B.S., Berman, S., 1966. Retinal damage by light in rats. Invest Ophthalmol. 5, 450-473.
200. Novak, C.M., Smale, L., Nunez, A.A., 1999. Fos expression in the sleep-active cell group of the ventrolateral preoptic area in the diurnal murid rodent, Arvicanthis niloticus. Brain Res. 818, 375-382.
201. Novak, C.M., Harris, J.A., Smale, L., Nunez, A.A., 2000. Suprachiasmatic nucleus projections to the paraventricular thalamic nucleus in nocturnal rats (Rattus norvegicus) and diurnal nile grass rats (Arvicanthis niloticus). Brain Res. 874, 147-157.
202. Novak, C.M., Parfitt, D.B., Sisk, C.L., Smale, L., 2007. Associations between behavior, hormones, and Fos responses to novelty differ in pre- and post-pubertal grass rats. Physiol Behav. 90, 125-132.
203. Nowak, R.M. 1991. Walker's Mammals of the World. 5th ed. vol 2. Baltimore: The Johns Hopkins University Press.
204. O'Day, W.T., Young, R.W., 1979. The effects of prolonged exposure to cold on visual cells of the goldfish. Exp Eye Res. 28, 167-187.
205. Organisciak, D.T., Darrow, R.M., Barsalou, L., Kutty, R.K., Wiggert, B., 2000. Circadian-dependent retinal light damage in rats. Invest Ophthalmol Vis Sci. 41, 3694-3701.
206. Organisciak, D.T., Vaughan, D.K., 2010. Retinal light damage: mechanisms and protection. Prog Retin Eye Res. 29, 113-134.
207. Orlov, V.N., Baskevich, M.I., Bulatova, N.Sh. 1992. Chromosomal sets of rats of the genus Arvicanthis (Rodentia, Muridae). Ethiopia Zool Zh. 71, 103–112.
208. Osborn, D.J., Helmy, I., 1980. The Contemporary Land Mammals of Egypt (Including Sinai). Date accessed: 04/29/2019. https://apps.dtic.mil/docs/citations/ADA098327
209. Otalora, B.B., Hagenauer, M.H., Rol, M.A., Madrid, J.A., Lee, T.M., 2013. Period gene expression in the brain of a dual-phasing rodent, the Octodon degus. J Biol Rhythms. 28, 249-261.
210. Ou, J., Ball, J.M., Luan, Y., Zhao, T., Miyagishima, K.J., Xu, Y., Zhou, H., Chen, J., Merriman, D.K., Xie, Z., Mallon, B.S., Li, W., 2018. iPSCs from a Hibernator Provide a Platform for Studying Cold Adaptation and Its Potential Medical Applications. Cell. 173, 851-863.e816.
211. Palacios, A.G., Lee, T.M., 2013. Husbandry and breeding in the Octodon degu (Molina 1782). Cold Spring Harb Protoc. 2013, 350-353.

212. Panda, S., Sato, T.K., Castrucci, A.M., Rollag, M.D., DeGrip, W.J., Hogenesch, J.B., Provencio, I., Kay, S.A., 2002. Melanopsin (Opn4) requirement for normal light-induced circadian phase shifting. Science. 298, 2213-2216.
213. Peichl, L., 2005. Diversity of mammalian photoreceptor properties: adaptations to habitat and lifestyle? Anat Rec A Discov Mol Cell Evol Biol. 287, 1001-1012.
214. Peirson, S.N., Butler, J.N., Duffield, G.E., Takher, S., Sharma, P., Foster, R.G., 2006. Comparison of clock gene expression in SCN, retina, heart, and liver of mice. Biochem Biophys Res Commun. 351, 800-807.
215. Pertusa, J.A., Nesher, R., Kaiser, N., Cerasi, E., Henquin, J.C., Jonas, J.C., 2002. Increased glucose sensitivity of stimulus-secretion coupling in islets from Psammomys obesus after diet induction of diabetes. Diabetes. 51, 2552-2560.
216. Pevet, P., Challet, E., 2011. Melatonin: both master clock output and internal time-giver in the circadian clocks network. J Physiol Paris. 105, 170-182.
217. Phillips, A.J.K., Fulcher, B.D., Robinson, P.A., Klerman, E.B., 2013. Mammalian rest/activity patterns explained by physiologically based modeling. PLoS Comput. Biol. 9, e1003213.
218. Pozdeyev, N., Taylor, C., Haque, R., Chaurasia, S.S., Visser, A., Thazyeen, A., Du, Y., Fu, H., Weller, J., Klein, D.C., Iuvone, P.M., 2006. Photic regulation of arylalkylamine N-acetyltransferase binding to 14-3-3 proteins in retinal photoreceptor cells. J Neurosci. 26, 9153-9161.
219. Provencio, I., Rollag, M.D., Castrucci, A.M., 2002. Photoreceptive net in the mammalian retina. This mesh of cells may explain how some blind mice can still tell day from night. Nature. 415, 493.
220. Rees, D.A., Alcolado, J.C., 2005. Animal models of diabetes mellitus. Diabet Med. 22, 359-370.
221. Refinetti, R., 2006. Variability of diurnality in laboratory rodents. J Comp Physiol A Neuroethol Sens Neural Behav Physiol. 192, 701-714.
Reid, C.A., Ertel, K.J., Lipinski, D.M., 2017. Improvement of Photoreceptor Targeting via Intravitreal Delivery in Mouse and Human Retina Using Combinatory rAAV2 Capsid Mutant Vectors. Invest Ophthalmol Vis Sci 58, 6429-6439.
222. Reme, C.E., Young, R.W., 1977. The effects of hibernation on cone visual cells in the ground squirrel. Invest Ophthalmol Vis Sci. 16, 815-840.
223. Rodriguez-Ramos Fernandez, J., Dubielzig, R.R., 2013. Ocular comparative anatomy of the family Rodentia. Vet Ophthalmol. 16 Suppl 1, 94-99.
224. Rosolen, S.G., Rigaudière, F., Le Gargasson, J.F., Chalier, C., Rufiange, M., Racine, J., Joly, S., Lachapelle, P., 2004. Comparing the photopic ERG i-wave in different species. Vet Ophthalmol. 7, 189-192.
225. Rousseau, S., McKerral, M., Lachapelle, P., 1996. The i-wave: bridging flash and pattern electroretinography. Electroencephalogr Clin Neurophysiol. Suppl. 46, 165-171.
226. Roy, M.S., Gunkel, R.D., Podgor, M.J., 1986. Color vision defects in early diabetic retinopathy. Arch Ophthalmol. 104, 225-228.
227. Ruan, G.X., Zhang, D.Q., Zhou, T., Yamazaki, S., McMahon, D.G., 2006. Circadian organization of the mammalian retina. Proc Natl Acad Sci USA. 103, 9703-9708.

228. Ruan, G.X., Allen, G.C., Yamazaki, S., McMahon, D.G., 2008. An autonomous circadian clock in the inner mouse retina regulated by dopamine and GABA. PLoS Biol. 6, e249.
229. Ruan, G.X., Gamble, K.L., Risner, M.L., Young, L.A., McMahon, D.G., 2012. Divergent roles of clock genes in retinal and suprachiasmatic nucleus circadian oscillators. PLoS One. 7, e38985.
230. Ruggiero, L., Connor, M.P., Chen, J., Langen, R., Finnemann, S.C., 2012. Diurnal, localized exposure of phosphatidylserine by rod outer segment tips in wild-type but not Itgb5-/- or Mfge8-/- mouse retina. Proc Natl Acad Sci USA. 109, 8145-8148.
231. Russart, K.L.G., Nelson, R.J., 2018. Light at night as an environmental endocrine disruptor. Physiol Behav. 190, 82-89.
232. Rutledge, A.C., Adeli, K., 2007. Fructose and the metabolic syndrome: pathophysiology and molecular mechanisms. Nutr Rev. 65, S13-23.
233. Saidi, T., Mbarek, S., Chaouacha-Chekir, R.B., Hicks, D., 2011a. Diurnal rodents as animal models of human central vision: characterisation of the retina of the sand rat Psammomys obesus. Graefes Arch Clin Exp Ophthalmol. 249, 1029-1037.
234. Saidi, T., Mbarek, S., Omri, S., Behar-Cohen, F., Chaouacha-Chekir, R.B., Hicks, D., 2011b. The sand rat, Psammomys obesus, develops type 2 diabetic retinopathy similar to humans. Invest Ophthalmol Vis Sci. 52, 8993-9004.
235. Sajdak, B., Sulai, Y.N., Langlo, C.S., Luna, G., Fisher, S.K., Merriman, D.K., Dubra, A., 2016. Noninvasive imaging of the thirteen-lined ground squirrel photoreceptor mosaic. Vis Neurosci. 33, e003.
236. Sajdak, B.S., Bell, B.A., Lewis, T.R., Luna, G., Cornwell, G.S., Fisher, S.K., Merriman, D.K., Carroll, J., 2018. Assessment of Outer Retinal Remodeling in the Hibernating 13-Lined Ground Squirrel. Invest Ophthalmol Vis Sci. 59, 2538-2547.
237. Sajdak, B.S., Salmon, A.E., Cava, J.A., Allen, K.P., Freling, S., Ramamirtham, R., Norton, T.T., Roorda, A., Carroll, J., 2019a. Noninvasive imaging of the tree shrew eye: Wavefront analysis and retinal imaging with correlative histology. Exp Eye Res. 185, 107683.
238. Sajdak, B.S., Salmon, A.E., Litts, K.M., Wells, C., Allen, K.P., Dubra, A., Merriman, D.K., Carroll, J., 2019b. Evaluating seasonal changes of cone photoreceptor structure in the 13-lined ground squirrel. Vision Res. 158, 90-99.
239. Sakai, T., Calderone, J.B., Lewis, G.P., Linberg, K.A., Fisher, S.K., Jacobs, G.H., 2003. Cone photoreceptor recovery after experimental detachment and reattachment: an immunocytochemical, morphological, and electrophysiological study. Invest Ophthalmol Vis Sci. 44, 416-425.
240. Sande, P.H., Fernandez, D.C., Aldana Marcos, H.J., Chianelli, M.S., Aisemberg, J., Silberman, D.M., Saenz, D.A., Rosenstein, R.E., 2008. Therapeutic effect of melatonin in experimental uveitis. Am J Pathol. 173, 1702-1713.
241. Sandu, C., Hicks, D., Felder-Schmittbuhl, M.P., 2011. Rat photoreceptor circadian oscillator strongly relies on lighting conditions. Eur J Neurosci. 34, 507-516.
242. Schmidt-Nielsen, K., Haines, H.B., Hackel, D.B., 1964. Diabetes mellitus in the sand rat induced by standard laboratory diets. Science. 143, 689-690.

243. Schwartz, M., Nunez, A., Smale, L., 2004. Differences in the suprachiasmatic nucleus and lower subparaventricular zone of diurnal and nocturnal rodents. Neuroscience 127, 13–23.
244. Schwartz, M.D., Urbanski, H.F., Nunez, A.A., Smale, L., 2011. Projections of the suprachiasmatic nucleus and ventral subparaventricular zone in the Nile grass rat (Arvicanthis niloticus). Brain Res. 1367, 146–161.
245. Sen, S., Raingard, H., Dumont, S., Kalsbeek, A., Vuillez, P., Challet E., 2017. Ultradian feeding in mice not only affects the peripheral clock in the liver, but also the master clock in the brain. Chronobiol Int. 34, 17-36.
246. Sengupta, A., Baba, K., Mazzoni, F., Pozdeyev, N.V., Strettoi, E., Iuvone, P.M., Tosini, G., 2011. Localization of melatonin receptor 1 in mouse retina and its role in the circadian regulation of the electroretinogram and dopamine levels. PLoS One. 6, e24483.
247. Shafrir, E., Ziv, E., 1998. Cellular mechanism of nutritionally induced insulin resistance: the desert rodent Psammomys obesus and other animals in which insulin resistance leads to detrimental outcome. J Basic Clin Physiol Pharmacol. 9, 347-385.
248. Shafrir, E., Ziv, E., Kalman, R., 2006. Nutritionally induced diabetes in desert rodents as models of type 2 diabetes: Acomys cahirinus (spiny mice) and Psammomys obesus (desert gerbil). Ilar J. 47, 212-224.
249. Shafrir, E., Ziv, E., 2009. A useful list of spontaneously arising animal models of obesity and diabetes. Am J Physiol Endocrinol Metab. 296, E1450-1452.
250. Shuboni, D.D., Cramm, S.L., Yan, L., Ramanathan, C., Cavanaugh, B.L., Nunez, A.A., Smale, L., 2015. Acute effects of light on the brain and behavior of diurnal Arvicanthis niloticus and nocturnal Mus musculus. Physiol Behav. 138, 75-86.
251. Sicard, B., Catalan, J., Ag-Atheyinine, S., Diarra, W., and Britton-Davidian, J. 1999. Biogeographical distribution of Arvicanthis niloticus Demarest 1822 and Arvicanthis ansorgei Thomas 1910 (Rodentia, Muridae) in Mali. In Abstracts of the 8th International Symposium on African Small Mammals, pp 2526, Paris.
252. Simo, R., Hernandez, C., & European Consortium for the Early Treatment of Diabetic Retinopathy, 2012. Neurodegeneration is an early event in diabetic retinopathy: therapeutic implications. Br J Ophthalmol. 96, 1285-1290.
253. Slijkerman, R.W., Song, F., Astuti, G.D., Huynen, M.A., van Wijk, E., Stieger, K., Collin, R.W., 2015. The pros and cons of vertebrate animal models for functional and therapeutic research on inherited retinal dystrophies. Prog Retin Eye Res. 48, 137-159.
254. Smale, L., Boverhof, J., 1999. The suprachiasmatic nucleus and intergeniculate leaflet of Arvicanthis niloticus, a diurnal murid rodent from East Africa. J Comp Neurol. 403, 190-208.
255. Solovei, I., Kreysing, M., Lanctot, C., Kosem, S., Peichl, L., Cremer, T., Guck, J., Joffe, B., 2009. Nuclear architecture of rod photoreceptor cells adapts to vision in mammalian evolution. Cell. 137, 356-368.
256. Solovei, I., Wang, A.S., Thanisch, K., Schmidt, C.S., Krebs, S., Zwerger, M., Cohen, T.V., Devys, D., Foisner, R., Peichl, L., Herrmann, H., Blum, H., Engelkamp, D., Stewart, C.L., Leonhardt, H., Joffe, B., 2013. LBR and lamin A/C sequentially tether peripheral heterochromatin and inversely regulate differentiation. Cell. 152, 584-598.

257. Staples, J.F., 2016. Metabolic Flexibility: Hibernation, Torpor, and Estivation. Compr Physiol. 6, 737-771.
258. Steinberg, R.H., Wood, I., Hogan, M.J., 1977. Pigment epithelial ensheathment and phagocytosis of extrafoveal cones in human retina. Philos Trans R Soc Lond B Biol Sci. 277, 459-474.
259. Storch, K.F., Paz, C., Signorovitch, J., Raviola, E., Pawlyk, B., Li, T., Weitz, C.J., 2007. Intrinsic circadian clock of the mammalian retina: importance for retinal processing of visual information. Cell. 130, 730-741.
260. Szabadfi, K., Estrada, C., Fernandez-Villalba, E., Tarragon, E., Setalo, G., Jr., Izura, V., Reglodi, D., Tamas, A., Gabriel, R., Herrero, M.T., 2015. Retinal aging in the diurnal Chilean rodent (Octodon degus): histological, ultrastructural and neurochemical alterations of the vertical information processing pathway. Front Cell Neurosci. 9, 126.
261. Szel, A., Rohlich, P., 1992. Two cone types of rat retina detected by anti-visual pigment antibodies. Exp Eye Res. 55, 47-52.
262. Tabor, G.A., Fisher, S.K., Anderson, D.H., 1980. Exp Eye Res. 30, 545-57
263. Tamai, M., Chader, G.J., 1979. The early appearance of disc shedding in the rat retina. Invest Ophthalmol Vis Sci. 18, 913-917.
264. Taomoto, M., Nambu, H., Senzaki, H., Shikata, N., Oishi, Y., Fujii, T., Miki, H., Uyama, M., Tsubura, A., 1998. Retinal degeneration induced by N-methyl-N-nitrosourea in Syrian golden hamsters. Graefes Arch Clin Exp Ophthalmol. 236, 688-695.
265. Terman, J.S., Reme, C.E., Terman, M., 1993. Rod outer segment disk shedding in rats with lesions of the suprachiasmatic nucleus. Brain Res. 605, 256-264.
266. Todd, W.D., Gall, A.J., Weiner, J.A., Blumberg, M.S., 2012. Distinct retinohypothalamic innervation patterns predict the developmental emergence of species-typical circadian phase preference in nocturnal Norway rats and diurnal nile grass rats. J Comp Neurol. 520, 3277-3292.
267. Tosini, G., Menaker, M., 1996. Circadian rhythms in cultured mammalian retina. Science. 272, 419-421.
268. Tosini, G., Ye, K., Iuvone, P.M., 2012. N-acetylserotonin: neuroprotection, neurogenesis, and the sleepy brain. Neuroscientist. 18, 645-653.
269. Touati, H., Ouali-Hassenaoui, S., Dekar-Madoui, A., Challet, E., Pevet, P., Vuillez, P., 2018. Diet-induced insulin resistance state disturbs brain clock processes and alters tuning of clock outputs in the Sand rat, Psammomys obesus. Brain Res. 1679, 116-124.
270. Touitou, Y., Reinberg, A., Touitou, D., 2017. Association between light at night, melatonin secretion, sleep deprivation, and the internal clock: Health impacts and mechanisms of circadian disruption. Life Sci. 173, 94-106.
271. Tu, D.C., Zhang, D., Demas, J., Slutsky, E.B., Provencio, I., Holy, T.E., Van Gelder, R.N., 2005. Physiologic diversity and development of intrinsically photosensitive retinal ganglion cells. Neuron. 48, 987-999.
272. Tzekov, R., Arden, G.B., 1999. The electroretinogram in diabetic retinopathy. Surv Ophthalmol. 44, 53-60.
273. Ulmansky, M., Ungar, H., Adler, J.H., 1984. Dental abnormalities in aging sand rats (Psammomys obesus). J Oral Pathol. 13, 366-372.

274. Van Den Pol, A.N., Cao, V., Heller, H.C., 1998. Circadian system of mice integrates brief light stimuli. Am J Physiol. 275, R654-657.
275. Van Hooser, S.D., Nelson, S.B., 2006. The squirrel as a rodent model of the human visual system. Vis Neurosci. 23, 765-778.
276. van Norren, D., Vos, J.J., 2016. Light damage to the retina: an historical approach. Eye (Lond). 30, 169-172.
277. Viswanathan, S., Frishman, L.J., Robson, J.G., Walters, J.W., 2001. The photopic negative response of the flash electroretinogram in primary open angle glaucoma. Invest Ophthalmol Vis Sci. 42, 514-522.
278. Vivanco, P., Rol, M.A., Madrid, J.A., 2010a. Pacemaker phase control versus masking by light: setting the circadian chronotype in dual Octodon degus. Chronobiol Int. 27, 1365-1379.
279. Vivanco, P., Otalora, B.B., Rol, M.A., Madrid, J.A., 2010b. Dissociation of the circadian system of Octodon degus by T28 and T21 light-dark cycles. Chronobiol Int. 27, 1580-1595.
280. Volobouev, V.T., Viegas-Paquignot, E., Petter, F., Dutrillaux, B. 1987. Karyotypic diversity and taxonomic problems in the genus Arvicanthis (Rodentia, Muridae). Genetica. 72, 147–150.
281. Volobouev, V.T., Viegas-Paquignot, E., Lombard, M., Petter, F., Duplantier, J.M., Dutrillaux, B. 1988. Chromosomal evidence for a polytypic structure of Arvicanthis niloticus (Rodentia, Muridae). Z Zool Syst Evolut-forsch. 26, 276–285.
282. von Schantz, M., Lucas, R.J., Foster, R.G., 1999. Circadian oscillation of photopigment transcript levels in the mouse retina. Brain Res Mol Brain Res. 72, 108-114.
283. Walder, K., Ziv, E., Kalman, R., Whitecross, K., Shafrir, E., Zimmet, P., Collier, G.R., 2002. Elevated hypothalamic beacon gene expression in Psammomys obesus prone to develop obesity and type 2 diabetes. Int. J. Obes. Relat. Metab. Disord. 26, 605–9.
284. Weng, J., Mata, N.L., Azarian, S.M., Tzekov, R.T., Birch, D.G., Travis, G.H., 1999. Insights into the function of Rim protein in photoreceptors and etiology of Stargardt's disease from the phenotype in abcr knockout mice. Cell. 98, 13-23.
285. Wenzel, A., Grimm, C., Samardzija, M., Reme, C.E., 2005. Molecular mechanisms of light-induced photoreceptor apoptosis and neuroprotection for retinal degeneration. Prog Retin Eye Res. 24, 275-306.
286. White, M.P., Fisher, L.J., 1989. Effects of exogenous melatonin on circadian disc shedding in the albino rat retina. Vision Res. 29, 167-179.
287. Wiechmann, A.F., Summers, J.A., 2008. Circadian rhythms in the eye: the physiological significance of melatonin receptors in ocular tissues. Prog Retin Eye Res. 27, 137-160.
288. Wiechmann, A.F., Vrieze, M.J., Dighe, R., Hu, Y., 2003. Direct modulation of rod photoreceptor responsiveness through a Mel(1c) melatonin receptor in transgenic Xenopus laevis retina. Invest Ophthalmol Vis Sci. 44, 4522-4531.
289. Wikler, K.C., Rakic, P., 1990. Distribution of photoreceptor subtypes in the retina of diurnal and nocturnal primates. J Neurosci. 10, 3390-3401.

290. Williams, T.P., Howell, W.L., 1983. Action spectrum of retinal light-damage in albino rats. Invest Ophthalmol Vis Sci. 24, 285-287.
291. Williams, D.S., 2008. Usher syndrome: animal models, retinal function of Usher proteins, and prospects for gene therapy. Vision Res. 48, 433-441.
292. Wilson, D.E., Reeder, D.M. 1993. Mammal Species of the World: A Taxonomic and Geographic Reference, Smithsonian Institute Press, Washington, DC.
293. Wisely, C.E., Sayed, J.A., Tamez, H., Zelinka, C., Abdel-Rahman, M.H., Fischer, A.J., Cebulla, C.M., 2017. The chick eye in vision research: An excellent model for the study of ocular disease. Prog Retin Eye Res. 61, 72-97.
294. Wong, J.C.Y., Smyllie, N.J., Banks, G.T., Pothecary, C.A., Barnard, A.R., Maywood, E.S., Jagannath, A., Hughes, S., van der Horst, G.T.J., MacLaren, R.E., Hankins, M.W., Hastings, M.H., Nolan, P.M., Foster, R.G., Peirson, S.N., 2018. Differential roles for cryptochromes in the mammalian retinal clock. FASEB J. 32, 4302-4314.
295. Wong, K.Y., 2012. A retinal ganglion cell that can signal irradiance continuously for 10 hours. J Neurosci. 32, 11478-11485.
296. Wong, T.Y., Klein, R., Islam, F.M.A., Cotch, M.F., Folsom, A.R., Klein, B.E.K., Sharrett, A.R., Shea, S., 2006. Diabetic Retinopathy in a Multi-ethnic Cohort in the United States. Am. J. Ophthalmol. 141, 446-455.e1.
297. Yamamoto, S., Kamiyama, M., Nitta, K., Yamada, T., Hayasaka, S., 1996. Selective reduction of the S cone electroretinogram in diabetes. Br J Ophthalmol. 80, 973-975.
298. Yan, L., Smale, L., Nunez, A.A., 2018. Circadian and photic modulation of daily rhythms in diurnal mammals. Eur J Neurosci. In press.
299. Yang, S., Luo, X., Xiong, G., So, K.F., Yang, H., Xu, Y., 2015. The electroretinogram of Mongolian gerbil (Meriones unguiculatus): comparison to mouse. Neurosci Lett. 589, 7-12.
300. Yoshizawa, K., Nambu, H., Yang, J., Oishi, Y., Senzaki, H., Shikata, N., Miki, H., Tsubura, A., 1999. Mechanisms of photoreceptor cell apoptosis induced by N-methyl-N-nitrosourea in Sprague-Dawley rats. Lab Invest. 79, 1359-1367.
301. Young, R.W., 1977. The daily rhythm of shedding and degradation of cone outer segment membranes in the lizard retina. J Ultrastruct Res. 61, 172-185.
302. Young, R.W., 1978. The daily rhythm of shedding and degradation of rod and cone outer segment membranes in the chick retina. Invest Ophthalmol Vis Sci. 17, 105-116.
303. Yuge, K., Nambu, H., Senzaki, H., Nakao, I., Miki, H., Uyama, M., Tsubura, A., 1996. N-methyl-N-nitrosourea-induced photoreceptor apoptosis in the mouse retina. In Vivo. 10, 483-488.
304. Zeitzer, J.M., Ruby, N.F., Fisicaro, R.A., Heller, H.C., 2011. Response of the human circadian system to millisecond flashes of light. PLoS One. 6, e22078.
305. Zhang, L., Storey, K.B., Yu, D.N., Hu, Y., Zhang, J.Y., 2016. The complete mitochondrial genome of Ictidomys tridecemlineatus (Rodentia: Sciuridae). Mitochondrial DNA A DNA Mapp Seq Anal. 27, 2608-2609.

306. Ziv, E., Shafrir, E., Kalman, R., Galer, S., Bar-On, H., 1999. Changing pattern of prevalence of insulin resistance in Psammomys obesus, a model of nutritionally induced type 2 diabetes. Metabolism. 48, 1549–54.

Figure Legends

Figure 1: Toluidine blue-stained histological section (left) and cone arrestin-immunostained cryostat section (right) of adult *Arvicanthis ansorgei* retina. The clear separation of cone (CCB) and rod (RCB) cell bodies within the outer nuclear layer (ONL) can be seen; CCB in the histological section have less intensely stained nuclei, and on the right are specifically and intensely stained with anti-cone arrestin. The antibody outlines the entire cell, including cone outer (COS) and inner (CIS) segments, with traces of cone axons visible running through the RCB layer and terminating in intensely stained cone synaptic pedicles in the outer plexiform layer (OPL). The rod OS (ROS) are unstained and extend beyond the COS to contact the overlying retinal pigmented epithelium (RPE). Additional abbreviations: Ch, choroid. Scale bar in bottom right = 25µm.

Figure 2: Immunostaining of *Arvicanthis* retina using antibodies directed against rod-, cone- or rod/conespecific proteins. A) DAPI staining of outer nuclear layer (ONL), divided clearly into the upper row of cone cell bodies (CCB) and lower rod cell bodies (RCB). Note the paler stained cone nuclei. Rod-specific antibodies: B) Same area stained with RET-P3, a monoclonal antibody specific for plasma membrane of rod cell bodies (Barnstable, 1980). The staining extending up through the CCB is actually on rod cell extensions joining to their inner/outer segments. C) Monoclonal antibody specific for cGMP-gated cation channel staines heavily the OS of rods. D) Phosducin antibody stains throughout the rod cell cytoplasm – notice the dark band corresponding to the absence of staining in CCB. Cone-specific antibodies: polyclonal antibodies to mid-wavelength cone opsin (E) and short wavelength cone opsin (F) respectively, label the OS in cones. The former are ~10 fold more numerous than the latter. Rod/cone antbodies: polyclonal antibodies to panarrestin (S-antigen) (G) and recoverin (H) stainheavily CCB and RCB, as well as IS and OS. Additional immunolabelled images can be seen in Bobu et al., 2006, 2008.

Figure 3: Phylogenetic analysis for selected retinal genes in *Arvicanthis ansorgei*. Multiple sequence alignment for the CDS of A) rhodopsin, B) short-wave-sensitive (blue) opsin, C) melanopsin and D)

cone-rod homeobox for *A. ansorgei* and other model organisms performed using MUSCLE. The Maximum Composition Likelihood model was used to construct Neighbor-Joining phylogenetic trees. Taken from Liu et al., 2017.

Figure 4: Comparative electroretinographic recordings from adult C57/Bl mice (black traces) and *Arvicanthis ansorgei* (grey traces). Animals (n=3 for each group) were anesthetised and stimulated with increasing intensities of white light. Representative single flash (A, B) and flicker (C) ERG recordings. The lightning symbol above the second vertical line indicates the time of the light flash. Comparison of representative records under dark-adapted (A) and light-adapted conditions (B, C). Open arrows indicate the a-wave, solid arrows indicate the trailing edge of the b-wave. The flash intensity for flicker recordings was 0.5 log cd×s/m2. ERG, electroretinogram. The overlay in (A) demonstrates lower amplitude rod responses in *A. ansorgei* compared to *M. musculus*, to be expected given the lower rod numbers; and the overlay in (B) shows clearly the higher corresponding cone responses in *A. ansorgei* for each flash intensity. The overlays further indicate the differential light sensitivities in the two species, since under scotopic conditions mice already give weak responses at 10^{-4} cd/s/m^2, not seen in *Arvicanthis*; and conversely pure cone responses are intiated in *Arvicanthis* at $5x10^{-2}$ cd/s/m^2, not seen in mice. Taken from Boudard et al., 2010.

Figure 5: Double-label immunohistochemistry of rod and cone phagocytosis, and quantitative analysis of rhythmic daily rod and cone phagocytosis in *A. ansorgei* retina. A-D: Sections obtained at 09.00 hours (1 hour after lights on) were stained with rho-4D2 anti-rhodopsin (staining rods and rod phagosomes, green) and red/green cone opsin antibody (staining cones and cone phagosomes, red). (A) Bright-field image showing the outer retina and RPE; (B) rho-4D2 labeling of the same field, including several immunopositive phagosomes (circles); (C) red/green cone opsin labeling of the same field, including several immunopositive phagosomes (white arrows); (D) merged image of (B) and (C), showing presence of both rod and red/green cone phagosomes in the RPE. Double-headed arrow: width of the RPE. ONL, outer nuclear layer; COS, cone outer segments; ROS, rod outer

segments. Scale bar, 15 µm. E, F: Phagosome counts were made every 3 hours throughout both the light and dark periods. (E) Rod phagocytosis: as seen in other species, a large burst in the number of rod phagosomes was seen 1 hour after light onset, significantly different from all other values ($P < 0.0001$). Phagosome numbers were lowest in late daytime, but showed a smaller but noticeable peak late at night. (F) Cone phagocytosis: similar to the kinetic profile for rods, cone phagocytosis peaked shortly after light onset, but the order of magnitude was always 10 times lower than that of rods (note difference in y-axis scales). When animals were raised under DD conditions, rod (G) and cone (H) phagosome counts actually increased, although there was a similar profile to LD. On the contrary, exposure to LL led to completely random profiles for both rods (I) and cones (J), and in addition cone phagosome numbers were significantly increased compared to LD. Modified from Bobu et al., 2006 and Bobu and Hicks, 2009.

Figure 6: Intense light exposure (ILE) does not elicit apoptosis in *A. ansorgei* photoreceptors but does injure mice photoreceptors. (A–D) Hematoxylin and eosin staining. (A) Control (-ILE) *A. ansorgei* retina; (B) *A. ansorgei* sacrificed one week after receiving 2 hour ILE at 12 klux. There was no observable alteration of retinal structure following exposure; (C) Control (-ILE) pigmented mouse (129S6) retina; (D) Pigmented mouse (129S6) sacrificed one week after receiving 2 hour ILE at 13 klux. There was complete loss of the ONL after light exposure. (E) Control (-ILE) *A. ansorgei*, and (F) +ILE *A. ansorgei* retinas taken 36 hours after exposure to 15 klux white light for 8 hours. No TUNEL reaction is seen in either case. (G) Retinal sections of albino Balb/c mice exposed to 5 klux for 1 hour (ie. 24 times less total light) already show widespread apoptotic nuclei within the ONL. Scale bar, 50 µm. Taken from Boudard et al., 2011).

Figure 7: Exposure to intense blue light does not lead to photoreceptor-specific light damage but thermal damage in *A. ansorgei* neural retina. Haematoxylin-stained retinal sections were prepared from animals exposed to (A) 15 minutes or (B) 45 minutes of narrow band intense blue light (30 mW/cm2, 403±10 nm) delivered via a fibre optics lamp apposed to the cornea, and killed 10 days

later. Retinal histology was normal 10 days after 15 minute exposure to blue light, whereas a ~1-mm-diameter circular lesion, corresponding to the area illuminated by the fibre optics beam, was observed after 45 minute exposure (flanked by arrows in the image B). (C) DAPI-stained section of same eye from animal 10 days after 45 min intense blue light exposure. Higher magnification of lesion site shown in C'. D-F, sections taken immediately adjacent to lesion site in 45 min-exposed animals, and D'-F' corresponding sections taken inside the lesion site. DAPI, rhodopsin and cone arrestin staining show typical staining in D, E and F respectively, with an intact ganglion cell layer (GCL, inner nuclear layer (INL) and outer nuclear layer (ONL). Rhodopsin immunorectivity was especially strong in the outer segments (OS), whereas cone arrestin immunoreactivity was visible throughout the cone cells. Within the lesion site, DAPI staining showed a disorganized mass of scar tissue (ST) (D'). No staining with rhodopsin or cone arrestin antibodies was detected within the lesion site, as seen in E' and F' respectively. (G, H) GFAP staining provides an indicator of general retinal stress. After 15 minutes of intense blue light exposure, outside the lesion site GFAP staining was confined to retinal astrocytes in the nerve fibre layer (NFL) (G), whereas in retinas exposed to 45 minutes of intense blue light there was generalized radial glial staining across the width of the retina, from the NFL to the external limiting membrane (ELM), outside of the lesion site (H). Notice the absence of GFAP immunoreactivity in the central retina denoted by * in G, and widespread staining in Müller glia in the same zone (*) in H. Scale bar in F': 300 µm (A-C); 100 µm (C'); 60 µm (D–H). Taken from Boudard et al., 2011 and thesis dissertation).

Figure 8: Immunohistochemistry labelling showing partial regional loss of rod- and cone-specific proteins in *Arvicanthis* receiving elevated doses of MNU. Fluorescence microscopy of an entire retinal section of 90 dpi (days post-injection)-MNU (100 mg/ml) *Arvicanthis* stained with DAPI (scale: 250 µm), showing the gradient of the degeneration along the vertical meridian from superior to inferior hemisphere. The entire section was reconstructed with adjacent images taken at ×20 magnification. Eight different regions (A–H) of this section are shown in higher detail (scale: 50 µm). (A–E) are located in the inferior hemisphere and (F–H) in the superior hemisphere. The approximate position

of the optic nerve head is shown with a white arrow (located 50-100 µm away in sister section). Same regions of adjacent sections labelled with rhodopsin, r-trans. (r-transducin), MW-cone opsin (red/green cone opsin), and cone arrestin (c-arr.) are shown in serial panels. Control (Ctrl) retina labelled with the same antibodies is given as reference. CCB, cone cell bodies; CIS, cone inner segments; COS, cone outer segments; GCL, ganglion cell layer; INL, inner nuclear layer; MNU, N-methyl-N-nitrosourea; MW opsin, red/green cone opsin; ONL, outer nuclear layer; RCB, rod cell bodies; RIS, rod inner segments; ROS, rod outer segments. Adapted from Boudard et al., 2010).

Figure 9: The molecular clock pathways and retinal clocks. Schematic representation of the transcriptional/translational feedback loops model for the molecular clock. The BMAL1/CLOCK (or BMAL1/NPAS2) dimer activates transcription of the Per and Cry genes upon binding to the Ebox sequences in their promoters. In turn, PER and CRY proteins form heterodimers able to inhibit transcriptional activity of BMAL1/CLOCK, thus turning down their own transcription. Meanwhile, these factors undergo posttranslational modifications, in particular, phosphorylation of PER proteins by the Casein Kinases 1δ or 1ε, signaling for ubiquitination and proteasomal degradation, and then allowing the cycle to restart. BMAL1/CLOCK likewise activates the expression of Rev-Erb and Ror genes, which products respectively repress and activate transcription of the Bmal1 gene at retinoic acid-related orphan receptor binding elements (RORE) sites. This generates an additional loop interlocked with the previous one, all together contributing to the robustness of the clockwork. The presence of Ebox and/or RORE sequences throughout the genome supports the rhythmic regulation of a set of target genes (CCG) for BMAL1/CLOCK, BMAL1/NPAS2, REV-ERB, and ROR transcription factors. Clock gene expression dynamics over the 24-hour cycle conforming to this model have been described in the ONL and in the inner retina (INL + GCL) in several ex vivo studies, as symbolized next to the eosin/hematoxylin stained transversal section of a rat retina shown in the upper-right corner of the figure. Taken from Felder-Schmittbuhl et al., 2018.

Figure 10: Expression profile of core clock genes Bmal1 over a single 24 h period in *Arvicanthis* maintained under different lighting conditions. Vertical columns, left to right : Bmal1, Per1, Per2, Cry1 and Cry2. Horizontal rows, top to bottom: top, 12 h light: 12 h dark cycle (LD); middle, constant darkness (DD); bottom, constant light (LL). Illumination conditions are depicted as backgrounds of white (light) and dark grey (darkness), right hatched (subjective day) and left hatched (subjective night). Statistically significant rhythmic changes are seen in all genes under LD, with most maxima occurring at the night-day transition point; the pattern is basically similar albeit dampened in DD. However LL leads to large phase shifts in expression profiles, with peak expression now occurring in early night. These data underline the highly disruptive effects of artifical light at night upon the retinal circadian clock. One-way analysis of variance (ANOVA) and cosinor levels of significance (PA and Pc respectively) are given in the upper right corner of each panel. Modified from Bobu et al., 2013.

Figure 11: Light-induced responses of ipRGCs in *Arvicanthis* (left) and mouse retina (right) to short flashes of constant irradiance (14.3 log NQ * cm-2 * s-1). The most sensitive ipRGC type (type I) responds to very short light flashes of 10 ms in *Arvicanthis* but only poorly to even 50 ms in the mouse, respectively. We did not try shorter pulses. Type II and type III ipRGCs were insensitive to flashes shorter than 1 s in both species, although *Arvicanthis* displayed greater activity. Modified from Karnas et al., 2013a.

Figure 12: Melatonin synthesis pathway shows two phase-opposed sites of expression in *Arvicanthis* retina. A, DAPI staining of a 10-µm section of *A. ansorgei* retina indicates the area of interest; from top to bottom. B, Aa-nat antisense probe at ZT19 (night time) stains inner segments (IS) and the scleral-most part of the outer nuclear layer (ONL). C, Aa-nat antisense probe at ZT6 stains ganglion cell layer (GCL). D, Immunostaining of *A. ansorgei* retina with anti-cone arrestin (red) clearly showing retinal organization with cone cell bodies (CCB) located sclerally to rod cell bodies (RCB). E, At ZT19, Aa-nat mRNA staining is restricted to the 2 scleral-most cell body rows (CCB) and IS. F, At ZT19 Aa-nat

antisense probe does not stain GCL. G and H, At ZT6, Aa-nat antisense probe stains GCL (H) but not ONL (G). I, Use of Aa-nat sense probe at ZT19 does not stain any structures. Scale bar, 10 µm. Additional abbreviations, INL, inner nuclear layer; OS, outer segments; RPE, retinal pigmented epithelium. Taken from Gianesini et al., 2015.

Figure 13: Scotopic and photopic electroretinograms of *Psammomys obesus*, humans and rats. Two different intensities are shown under scotopic mode, faint intensity (0.01 cd/s/m^2) to evoke a pure rod response, and high intensity (3 cd/s/m^2) to evoke a mixed rod-cone reponse. The single photopic recording, under background light adaptation (3 cd/s/m^2), shows a pure cone response. The greater similarities between recordings from *P. obesus* and humans compared to those made in Wistar rats can be seen, including similar amplitudes and waveforms under scotopic conditions, and the presence of post b wave components (the i wave and photoreceptor negative response, PhNR) not seen in rats. Other abbreviations: a = a wave (hyperpolarisation), b = b wave (depolarisation). Modified from Dellaa et al., 2017.

Figure 14: Fundus Fluorescent angiography showing organisation of major blood vessels in *Psammomys obesus*. Vessels present as two beds, one spreading laterally from the optic nerve head (ONH), the other branching laterally in the superior hemisphere. Between the two lies a poorly vascularized region corresponding to the area centralis (outlined by dotted lines). Photoimage made from images captured using Phoenix Micron III camera and anaethetised adult female *P. obesus* injected i.v. with fluorescein, courtesy of Dr. M. Roux, IGBMC, Illkirch, France.

Figure 15: Vascular modifications during diabetes in *P. obesus*. (A–D) Retinas stained with *B. simplicifolia* isolectin. Although the vessel aspect in control retinas (lean normal, LN) showed a regular smoothly branching aspect (A), diabetic retinas (obese hyperglycemic, OH) showed a range of abnormalities, including irregular diameter and constrictions (B, open bracket), neovascular buds (C, arrow), and balloon-like swellings (D, arrow). Vascular and blood-retinal barrier modifications during diabetes in *P. obesus*. LN retinas labeled with *B. simplicifolia* lectin (Bs, red) to outline blood vessels

(E) and anti-smooth muscle actin antibody (SMA, green) to stain pericytes (F) demonstrate the dense pericyte coverage (examples shown by arrows). On the contrary, OH retinas labeled under identical conditions showed that lectin-stained vessels (G) are completely lacking pericytes (H). Modified from Saidi et al., 2011b.

Figure 16: Pro-angiogenic and anti-angiogenic growth factors in the vitreous of control and diabetic eyes from *P. obesus*. (A) top panel: VEGF-immunoreactive bands in vitreous samples from three control (lean normal, LN, left) and three diabetic (obese hyperglycemic, OH, right) animals. Lower panel: the bands were analyzed by densitometry and normalized to tubulin in stripped membranes from the same samples. Black column: LN controls; white column: OH animals. ***P<0.001. (B) top panel : PEDF-immunoreactive bands in vitreous samples from three control (LN, left) and three diabetic (OH, right) animals. Lower panel: the bands were analyzed by densitometry and normalized to tubulin in stripped membranes from the same samples. Black column: LN controls; white column: OH animals. ***P<0.001. Relative levels given in arbitrary units. Modified from Saidi et al., 2011b.

Figure 17: Rod and cone photoreceptor opsins in control and diabetic *P. obesus* retina. A-C: Rhodopsin (Rho) immunolabeling showed strong expression in rod outer segments (OS, green) in lean normal (LN), obese normoglycemic (ON), and obese hyperglycemic (OH) animals respectively. D-F: Staining of red/green, or mid-wavelength, cone opsin (MOp) was localized to numerous cone outer segments (OS, red) in LN (D) and ON (E) animals, whereas there were many less immunolabeled cells in OH tissue (F). This was also the case for blue or short wavelength cone opsin (SOp) immunostaining in OS of LN (G) and OH animals (H). To the right of each immunostaining series are shown western blot analyses and quantification of Rho, MOp, and SOp expression. (I) Rho and tubulin (Tub) immunoreactivity showed no difference in intensity between samples. Triplicate samples are shown above corresponding columns: LN (black), ON (gray), OH (white). (J) MOp immunoreactivity showed a roughly 50% decrease in OH retinas when normalized to Tub (***P <

0.001, ANOVA). (K) Similarly, SOp immunoreactivity was also reduced by 50% in OH retinas (***P< 0.001, ANOVA). Scale bar, 80 µm. Modified from Saidi et al., 2011b.

Figure 18: Use of Adaptive Optics Scanning Light Ophthalmoscopy (AOSLO) to show the similar appearance of cone photoreceptors between human fovea (left) and 13-Lined ground squirrel visual streak (right) *in vivo.* Scale bar = 20 µm.

Figure 19: Chromatin organization in nocturnal and diurnal rodent retinas. (A) *Mus musculus* rod nuclei have a uniquely inverted chromatin structure, with heterochromatin (HC, red) concentrated into a central mass surrounded by euchromatin (EC, green). This is the opposite of the situation seen in every other differentiated cell type, in which EC forms a large central area surrounded by a shell of HC (see nuclei in INL). This conventional organization is also seen in rods of diurnal rodents like the ground squirrel, shown at low (B) and high magnification (C) (HC in red, EC in green). Surprisingly, *Psammomys obesus* (and *Arvicanthis*, not shown) possess inverted rod nuclei similar to nocturnal *Mus musculus*, again shown at low (D) and high magnification (E) (HC in red, EC in green). Panel A modified from Solovei et al., 2009, other panels unpub. data and pers. comm. Dr. I. Solovei, with permission).

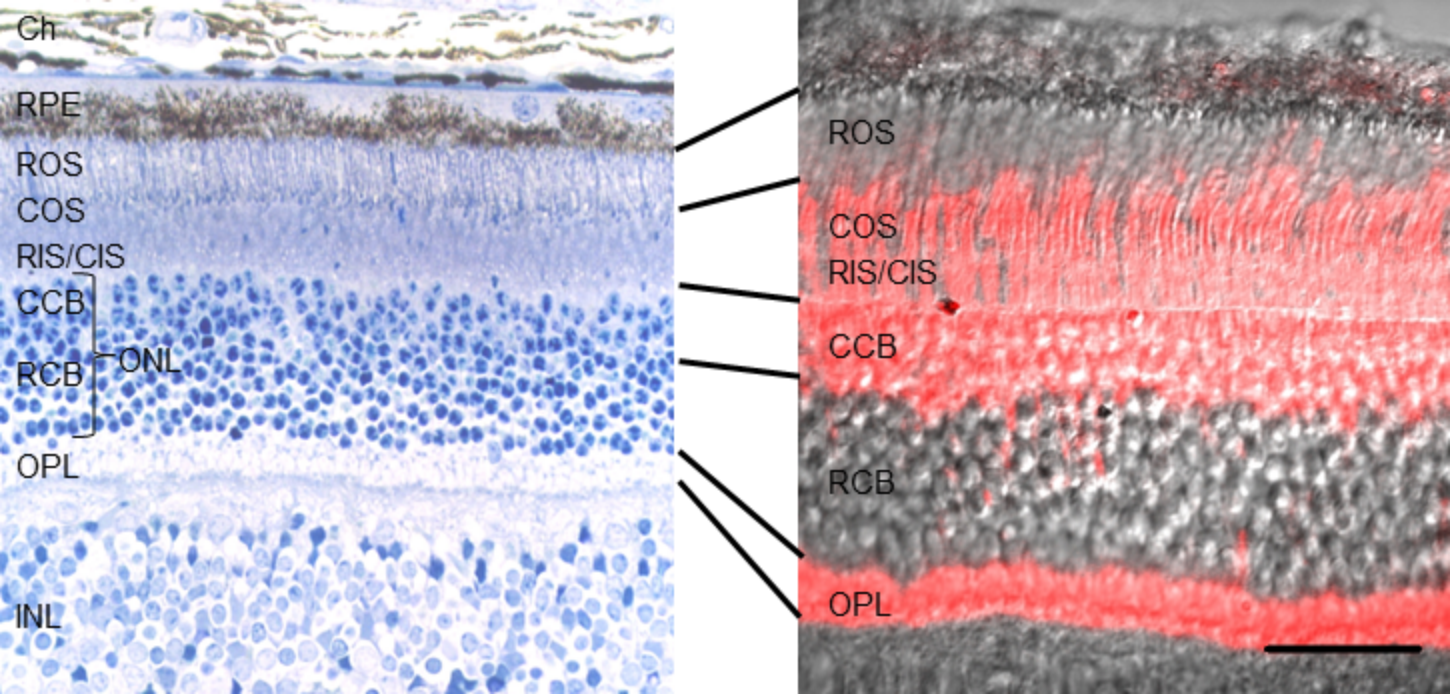
Ch
RPE
ROS
COS
RIS/CIS
CCB
RCB
ONL
OPL
INL
ROS
COS
RIS/CIS
CCB
RCB
OPL

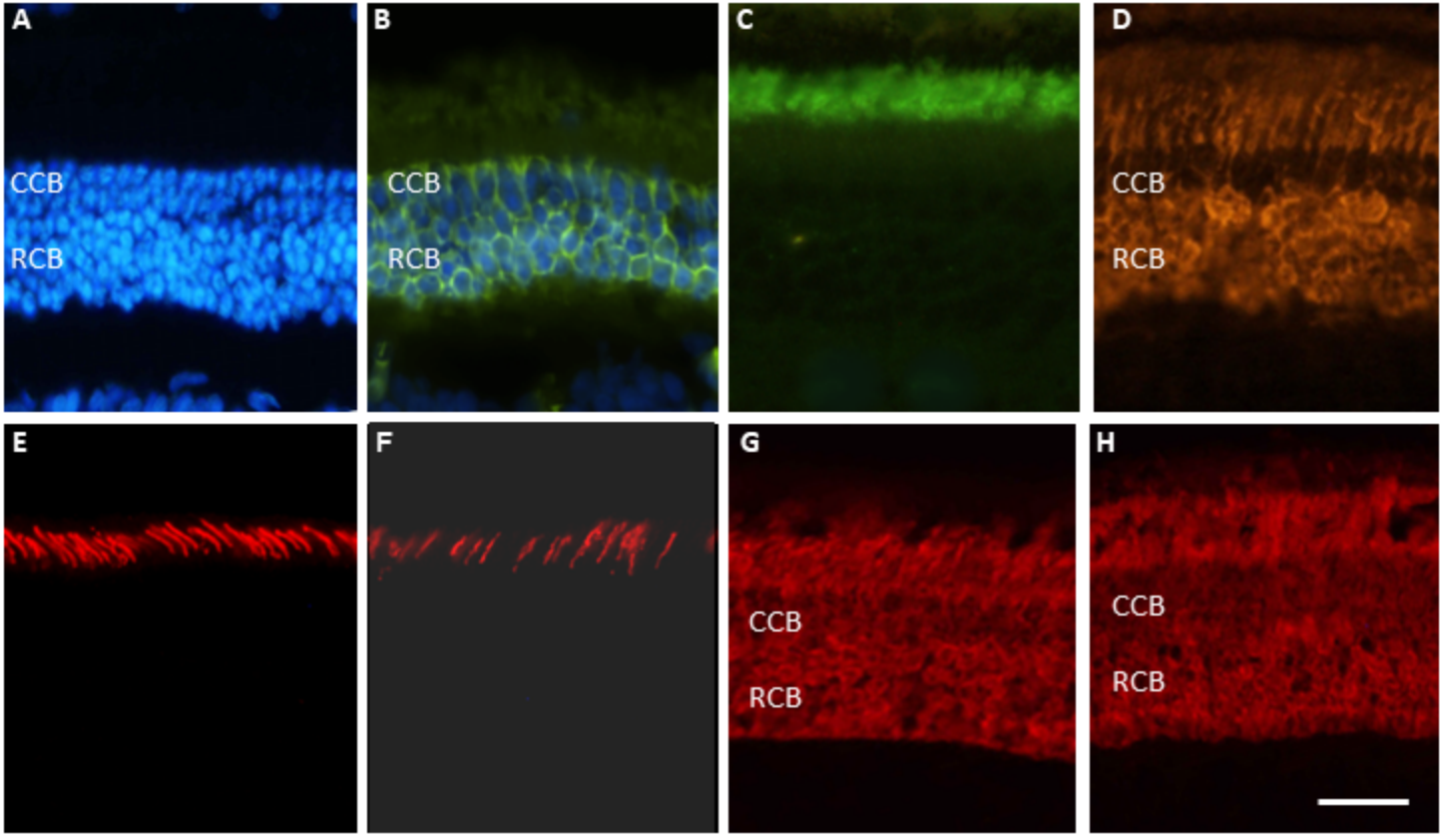
A
CCB
RCB
B
CCB
RCB
C
D
CCB
RCB
E
F
G
CCB
RCB
H
CCB
RCB

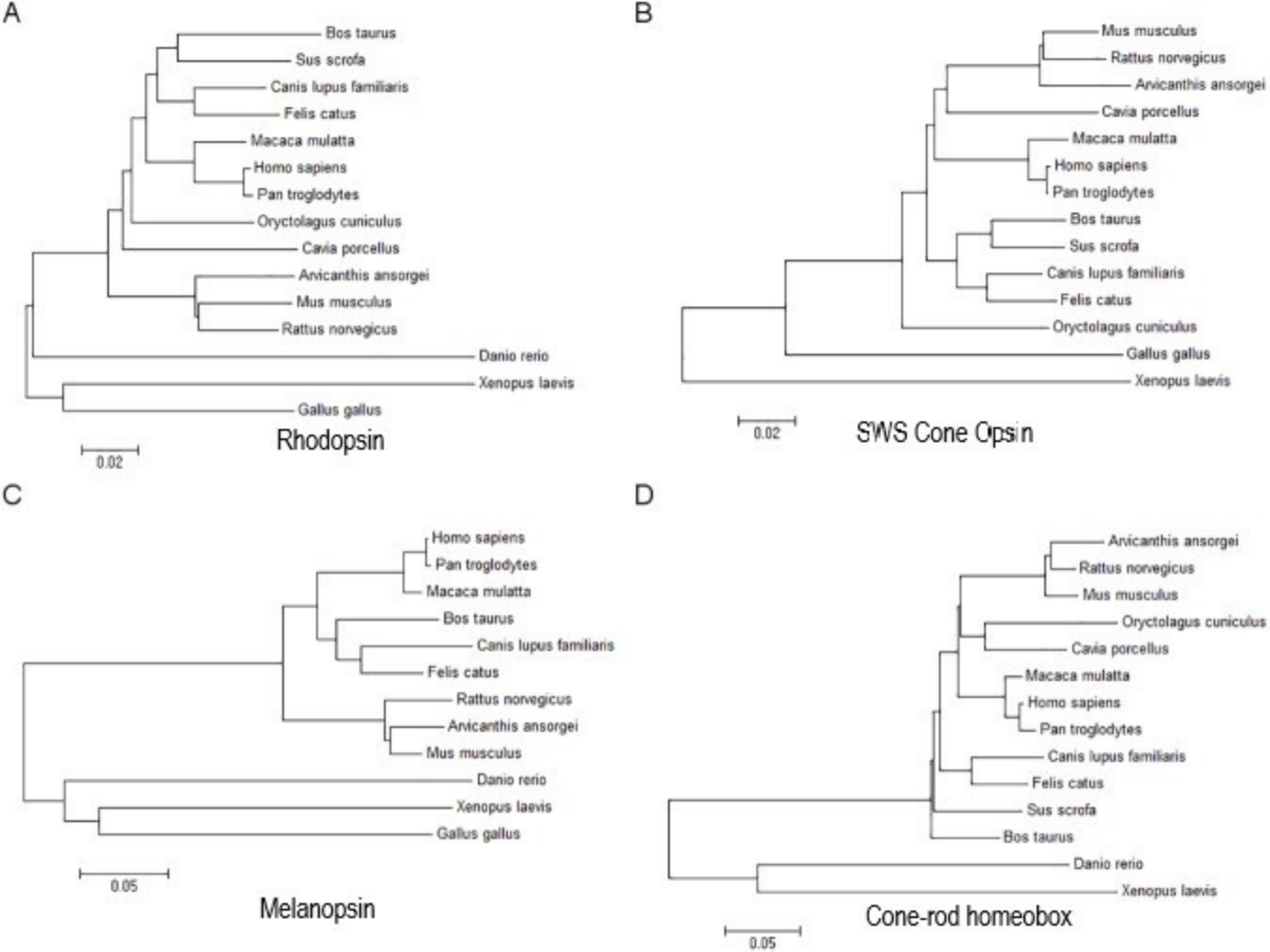
A
Bos taurus
Sus scrofa
Canis lupus familiaris
Felis catus
Macaca mulatta
Homo sapiens
Pan troglodytes
Oryctolagus cuniculus
Cavia porcellus
Arvicanthis ansorgei
Mus musculus
Rattus norvegicus
Danio rerio
Xenopus laevis
Gallus gallus
0.02
Rhodopsin
B
Mus musculus
Rattus norvegicus
Arvicanthis ansorgei
Cavia porcellus
Macaca mulatta
Homo sapiens
Pan troglodytes
Bos taurus
Sus scrofa
Canis lupus familiaris
Felis catus
Oryctolagus cuniculus
Gallus gallus
Xenopus laevis
0.02
SWS Cone Opsin
C
Homo sapiens
Pan troglodytes
Macaca mulatta
Bos taurus
Canis lupus familiaris
Felis catus
Rattus norvegicus
Arvicanthis ansorgei
Mus musculus
Danio rerio
Xenopus laevis
Gallus gallus
0.05
Melanopsin
D
Arvicanthis ansorgei
Rattus norvegicus
Mus musculus
Oryctolagus cuniculus
Cavia porcellus
Macaca mulatta
Homo sapiens
Pan troglodytes
Canis lupus familiaris
Felis catus
Sus scrofa
Bos taurus
Danio rerio
Xenopus laevis
0.05
Cone-rod homeobox

A

mouse

Arvicanthis

overlay

log (cdxs/m²)

-4.0
-3.0
-2.0
-1.5
-1.0
-0.5
0.0
0.5
1.0
1.5

400µV/div.

40 ms/div.

B

log (cdxs/m²)

-2.0
-1.5
-1.0
-0.5
0.0
0.5
1.0
1.5

200µV/div.

40 ms/div.

C

mouse

Arvicanthis

overlay

200µV/div.

0.5 Hz
1 Hz
2 Hz
3 Hz
5 Hz
7 Hz
10 Hz
12 Hz
15 Hz
18 Hz
20 Hz
29 Hz

50 ms/div.

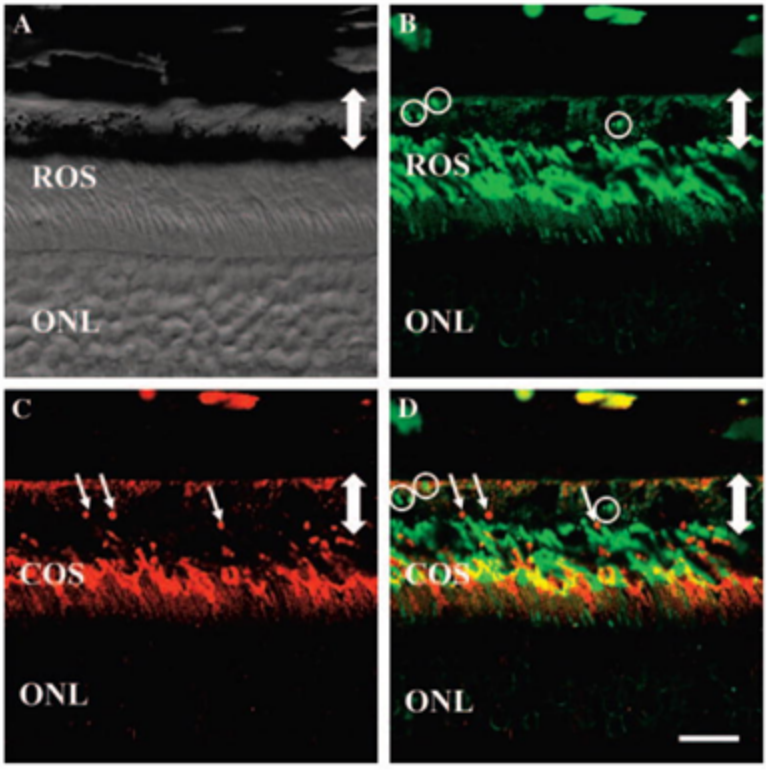
A
ROS
ONL
B
ROS
ONL
C
COS
ONL
D
COS
ONL

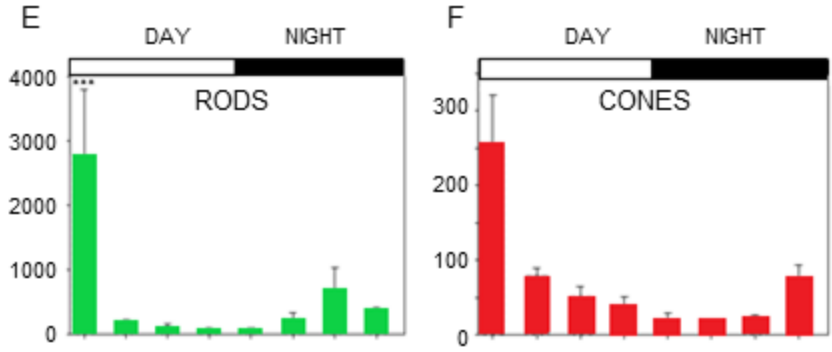
E
DAY
NIGHT
RODS
4000
3000
2000
1000
0
F
DAY
NIGHT
CONES
300
200
100
0
ZEITGEBER TIME (HRS)

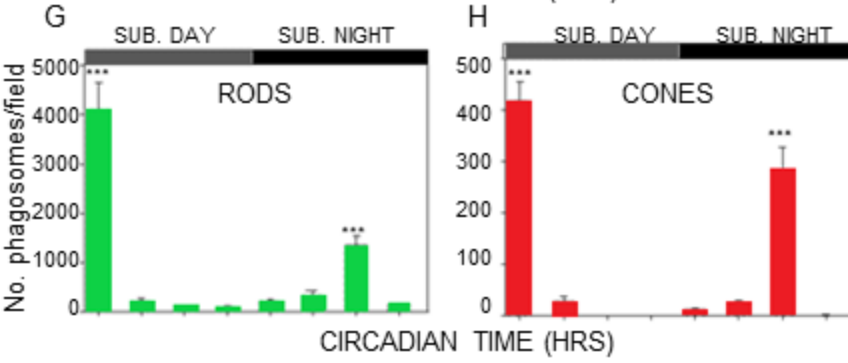
G
SUB. DAY
SUB. NIGHT
RODS
No. phagosomes/field
5000
4000
3000
2000
1000
0
H
SUB. DAY
SUB. NIGHT
CONES
500
400
300
200
100
0
CIRCADIAN TIME (HRS)

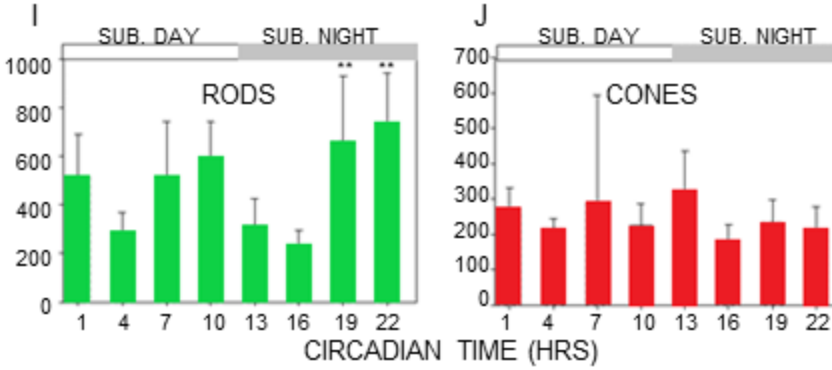
I
SUB. DAY
SUB. NIGHT
RODS
1000
800
600
400
200
0
1 4 7 10 13 16 19 22
J
SUB. DAY
SUB. NIGHT
CONES
700
600
500
400
300
200
100
0
1 4 7 10 13 16 19 22
CIRCADIAN TIME (HRS)

Haematoxylin/eosin staining

TUNEL staining

-ILE

+ILE

-ILE

+ILE

Arvicanthis

mouse

A

ONL

INL

GCL

B

ONL

INL

GCL

(12 klux, 2 h., recov.: 1 week)

E

ONL

INL

GCL

F

ONL

INL

GCL

(15 klux, 8 h ., recov.: 36 h)

C

ONL

INL

GCL

D

INL

GCL

(13 klux, 2 h ., recov.: 1.5 mo)

G

ONL

INL

GCL

(5 klux, 1 h ., recov.: 36 h)

pigmented mouse (129S6)

albino mouse
(BALB/c)

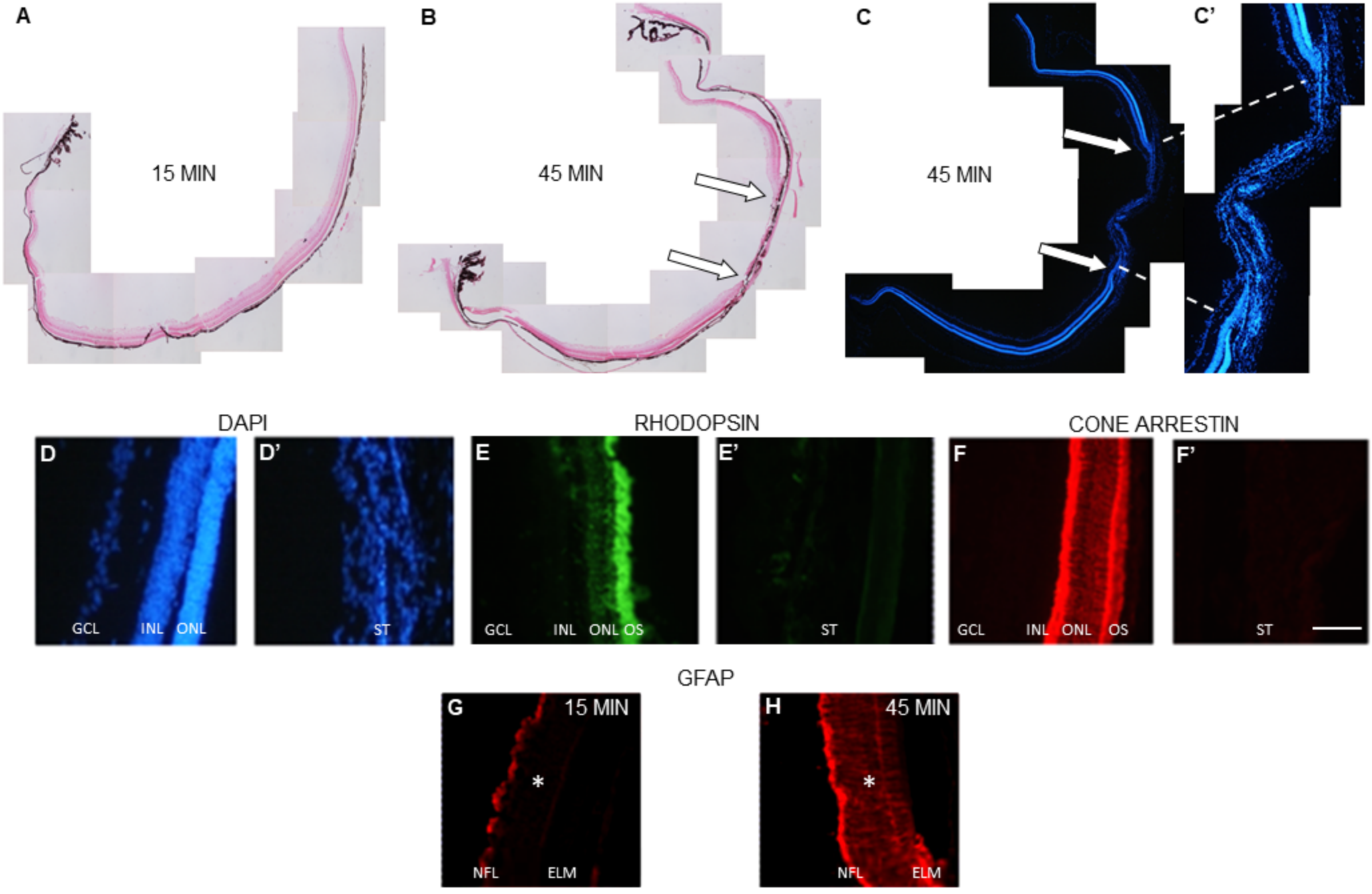
A
15 MIN
B
45 MIN
C
C'
45 MIN
DAPI
RHODOPSIN
CONE ARRESTIN
D
D'
E
E'
F
F'
GCL
INL
ONL
ST
OS
GFAP
G
15 MIN
H
45 MIN
*
NFL
ELM

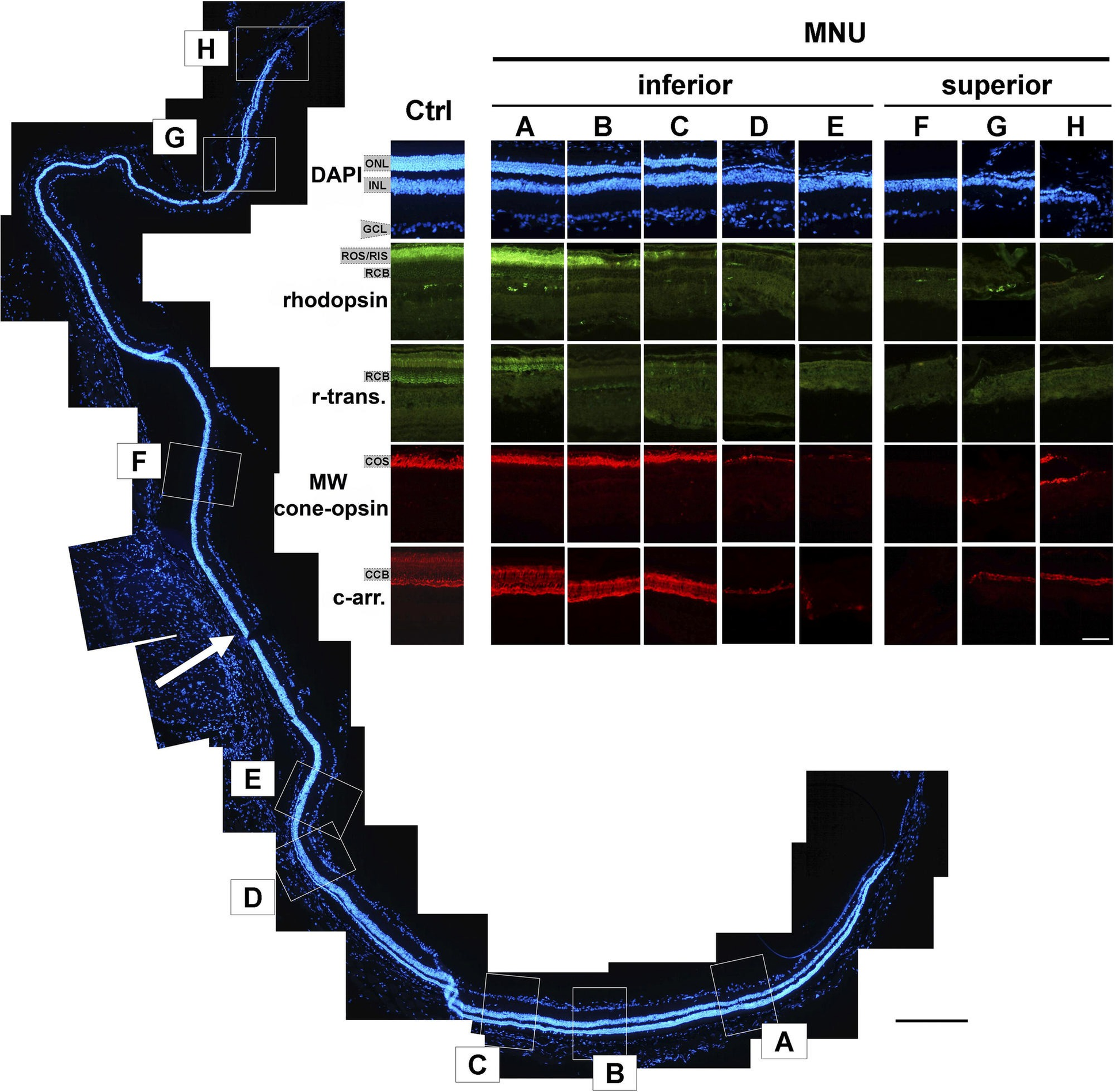
MNU
inferior
superior
Ctrl
A
B
C
D
E
F
G
H
DAPI
ONL
INL
GCL
ROS/RIS
RCB
rhodopsin
RCB
r-trans.
COS
MW
cone-opsin
CCB
c-arr.

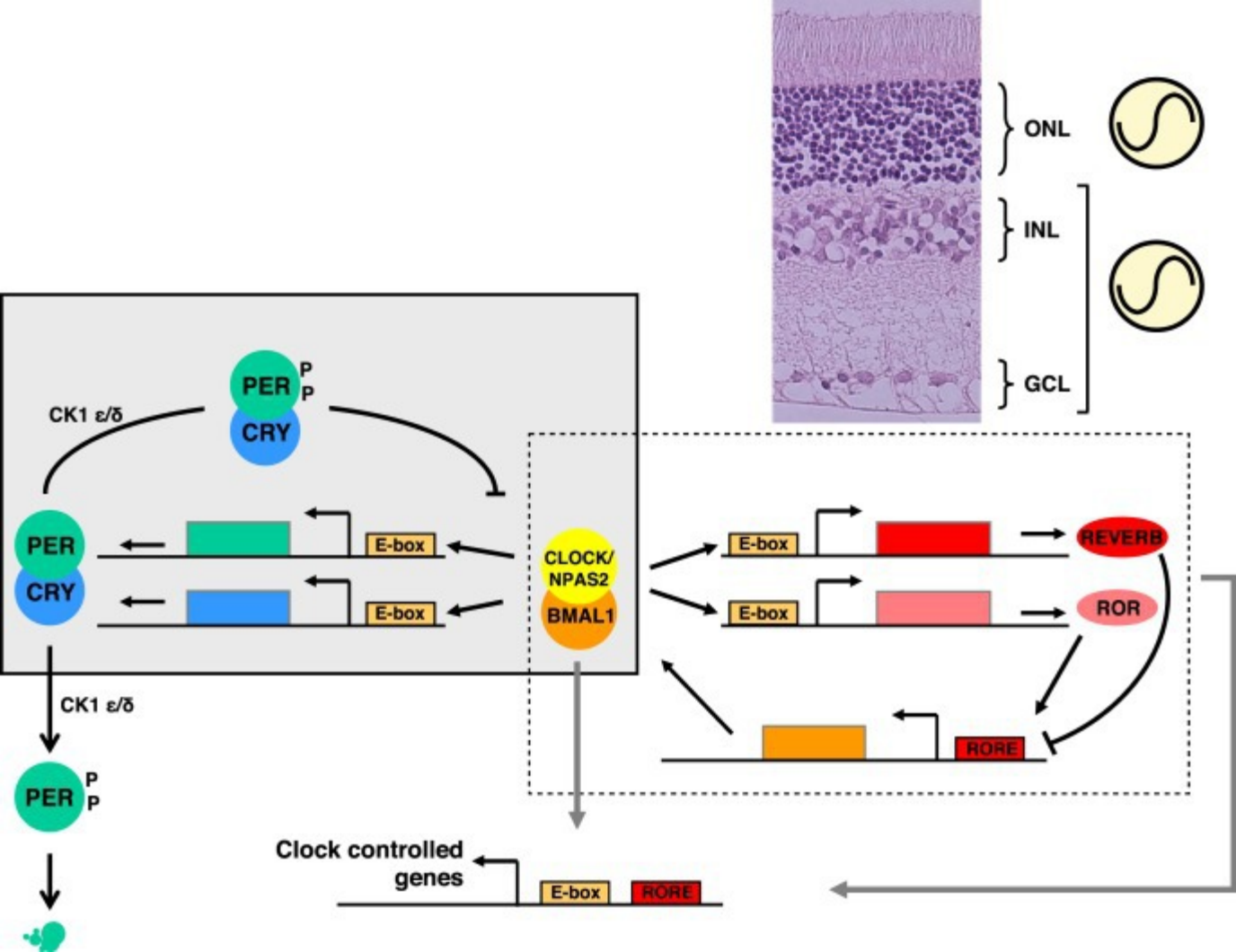
ONL
INL
GCL
PER
P
P
CRY
CK1 ε/δ
PER
CRY
E-box
E-box
CLOCK/
NPAS2
BMAL1
E-box
E-box
REVERB
ROR
RORE
CK1 ε/δ
PER
P
P
Clock controlled
genes
E-box
RORE

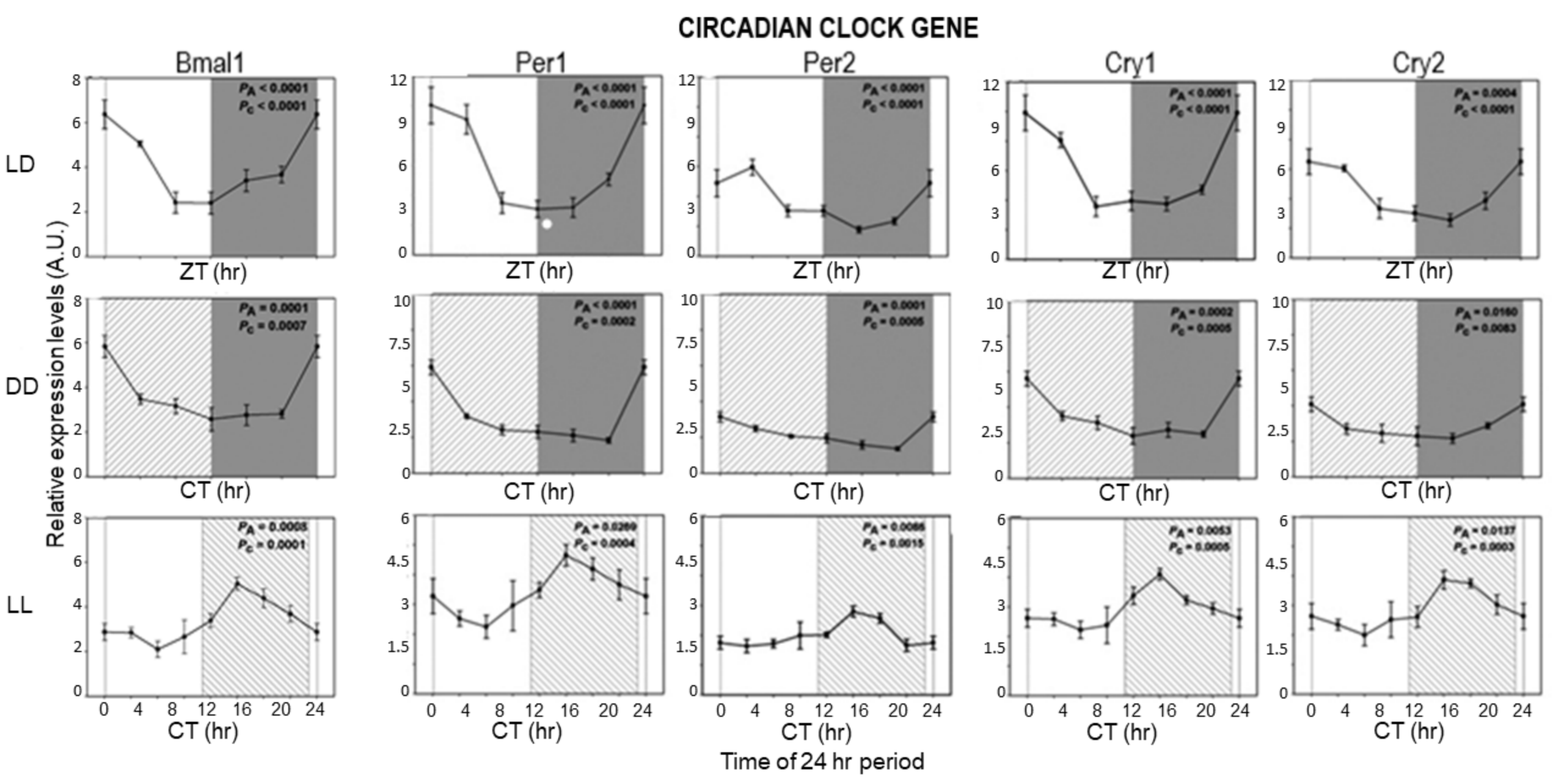
CIRCADIAN CLOCK GENE
Bmal1
Per1
Per2
Cry1
Cry2
LD
DD
LL
Relative expression levels (A.U.)
ZT (hr)
CT (hr)
Time of 24 hr period

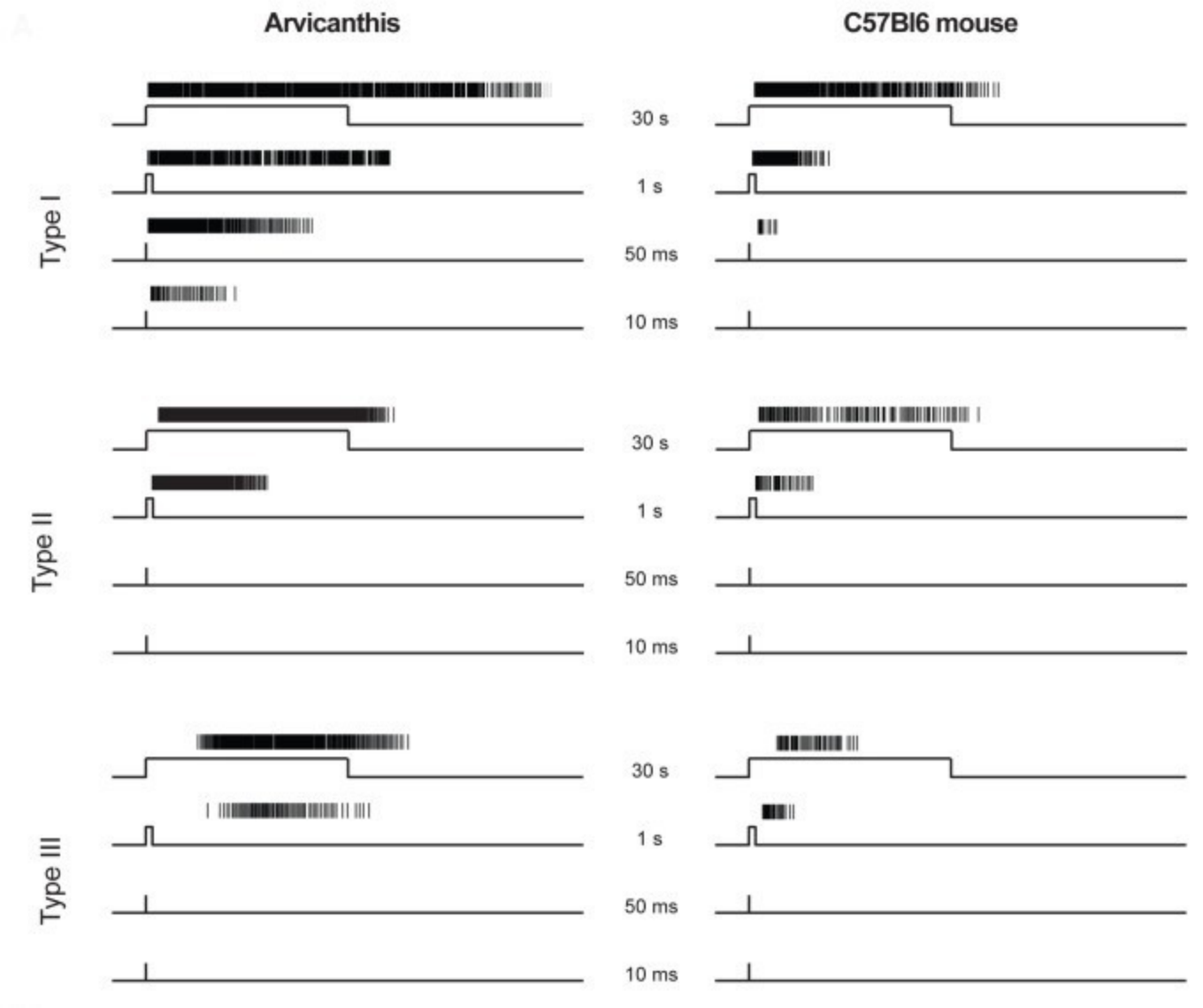
Arvicanthis
C57Bl6 mouse
Type I
Type II
Type III
30 s
1 s
50 ms
10 ms
30 s
1 s
50 ms
10 ms
30 s
1 s
50 ms
10 ms

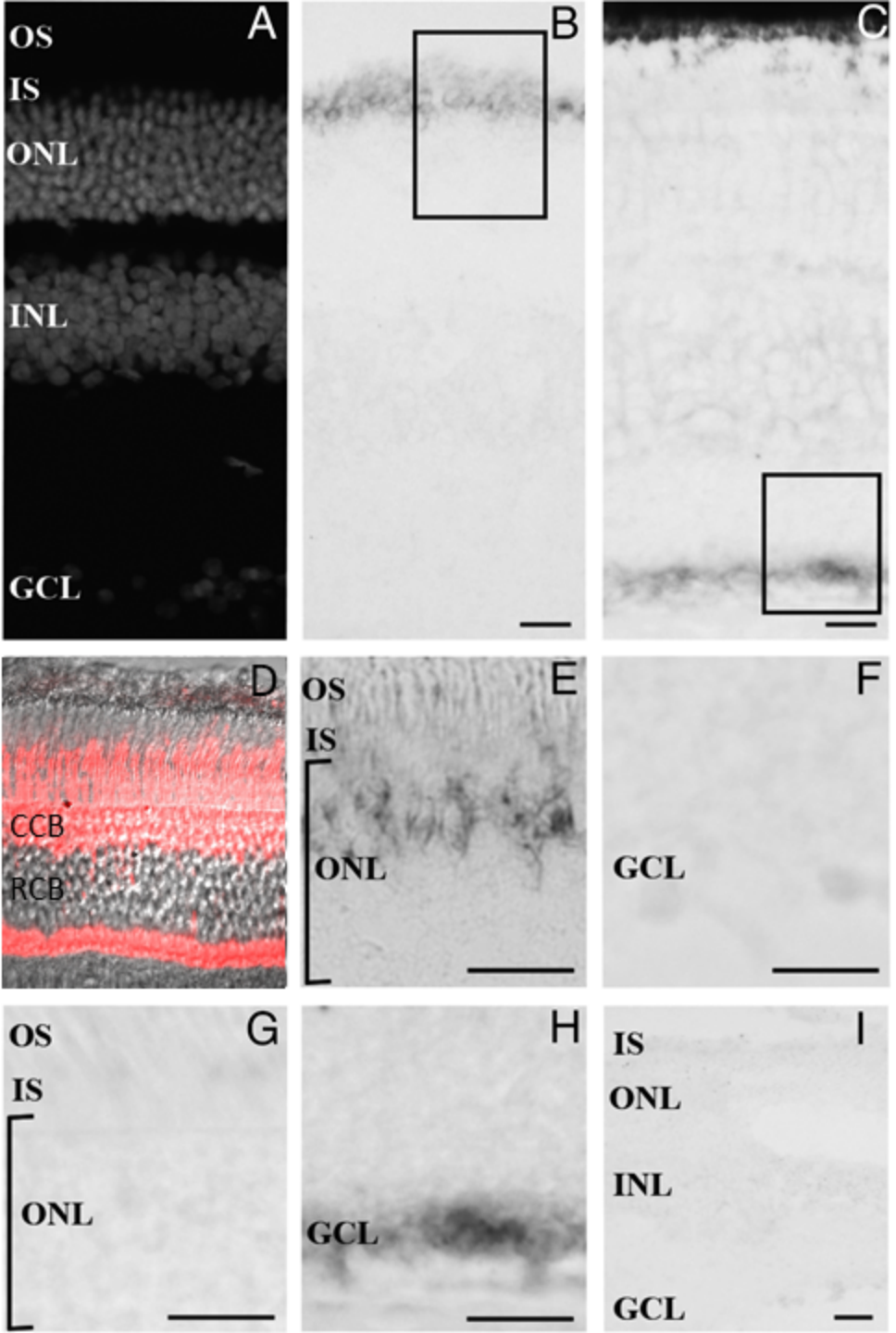
A
OS
IS
ONL
INL
GCL
B
C
D
CCB
RCB
E
OS
IS
ONL
F
GCL
G
OS
IS
ONL
H
GCL
I
IS
ONL
INL
GCL

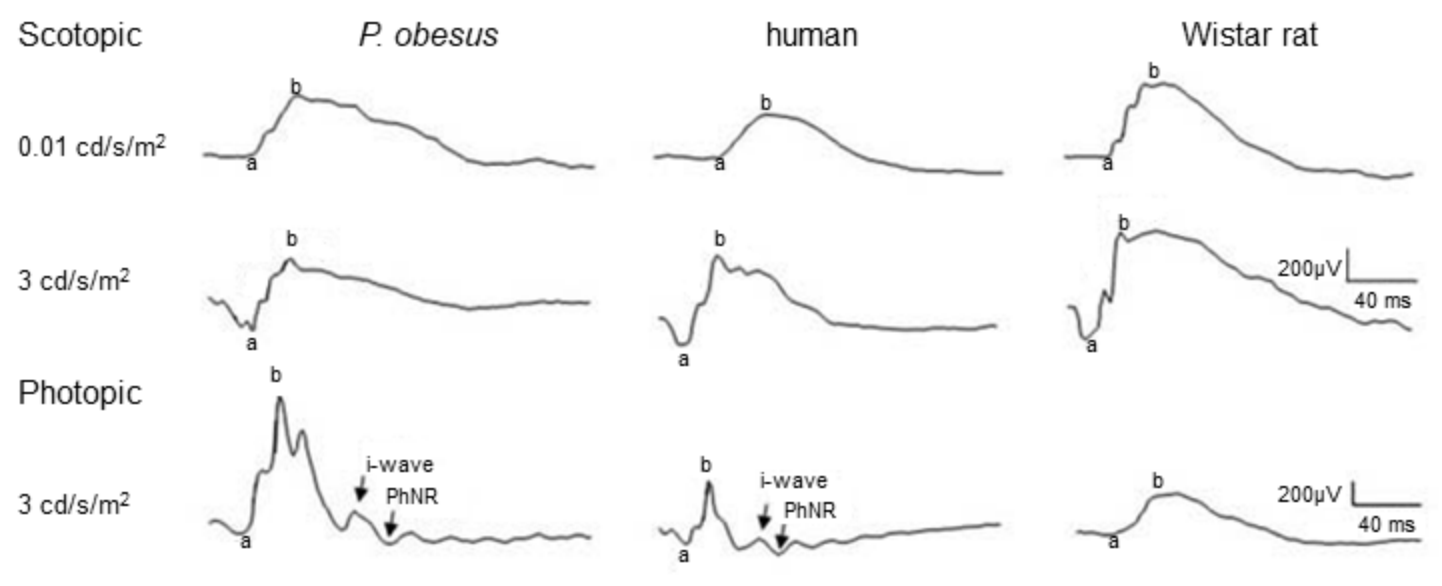
Scotopic
P. obesus
human
Wistar rat
0.01 cd/s/m2
3 cd/s/m2
Photopic
3 cd/s/m2
a
b
i-wave
PhNR
200μV
40 ms

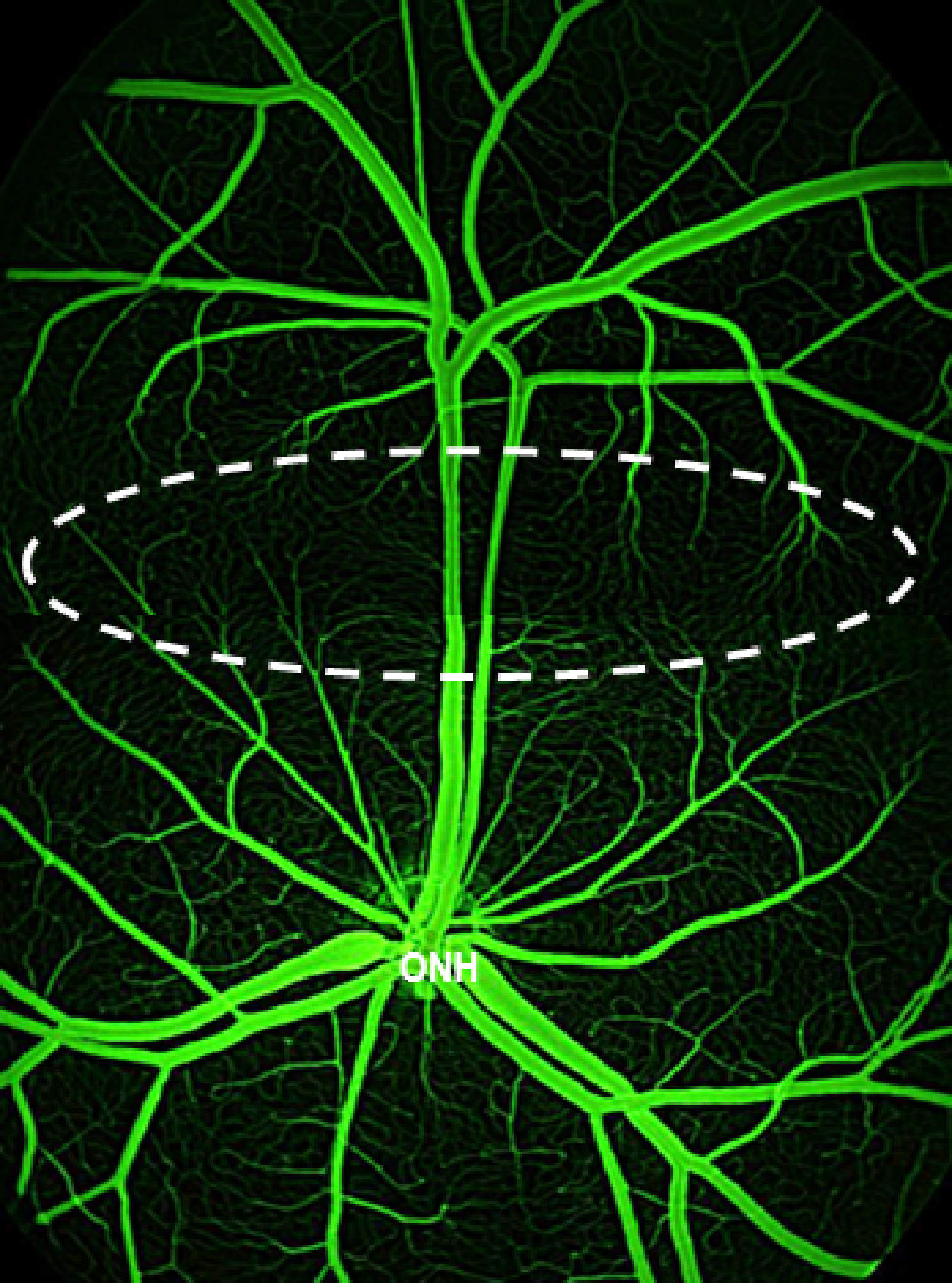
ONH

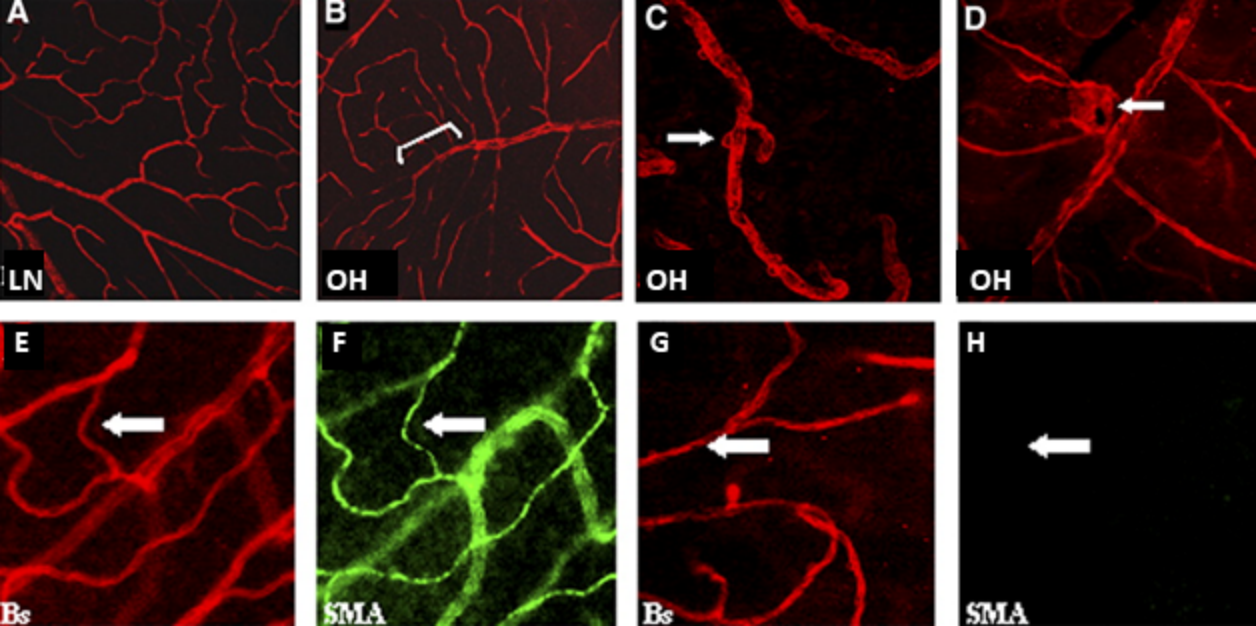
A
LN
B
OH
C
OH
D
OH
E
Bs
F
SMA
G
Bs
H
SMA

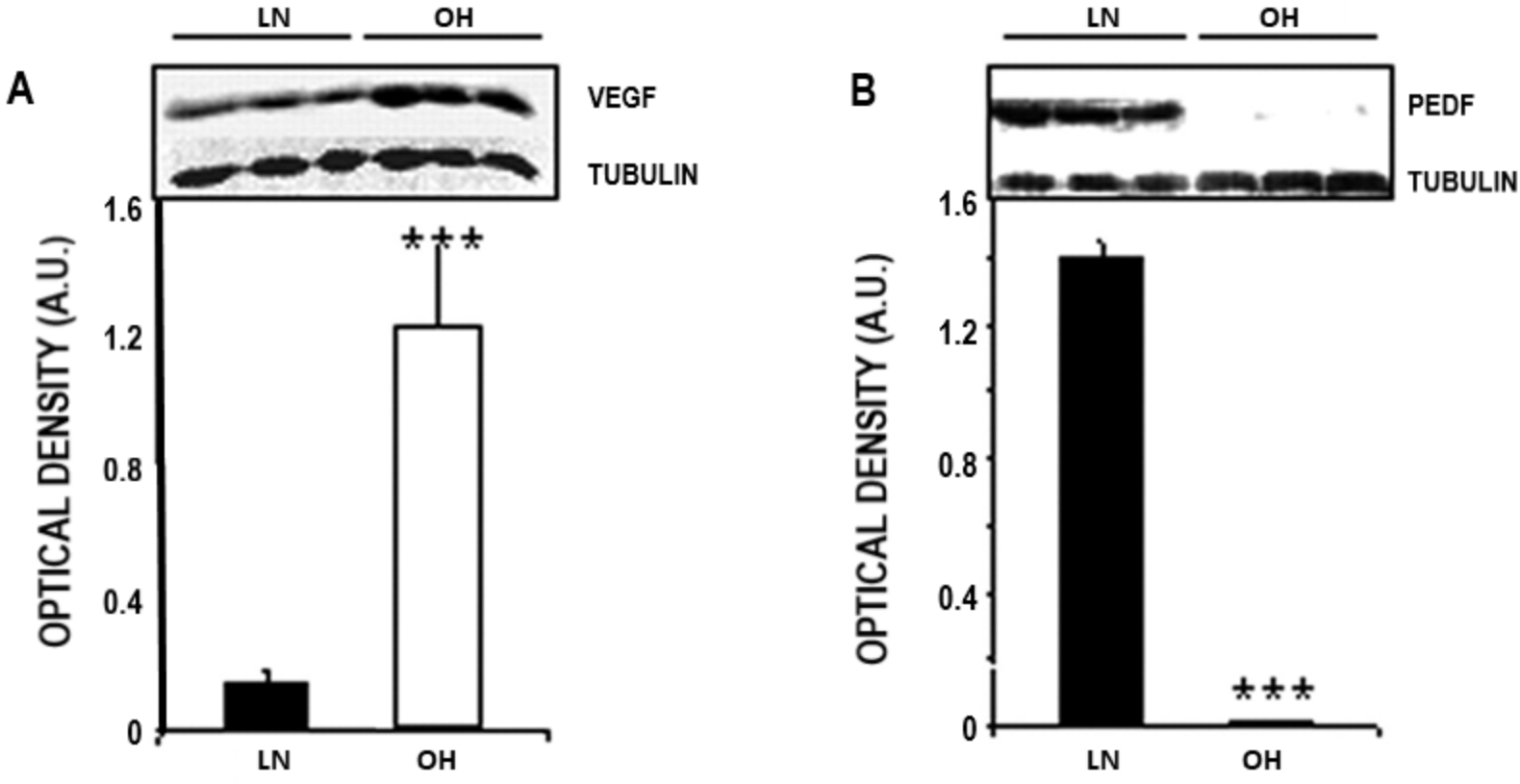
A
LN
OH
VEGF
TUBULIN
OPTICAL DENSITY (A.U.)
1.6
1.2
0.8
0.4
0
***
LN
OH
B
LN
OH
PEDF
TUBULIN
OPTICAL DENSITY (A.U.)
1.6
1.2
0.8
0.4
0
***
LN
OH

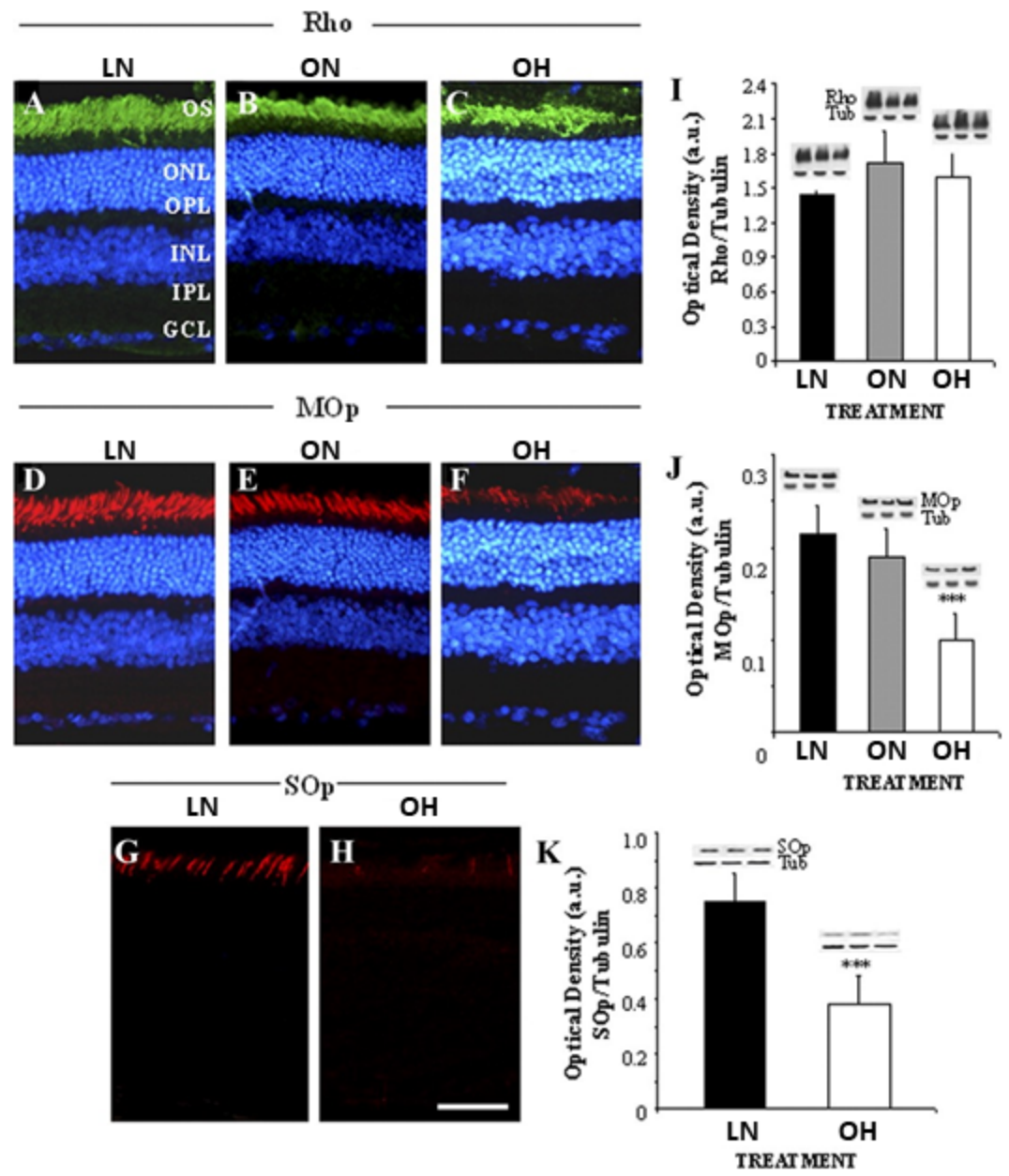
Rho
LN
ON
OH
A
OS
ONL
OPL
INL
IPL
GCL
B
C
I
Optical Density (a.u.)
Rho/Tubulin
Rho
Tub
2.4
2.1
1.8
1.5
1.2
0.9
0.6
0.3
0
LN
ON
OH
TREATMENT
MOp
LN
ON
OH
D
E
F
J
Optical Density (a.u.)
MOp/Tubulin
MOp
Tub
0.3
0.2
0.1
0
***
LN
ON
OH
TREATMENT
SOp
LN
OH
G
H
K
Optical Density (a.u.)
SOp/Tubulin
SOp
Tub
1.0
0.8
0.6
0.4
0.2
0
***
LN
OH
TREATMENT

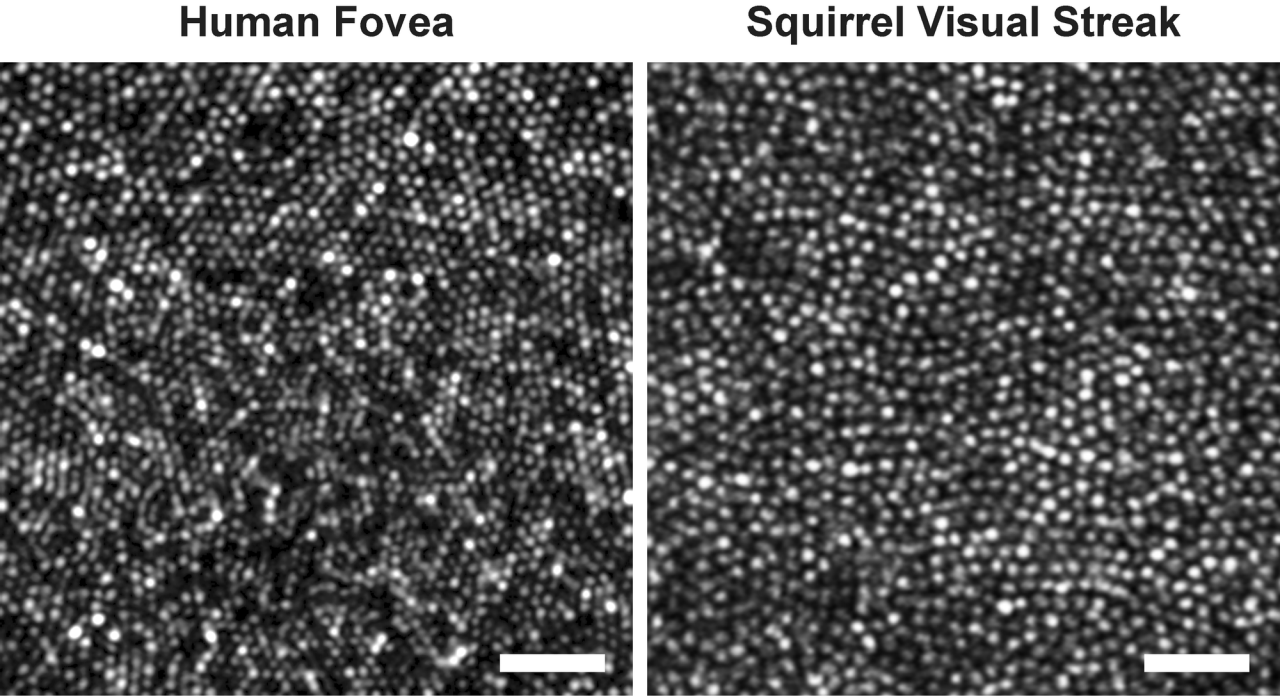
Human Fovea
Squirrel Visual Streak

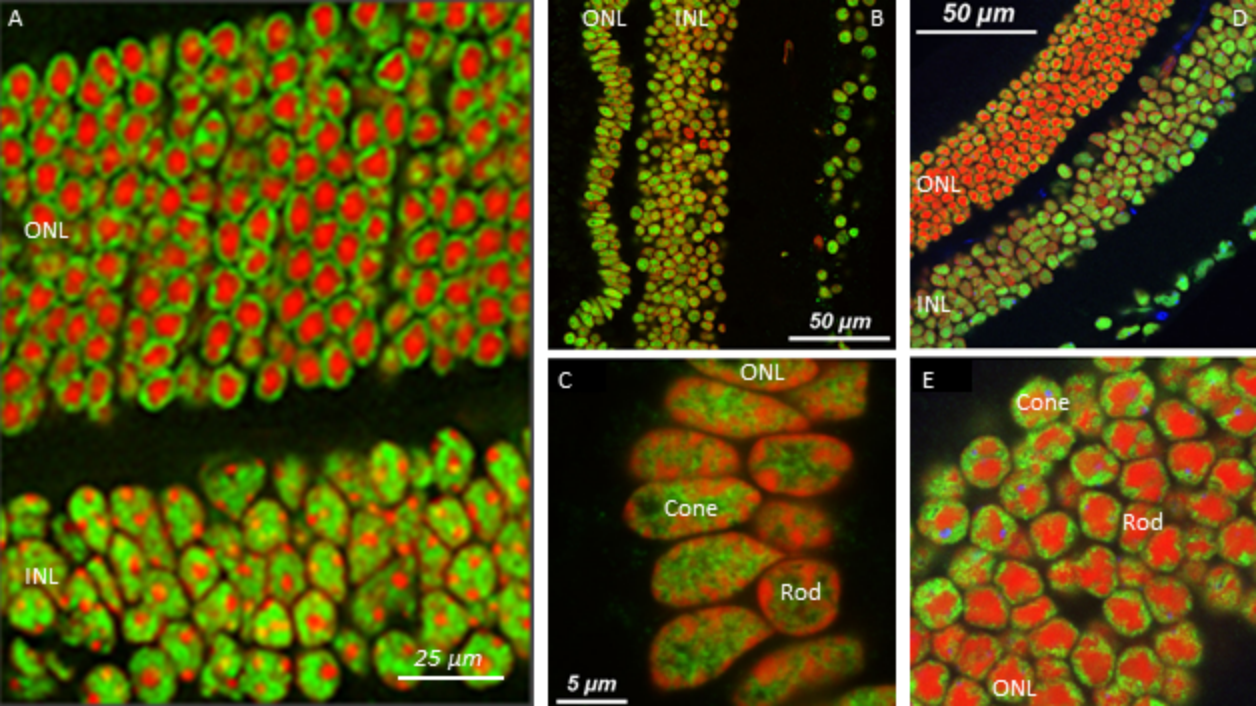
A
ONL
INL
25 μm
ONL
INL
B
50 μm
50 μm
D
ONL
INL
C
ONL
Cone
Rod
5 μm
E
Cone
Rod
ONL